Politecnico di Milano

Facoltà di Ingegneria Industriale e dell'Informazione

Corso di laurea Magistrale in Ingegneria dell'Automazione

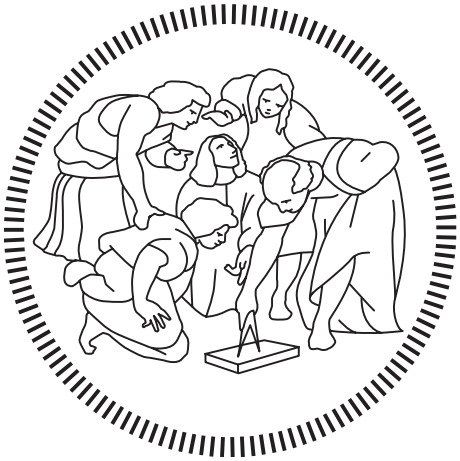

Model predictive control for microgrid management

Relatore

Fredy Orlando RUIZ PALACIOS

Tesi di laurea magistrale di:

Andree Jheyson ROJAS GRANADOS – 914850

Anno academico 2019 - 2020

Abstract

In recent years, generation of energy using renewable resources such as wind or sun radiation has become popular due to pollution reduction policies and economic benefits involved. In the case of solar generation, initially large fields containing several photovoltaic panels were needed to produce energy at large scale; typically these systems were owned by energy generation companies. However, production of energy at small scale using panels on condominiums is also gaining popularity because of bill reduction for the residents. Due to the natural uncertainty of renewable generation and electrical demand, these systems are used together with a storage system to make use of the energy stored when the solar irradiation is not enough to satisfy the demand and to store energy when the energy generation is greater than the demand. The operation of the storage impacts in the performance of the microgrid, hence in this thesis a control strategy to manage the storage of a microgrid is proposed. The proposed control strategy is based on Model Predictive Control (MPC) which aims to control the system optimally according to certain objectives and subjected to operational restrictions. MPC is based on solving an optimization problem at each time instant and in this thesis the optimization problem is formulated as a mixed integer linear programming (MILP). The control strategy is evaluated through simulations and two different microgrids are considered which differ in the type of storage system, but equivalent storage capacity is considered. One of them is based on regeneration of hydrogen through electrolysis whereas the other storage system is based on batteries. Additionally, for each microgrid two objectives are considered in the optimization problems: minimization of energy exchange with the grid and minimization of energy costs. Then, a simpler heuristic algorithm based on logical rules is presented with the sole purpose to compare the performance of both control systems. The results of the simulations show the effectiveness of the proposed control strategy and that each type of storage system is suitable for a certain objective.

Sommario

Negli ultimi anni, la produzione di energia usando risorse rinnovabili come il vento o la radiazione solare è diventata piuttosto comune grazie alle politiche di riduzione dell'inquinamento e anche dei benefici economici. Nel caso della produzione solare, inizialmente erano necessari per la produzione di energia in larga scala ampi spazi che contenessero una moltitudine di pannelli fotovoltaici; tipicamente questi sistemi erano di proprietà delle compagnie di produzione energetica. Tuttavia, oggigiorno, la produzione di energia in piccola scala mediante pannelli all'interno di condomini sta diventando sempre più comune grazie alla riduzione dei costi in bolletta per i residenti. A causa della naturale incertezza della produzione rinnovabile e della domanda di corrente elettrica, questi sistemi vengono usati insieme a un apparato di immagazzinamento per poter fare uso di tale energia ogni qual volta la radiazione solare non sia sufficiente per soddisfare la richiesta e per poterla immagazzinare nei casi in cui la produzione energetica sia maggiore della domanda. L'operazione di stoccaggio influisce sulla performance della microgrid: è per questo che in questa tesi si propone una strategia di controllo per gestire l'immagazzinamento di energia di tale sistema. La strategia di controllo proposta è basata sul Model Predictive Control (MPC) che ambisce a controllare in modo ottimale il sistema secondo diversi obiettivi e sottostando ad altre restrizioni operative. L'MPC si basa sulla risoluzione e sull'ottimizzazione del problema in ogni istante di tempo, e in questa tesi il problema dell'ottimizzazione è formulato come un Mixed Integer Linear Programming (MILP). La strategia di controllo è valutata tramite simulazioni, e sono considerate due diverse microgrid che differiscono per tipologia del sistema di stoccaggio, ma sono equivalenti se viene considerata la capacità di stoccaggio. Una di esse è basata sulla rigenerazione dell'idrogeno mediante elettrolisi, mentre l'altro sistema di immagazzinamento è fondato su batterie. In più, per ogni microgrid, nei problemi di ottimizzazione, si considera due obiettivi: la minimizzazione dello scambio di energia con la rete e la minimizzazione dei costi dell'energia. Viene presentato, inoltre, un più semplice algoritmo euristico basato su regole logiche con il solo proposito di comparare la performance dei due sistemi di controllo. I risultati delle simulazioni mostrano l'efficacia della strategia di controllo proposta e che ogni tipo di sistema di stoccaggio è più adatto a un obiettivo diverso.

Table of Contents

List of Figures

List of Tables

Chapter 1 Introduction

In recent years there has been a continuous increase in the use of renewable energy at low scales. Due to the nature of these kind of resources, the maximum levels of generation does not coincide with the maximum levels of consumption so they are often used together with other components such as gas generators and energy storage which can be regulated to provide energy when there is deficit and store energy when there is surplus. The combination of different devices that can produce and consume energy locally is known as a microgrid. However, the management of these controllable devices cannot be aleatory otherwise its use may imply greater economic costs, undesired technical behaviour, or simply suboptimal performance. In this context, the objective of this thesis is to present a control structure for the efficient management of an electrical microgrid. This control structure is based on a technique called Model Predictive Control (MPC) which is based on numerical optimization. This thesis considers two kind of microgrids: one with energy storage based on hydrogen and other that uses batteries as storage. Then, for each microgrid different objectives are stated: minimization of energy exchange with the grid and reduction of energy costs. Simulations based on mathematical models are performed to show the behaviour of the proposed control strategy.

This thesis is structured as follows:

- In chapter 2 theoretical background concerning microgrids is presented. It describes the concept of microgrids, their benefits, types, main components, and the mathematical models of the components used in this thesis.
- In chapter 3 theoretical background corresponding to numerical optimization is presented. In this thesis mixed integer linear programming is used, so in this section is described this kind of optimization problem and how to cast functions or expressions as a mixed integer linear program. It is also described the Branch& Bound methods which are main algorithm used to solve this kind of problems. This description allows to understand how the optimization problem statement affects the computation time to solve these problems.

- In chapter 4 is introduced theoretical background of MPC, its formulation for linear systems and how to include it in the formulation of a mixed integer linear program
- Chapter 5 describes the microgrids considered and their mathematical models are validated and then simplified for their use in MPC. Then the control strategy is described. The cost functions for each objective and microgrid are presented as well as the operational constraints for each case. Next, it is presented how is generated the photovoltaic generation and electrical demand data used in the simulations. Finally, an alternative simpler algorithm is described is described to compare it with the performance of MPC.
- Chapter 6 defines comparison criteria and shows the results of simulations. The results are compared with the previous define criteria and some comments are given for these results.

Theoretical background

Chapter 2 Electrical microgrids

2.1 Introduction

A conventional grid electrical grid is a system whose main objective is to provide electrical energy to consumers and is conventionally based on three stages: generation, transmission, and distribution. Power plants generate large amounts of electric energy by transforming primary sources of energy found in nature into electric energy. These plants are usually located near the natural resources and far from consumers, so energy is transported to urban areas by transmission networks. These networks move electric energy for long distances, so they operate at high voltage to minimize the power losses due to Joule effect. Once in urban areas, there are electrical distribution substations which step down voltage to user levels and then electrical energy is delivered to final users [1].

An important characteristic of current electrical grids is that considerable part of total electric energy is generated by using natural resources which release CO_2 to the environment and contribute to global warming. For this reason, electrical generation using renewable energy resources (RER) such as sunlight and wind, which have experienced a high development in recent years, appear as an interesting solution to reduce CO_2emissions [2]. Moreover, the introduction of these resources in the generation of energy makes the prices of electrical energy less dependent of the fluctuating price of fossil fuels providing in this way financial stability [3]. However, the use of these resources also has some drawbacks. An issue is their relatively high investments costs since they are a technology which is not yet consolidated, so economic incentives are needed. Although they have gained great popularity in recent years and are in continuous development, so these costs are expected to decrease in time [3]. Another disadvantage is that electrical power produced by RER's cannot be controlled because these resources are intermittent i.e. electrical power depends on external factors such as the availability of sunlight or speed of wind. In a grid with only conventional resources, power is regulated to satisfy the demand. However, when RER

generation is included these resources have a priority over other types of generation types in the scheduling, i.e. they produce all the energy they can provide and variability of RER's is assumed by regulating power of plants that work with conventional resources. So far in most countries participation of RER's in conventional grids is relatively small so their intermittency can be assumed by other generation types; although, an increase of participation of RER's in a conventional electrical system will degrade power reliability because the intermittency of RER's will predominate in the grid and generation-demand balance will be harder to achieve [3]. On the other hand, another inconvenient of current electrical grids is that distribution networks experience significant power losses in form of heat since they transport electricity at relatively low voltages. A solution for this issue could be distributed generation (DG) which stands for the installation of small generation plants close to consumers to avoid the losses due to transportation [4]. Although small power plants based on RER's can be installed, the problem of their intermittency remains and therefore is still present the degradation of power quality if RER predominate on the grid. In this context, microgrids appear as a concept to facilitate the integration of RER's and DG in electrical grids. In this chapter basic notions of microgrids will be given as well as description of the main components putting more emphasis in the qualitative description and mathematical models of the components that will be used in this thesis

2.2 Basic concepts

In the EU research project [5] the following definition is given:

Microgrids comprise LV distribution systems with distributed energy source, such as micro-turbines, fuel cells, PV's, etc ... together with storage devices, i.e. flywheels, energy capacitors and batteries, and controllable loads, offering considerable control capabilities over the network operation. These systems are interconnected to the Medium Voltage Distribution network, but they can also be operated isolated from the main grid.

From this definition it can be derived that a microgrid is a small electrical system that operates at relatively low voltages and integrates small sources of generation, small consumers, storage systems and a control system. The term "small" is relative since microgrids can operate with generation of few kW to satisfy domestic electrical demands for a residence or can also work with generation of several kW to satisfy electrical demand for example in a commercial centre [6]. The difference with a conventional grid is that there is a storage system that allows to store excess of generated energy when it is not needed and use it later when there is a deficit of

generation. In this way it allows to introduce RER's massively despite of their intermittency. Another difference is the inclusion of DG where generation units are physically close to the load, so power flows through the distribution networks are reduced and therefore the power losses are also reduced. An important component is the management system which constantly monitors the operation of the microgrid and uses these measurements together with algorithms to make decisions and operate the grid in an efficient way according to certain objectives.

2.3 Benefits

Adoption of microgrids leads to economic, technical, environmental, and social benefits [6]:

Economic benefits

- Storage of energy generated in excess for later use leads to reduction of bills paid by users.
- Microgrids can assume the expected growing demand so investments needed to build or renew infrastructure are reduced.
- The price of energy becomes more independent from the price of fossil fuels which makes the electrical sector financially less vulnerable to fossil fuels price fluctuations.

Technical benefits

- Installation of generation units close to the loads decreases power losses in the distribution network, so the electrical system becomes more efficient.
- Storage devices can help the grid by mitigating power disturbances making it more reliable.
- Power fluctuations inherent to intermittent nature of RER's is reduced so the adoption of RER's is favoured.
- Availability of energy in case of partial or total failures in the main grid.

Environmental benefits

- Decrease of the CO_2 emissions due to increase of use RER's.

Social benefits

- Electrification of remote small areas where the installation of transmission lines represents an elevated cost

2.4 Architecture

A microgrid is typically constituted by [6]:

- Controllable energy sources: The power output of these resources can be regulated as requested. Example of these plants are small gas generators for domestic microgrids or small hydro plants for greater applications.
- Non-controllable energy sources: The power output cannot be regulated since it depends on external factors. Example of these plants are photovoltaic panels and wind generators.
- Controllable loads: Also known as non-essential loads and refer to devices whose power consumption can be curtailed or shifted for some amount of time by a management system. Example of these loads can be water heaters and air conditioning.
- Non controllable load: The operation of these devices can only be controlled manually by the users.
- Energy storage system: System that can store and provide energy according to the setpoint requested by the management system. Examples of these are …
- Monitoring and control system: It is the management system that monitors the components of the grid and regulates the power outputs of the controllable loads, energy sources and energy storage to achieve an optimal operation of the plant according to certain objective.

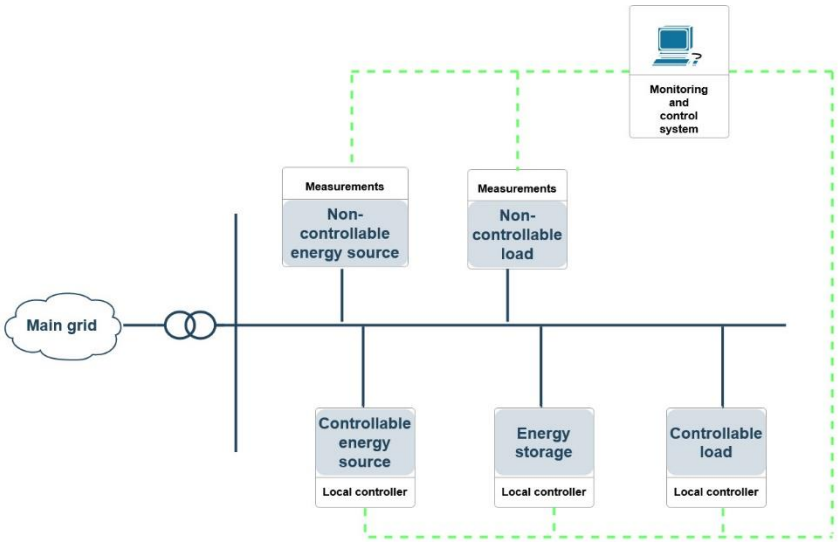

Fig. 2.1: Architecture of a microgrid

2.5 Management system

The management system is the responsible for the monitoring and control of the microgrid. This system is composed of several controllers each of them performing a specific control function. These control functions operate at different timescales, so a hierarchical structure is used [3]. A common structure is to divide controllers in two groups:

- Primary controllers: They perform control functions that have fast behaviour and operate in timescales that range from milliseconds to seconds. These devices control a single device and examples of their functions can be voltage control and current control.
- Secondary controllers: They perform control functions that do not need to operate fast, so they operate at timescales that range from minutes to hours. These controllers acquire measurement signals from primary controllers and give them back reference signals. Examples of their control functions can be storage management and power flows optimization.

The following scheme represent this hierarchical structure:

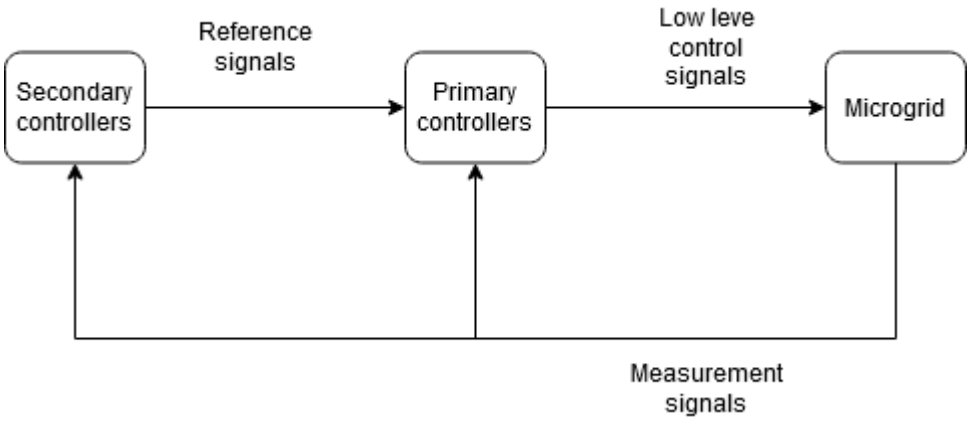

Fig. 2.2: Control hierarchy scheme

2.6 Energy sources

There are several types of natural resources used for generation of energy and the definition of microgrids does not restrict the type of natural resource used for power generation. So, production of energy using non-renewable sources is also possible. In general, natural resources can be classified in two groups: those that allow regulation of power and those that are intermittent by nature and therefore cannot regulate their power output. Furthermore, depending on the type of resource there is the necessity

of certain power electronics interfaces to make the output of generation compatible to the grid voltage level. Those systems which generate AC electricity usually use a DC rectifier and then an inverter to obtain the desired voltage and frequency; whereas systems that produce DC electricity only need the inverter. Some sources of energy used in microgrids will be described.

Solar power generation

Sun emits radiant light and heat that can be used directly or indirectly to produce electricity [7]. On the one hand, heat from sun can be used to boil water which produces steam that can be used in a steam turbine to generate electricity whereas on the other hand, photovoltaic panels made of semiconductor materials can take advantage of sunlight irradiance to produce electricity. Among these options to transform solar energy, photovoltaic generation has gained popularity in recent years.

In [7], the following definition is given:

The main element of photovoltaic generation is a solar cell which is basically a PN junction diode. Solar radiation causes a large number of electron-hole pairs to be created in the semiconductor material. The asymmetry in a PN junction provides a built-in electric field at the junction, therefore the generated electrons and holes flow from the P-side to the N-side and from the N-side to the P-side, respectively. A voltage appears across the diode, which can drive current into an external circuit and deliver power to it.

Cells are combined in series and parallel to form a module with desired voltage and power. The adoption of this technology involves the following benefits [7]:

- Conversion of energy is quiet, so it does not disturb users
- Their costs are continuously falling in recent years due to their popularity
- At small-scale generation, solar panels can be installed on the roofs of residences, so their installation is relatively easily when compared with other types of generation. This feature facilitates their adoption by small users.

In [8], the following equations are given to compute the photovoltaic generation:

$$T_C = T_a + \frac{NOCT}{800} \cdot G \tag{2.1}$$

$$\eta_{th} = 1 - \alpha_{th} \cdot (T_c - 25) \tag{2.2}$$

$$\frac{P_{AC}}{P_{nom}} = \eta_{DC-AC} \cdot \frac{G}{1000} \cdot \eta_{th} \tag{2.3}$$

where T_a is the temperature of the air in °C, NOCT is the nominal operating cell temperature, G is the solar irradiance in W/m^2, T_C represents the cell temperature, η_{th} represent the reduction of production due to cell temperature and α_{th} is an empirical parameter that allows to calculate this loss, η_{th} represents the losses due to the conversion of energy from DC to AC.

This model allows to convert solar irradiance into a dimensionless value that represents the ratio between the produced power and the nominal power.

2.7 Energy storage systems

In conventional grids the balance between generation and load is achieved by regulating power from generators by using frequency as feedback signal. At operating conditions, variations of electrical frequency are inversely proportional to changes of load, i.e. when the load increases the frequency of the grid tends to decrease and vice versa. So, the controllers of the generators automatically regulate power to maintain frequency constant as much as possible. However, this mechanism only works for small variations of load and therefore base generation is prior scheduled based on load forecasts. In this way, generation is regulated to satisfy the energy balance between generation and demand. As explained before, power output from renewable resources is highly variable and cannot be regulated, therefore conventional generation needs to be capable to deal with uncertainties coming not only from demand but also from renewable generation. Moreover, congestion of energy in the grid and peaks of renewable generation occur at different interval of hours. For these reasons, renewable generation cannot predominate in a conventional grid. In this context, the availability of energy storage systems can solve these issues.

There are many types of storage systems used in microgrids among which can be found: hydrogen compressed and batteries. To compare these storage technologies the following criterions can be used:

Self-discharge losses: Losses of stored energy while power is not consumed.

Roundtrip efficiency: Ratio between the energy that can be obtained from the storage and the energy needed to charge the storage.

Cycle lifetime: The number of charge-discharge cycles obtained from a storage system in its lifetime.

Energy density: Space of a storage system to store certain amount of energy.

In the following sections hydrogen-based storage and batteries will be described in more detail.

2.7.1 Regenerative Hydrogen Fuel Cell

The use of hydrogen as a mean to store hydrogen is today a technology in development and it is expected to play an important role in the energy sector in the future. The following characteristics make it an attractive mean to store energy [4] [9]:

- It has the highest energy density than other energy storage types.
- Its adoption by small users is possible since it does not have geographical restrictions as other technologies such as pumped hydro
- It has a low self-discharge rate which makes it an interesting option for seasonal storage, e.g. solar energy produced in summer can be stored for months and then used in winter when solar irradiance levels are low

In this context an important technology that uses hydrogen to store energy is Regenerative Hydrogen Fuel Cell (RHFC). It is a system that accumulates hydrogen when there is a surplus of electrical energy and when needed produces electrical energy consuming the stored hydrogen. It consists of three main components: electrolyser, storage tank and fuel cell. At a first stage the electrolyser absorbs electrical energy and water to produce hydrogen and oxygen by electrolysis of water. Then, hydrogen is stored in a tank. Finally, the fuel cell absorbs hydrogen from the tank and oxygen to produce electricity and water. Fig. 2.3 obtained from [9] depicts the operation of this system:

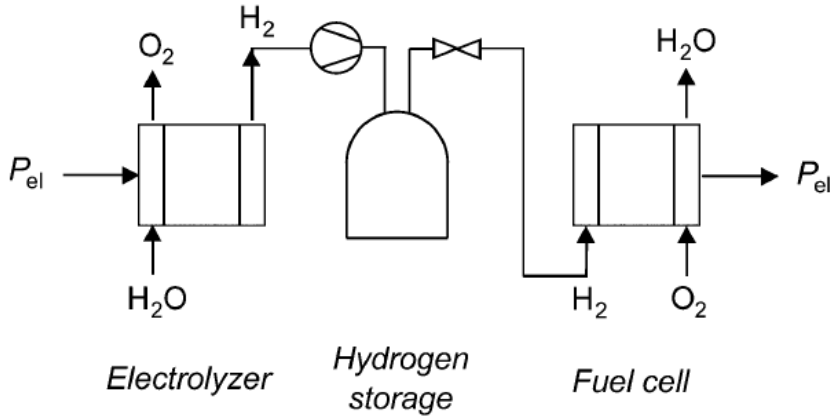

Fig. 2.3: Scheme of regenerative hydrogen fuel cell

However, all the benefits of hydrogen are overshadowed by the low round-trip efficiency of this system, which is particularly low - around 30% - when compared with

other technologies. This low value is due to the low efficiencies of electrolyser and fuel cell with typical values of 70% and 47% respectively [9].

2.7.1.1 Electrolyser

An electrolyser is a device that receives electrical current and water flow as inputs and produces hydrogen. It is based on water electrolysis by which a water molecule is separated into hydrogen and oxygen by applying current [10]. The following expression represents the electrolysis reaction for an electrolyser:

$$H_2O \rightarrow H_2 + \frac{1}{2}O_2 \tag{2.4}$$

This chemical process is endothermic, i.e. the process absorbs heat and is also non-spontaneous, i.e. for the reaction to take place it needs an external source of energy. The electrolysis cell is the basic unit of an electrolyser, and since the values of voltage and current of a single cell are small, cells are interconnected to use a desired voltage and current. The interconnection of cells can be in series or parallel, but series connections are nowadays the most adopted solution by manufacturers. Fig. 2.4 obtained from [10] depicts these types of connections:

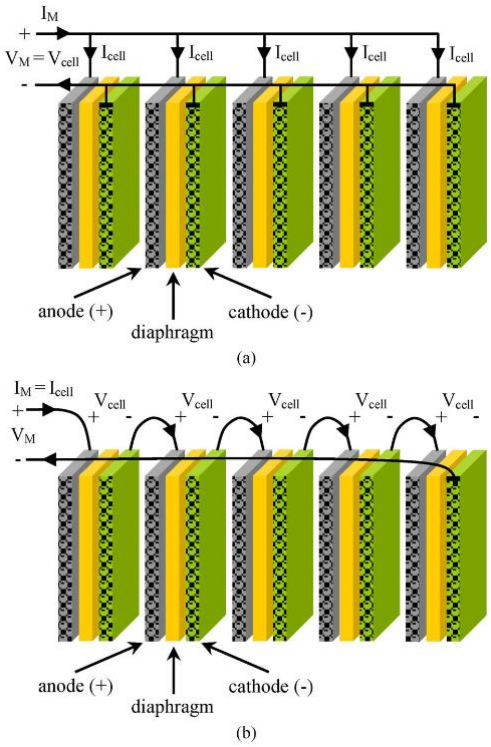

Fig. 2.4: (a) interconnection of cells in parallel, (b) interconnection of cells in series

The electrolysis chemical reaction depends on ion-conductivity, so electrolysers can be classified depending on the technology used to allow ion mobility. In this thesis alkaline electrolyser will be used which use an alkaline solution to allow the chemical reaction. For this case, the chemical reactions are:

$$Cathode: 2H_2O + 2e^- \rightarrow H_2 + 2OH^- \tag{2.5}$$

$$Anode: 2OH^- \rightarrow \frac{1}{2}O_2 + 2e^- \tag{2.6}$$

At low levels of power supply, there is hydrogen contamination in the oxygen stream due the low permeability of liquid electrolyte which is flammable mixture. For these reason safety shutdowns occur when the power supply is lower than a certain percentage of the nominal power [10].

Model description

In this section the model described in [11] for an alkaline electrolyser is presented.

a) Thermodynamical sub model

The reversible voltage (U_{rev}) is the minimum required voltage for electrolysis to take place. At standard conditions of temperature and pressure, i.e. 1 atm and 25°, $U_{rev} =$ 1.229 V

b) Electrical sub model

In this model is considered an empiric relation between current and voltage. This relation is described in the following equation:

$$U_{cell} = U_{rev} + \frac{r}{A} I + s \cdot log(\frac{t}{A} I + 1) \tag{2.7}$$

Where r, s and t are empirical parameters; I is the current of each stack and A is electrolyser stack area.

In [12] is presented Fig. 2.5 that shows that the relation between current and voltage depends on temperature:

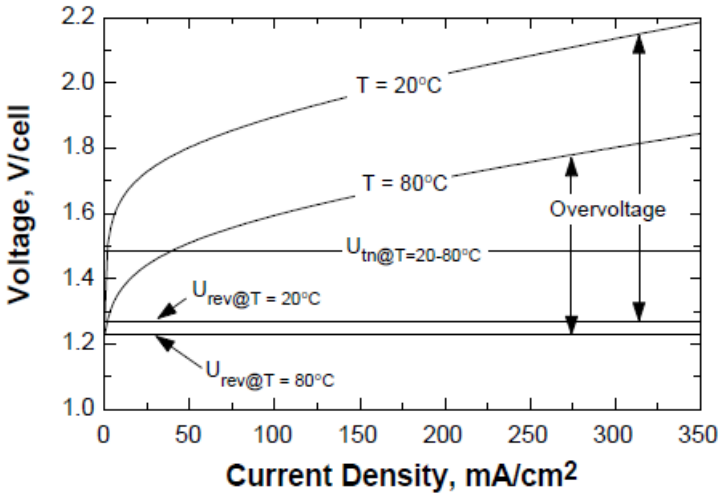

Fig. 2.5: relationship between current density and cell voltage for an alkaline electrolyser

The main difference between the curves is due to overvoltage which is caused by temperature so to describe better the process, temperature is included in the second and third terms of equation (2.8):

$$U_{cell} = U_{rev} + \frac{(r_1 + r_2 \cdot T)}{A} I + s \cdot log(\frac{(t_1 + t_2 \cdot T + t_2 \cdot T^2)}{A} I + 1) \quad (2.8)$$

Since electrolysers are built with arranges of cells connected in series and parallel, the voltage of the electrolyser is defined by the product of the cell voltage by the number of cells in series, while the current passing through each stack in parallel multiplied by the number of cells in parallel is equal to the current of the electrolyser. Then the power of the cell is the product of the current and voltage.

The Faraday efficiency's definition is the ratio between the real and maximum theoretical production of hydrogen by the electrolyser. The following empirical expression describe this efficiency:

$$\eta_f = \frac{(I/A)^2}{f_1 + (I/A)^2} f_2 \quad (2.9)$$

where f_1 and f_2 are empirical parameters

The production rate of hydrogen is directly proportional to the electrical current. Since typically an electrolyser is formed by cells connected in series the hydrogen production rate can be described by the following expression:

$$\dot{m}_{H_2} = \eta_f \frac{n_c I}{zF} \tag{2.10}$$

where n_c is the number of cells in series, z is the number of electrons of hydrogen (z=2) and F represents the Faraday constant which is 96485. The production of hydrogen $\dot{m}_{H_2}$ is expressed in mol/s

c) Thermal sub model

As mentioned before, temperature has an effect on the voltage of the cell, so it is important to model the behaviour of temperature in this process.

The thermal energy balance can be expressed as:

$$C_t \frac{dT}{dt} = \dot{Q}_{gen} - \dot{Q}_{loss} - \dot{Q}_{cool} \tag{2.11}$$

where $\dot{Q}_{gen}$ refers to the heat released by electrolysis, $\dot{Q}_{loss}$ represent the heat exchange to the ambient due to the system operates at a higher temperature; and $\dot{Q}_{cool}$ is due to external cooling of the system. The following equations describe these terms:

$$\dot{Q}_{gen} = n_c(U - U_{tn})I \tag{2.12}$$

where n_c is the number of cells, U is the voltage of the stack, U_{tn} thermoneutral voltage and I the current of the stack

$$\dot{Q}_{loss} = \frac{1}{R_t}(T - T_a) + h_f(T - T_a) + h_n(T - T_a) \tag{2.13}$$

where R_t is the thermal resistance of the electrolyser, h_f is the film coefficient for forced convection, h_n is the film coefficient for natural convection, T is the operating temperature and T_a is the ambient temperature.

For the cooling term, the model described in [11] considers a fan to evacuate heat and it is based on hysteresis to maintain the temperature inside a range. The amount of heat that the fan can evacuate should be higher than the heat produced by electrolysis.

2.7.1.2 Fuel cell

A fuel cell, inversely to an electrolyser, is a device that produces electrical energy when is fed with gas rich in hydrogen and oxygen. The following expression represents this chemical reaction [13]:

$$2H_2 + O_2 \rightarrow H_2O \tag{2.14}$$

Inversely to the electrolyser, this chemical reaction is exothermic and spontaneous which implies that it does not need to absorb energy to occur.

The basic configuration of a fuel cell consists of an electrode in contact with O_2 and another electrode in contact with H_2 and an electrolyte in contact with both electrodes. The reactions taking place at each electrode depend on the type of fuel cell. In this thesis, a PEM (proton exchange membrane) fuel cell is considered and its main characteristic is that the electrolyte consists of a solid membrane that is impermeable enough to separate oxygen and hydrogen but has high ion conductivity to allow protons flow. The chemical reactions for these fuel cells are the following [14]:

$$Anode: H_2 \rightarrow 2H^+ + 2e^- \tag{2.15}$$

$$Cathode: \frac{1}{2}O_2 + 2H^+ + 2e^- \rightarrow H_2O \tag{2.16}$$

At the anode hydrogen splits into electrons and protons. Then electrons move from the terminal of the electrode to the outside, form electrical current and return to the fuel cell at the cathode. On the other hand, protons move from the anode to the cathode through the membrane where they meet, oxygen and the electrons that return to the system. These particles combine and produce water which is pulled out of the fuel cell. This chemical reaction is described in Fig. 2.6:

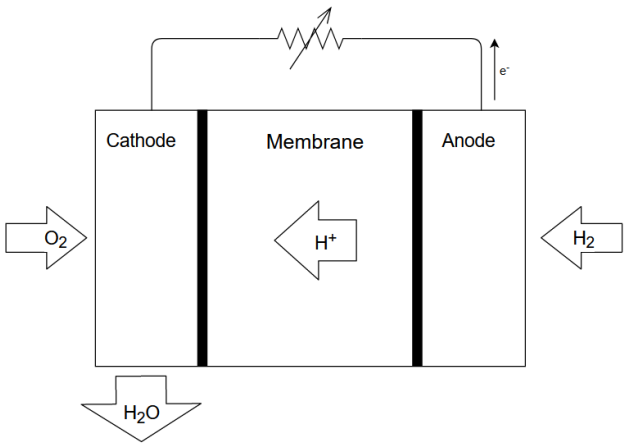

Fig. 2.6: Operation principle of PEM fuel cell

An important characteristic of this these fuel cells is that they are compact due to the thinness of the membrane electrodes assembly. Similarly to electrolysers, there are also alkaline fuel cells, but PEM technology has gained popularity in recent years and is the preferred technology by most manufacturers and the research community. Differently to alkaline technology, PEM fuel cells do not have the limitation of low power and can operate in the full range [15].

Model description

In this section the model for a PEM fuel cell taken from [16] is described. For a single cell, the equation of the voltage is:

$$V_{cell} = E_{Nernst} - V_{act} - V_{con} - V_{ohm} \tag{2.17}$$

where E_{Nernst} is the thermodynamical potential, V_{act} represents activation overvoltage at the electrodes, V_{con} is a loss related to mass transportation and V_{ohm} is the ohmic overvoltage that represent losses for the proton conductivity of internal electric resistances.

a) Nernst voltage

The standard expression for this voltage can be written as:

$$E_{Nernst} = 1.229 - (8.5 \cdot 10^{-4})(T - 298.15) + (4.308 \cdot 10^{-5})T(ln\, p_{H_2} + 0.5 \cdot ln\, p_{O_2}) \tag{2.18}$$

where T is the cell temperature in Kelvin, p_{H_2} and p_{O_2} are the partial pressure of H_2 and O_2 respectively expressed in atm.

b) Activation voltage

There is a barrier energy that has to be overcome for the reactions at the electrodes to take place. The activation overvoltage can be expressed as:

$$V_{act} = \xi_1 + \xi_2 T + \xi_3 T\left[ln\, C_{O_2}\right] + \xi_4 [ln\, I] \tag{2.19}$$

where I is the current of the fuel cell, ξ are empirical parameters, T is the temperature of the system in kelvin and C_{O_2} is the concentration of oxygen in mol/cm^3

c) Concentration overvoltage

This voltage drop is due to reduction of concentration of the gases. The following expression describes it:

$$V_{act} = -B \cdot ln\left(1 - \frac{I}{I_{max}}\right) \tag{2.20}$$

where B is an empirical parameter

d) Ohmic voltage

This loss of voltage is due to the resistance of electrons to flow through the electrodes and protons to move through the electrolyte. It is noted by [17] that the resistance to ions movement is predominant. This loss can be expressed as:

$$V_{ohm} = I \cdot (R_m + R_c) \tag{2.21}$$

where R_m and R_c represent the resistance to the flow of ions and electrons, respectively.

The resistance R_m is described by the following expression

$$R_m = \frac{r_m \cdot l_{mem}}{A} \tag{2.22}$$

where r_m is the membrane resistivity, $l_{mem}$is the membrane thickness and A is the cell area.

r_m is related to the current density and temperature:

$$r_m = \frac{181.6 \cdot \left[1 + 0.03\left(\frac{I}{A}\right) + 0.062\left(\frac{T}{303}\right)^2\left(\frac{I}{A}\right)^{2.5}\right]}{\left[\lambda - 0.6343 - 3\left(\frac{I}{A}\right)\right] e^{[4.18((T-303)/T)]}} \tag{2.23}$$

where λ is an adjustable parameter which is related the membrane humidity and ranges from 0 to 23 and, its usually value in most applications is 14.

The consumption rate of hydrogen is obtained by Faraday's law:

$$\dot{m}_{H_2} = \frac{n_c I}{zFx} \tag{2.24}$$

where n_c is the number of cells, z is the number of electrons of hydrogen, F is the constant of Faraday and x is the concentration percentage of hydrogen of the inlet flow. The consumption rate of hydrogen by this formula is expressed in mol/s.

2.7.1.3 Hydrogen storage tank

This device accumulates the hydrogen produced by the electrolyser and supplies it to the fuel cell. The previous equations given for the electrolyser and fuel cell express flow in mol/s but it is common practice to use volumetric flow rates in litres per minute. However, volume of gases depends on the ambient conditions. Hence, to compare flows of gases at different conditions, volumes are expressed at standard conditions, i.e. 1 atm and 273 K. The equation of ideal gases is stated as:

$$\mathrm{PV} = RTn \tag{2.25}$$

Considering standard conditions, for hydrogen this expression becomes:

$$\mathrm{V} = 22.4 \cdot n \tag{2.26}$$

From this equation it is clear to see that 1 mol of hydrogen at standard conditions is equivalent to 22.4 litres. Therefore the following expression can be used to convert from mol/s to litres per minute:

$$\dot{m}_{slpm} = \dot{m}_{mol/s} \cdot 22{,}4 \cdot 60 \tag{2.27}$$

where slpm in the previous equation stands for litres per minute at standard conditions

The dynamics of the amount of hydrogen in the tank can be expressed as:

$$x_{(k+1)} = x_{(k)} + \frac{100 \cdot \Delta t}{Q_{max}} \cdot (\dot{m}_{ely} - \dot{m}_{fc}) \tag{2.28}$$

where $\dot{m}_{ely}$ represents the flow of hydrogen produced by the electrolyser, $\dot{m}_{fc}$is the flow of hydrogen consumed by the fuel cell, Q_{max} is the capacity of the tank expressed in litres at standard conditions, Δt is the sampling time and $x_{(k)}$is the percentage of hydrogen in the tank with respect to the capacity of the tank where 0 and 100 represent empty and full tank respectively.

2.7.2 Battery

2.7.2.1 Main concepts

Similarly to the previous storage system, batteries are also based on transformation of chemical energy into electrical energy. However, for batteries it is not needed to constantly provide external reactants such as water or oxygen to produce the chemical reactions. Instead, in this case the chemical reactions directly affect the electrodes. Batteries can provide energy when connected to an external circuit and absorb energy when the electrical current is inverted [18].

When discharging:

An oxidation reaction ($A \rightarrow A^+ + e^-$) of the anode occurs and thus this electrode is considered the negative terminal. When the battery is connected to an external circuit, the electrons produced by oxidation travel through the external connection forming electrical current and return to the battery by the positive terminal. Then, the returning electrons allow a reduction reaction ($B^+ + e^- \rightarrow B$) of this terminal which in this case is the cathode. Fig. 2.7 taken from [19] depicts this process:

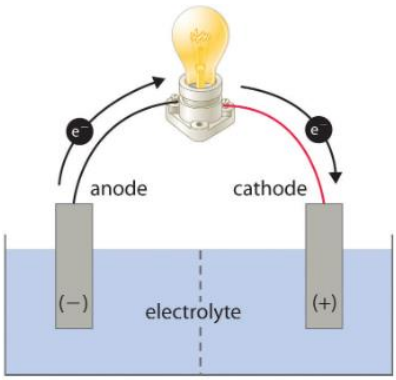

Fig. 2.7: Scheme of principle when a discharging a battery

When charging:

In this case the redox reaction is non-spontaneous, so an external source of electrons is needed. The electrons supplied enter by the negative terminal and a reduction reaction ($B^+ + e^- \rightarrow B$) takes place. Differently from discharging, in this case the

negative terminal is the cathode. Then an oxidation reaction ($A \rightarrow A^{+} + e^{-}$) of the anode takes place generating the electrons that leave the battery and return to the source. In this case the anode becomes the positive terminal. Fig. 2.8 taken from [19] depicts this process:

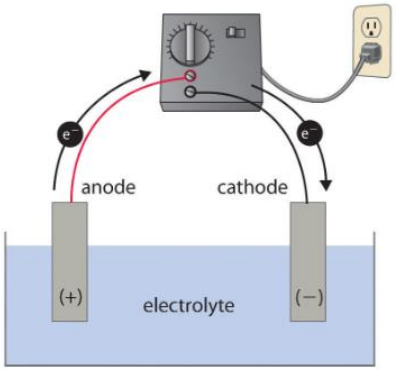

Fig. 2.8: Scheme of principle when charging a battery

Some of the technical specification of batteries is provided below [18] [20]:

Discharge rate: It is the value of the current that will discharge the battery within a certain amount of time. It is typically expressed as hC where h is the number of hours to discharge the battery. For instance, 1C rate represent the discharge current needed to discharge the battery in 1 hour.

Energy capacity: It is the amount of energy expressed in Wh available when the battery is discharged at a certain discharge rate. It is computed by multiplying the discharge rate by the time needed to discharge. The energy capacity decreases when the battery is subjected to high discharge rates due to higher losses.

State of charge (SoC %): It is a term that indicates the amount of energy available in a battery at a specific point in time.

Depth of Charge (DoD %): It is a term opposite to SoC and represents the percentage of battery capacity that has been used.

Lifetime: The number of cycles a battery can complete until its capacity its reduced to 80% of its original value. This value is reduced when the battery is subjected to high discharge depths.

The types of batteries used nowadays differ in the materials used for the electrodes and electrolyte. In [21], two types of batteries commonly used are described:

- Lithium-ion (Li-ion): They use lithium as material for the electrodes. These batteries have high energy density when compared to other batteries and are mainly used in domestic appliances but also in electric vehicles and aerospace applications due to their low weight.
- Lead- acid: They use lead oxide (PbO2) and lead (Pb) for the electrodes, and sulfuric acid as electrolyte. This type of batteries is the oldest, but it is still used in many applications. These batteries have low energy density which means that to store certain amount of energy they are heavier and occupy more space than other batteries. However, their low price makes them an attractive solution.

In the following table some characteristics of these types of batteries are presented [22] [23] [24] [25]:

Type	Energy efficiency	Energy density (Wh/L)	Cost ($ per kWh)	Life cycle (number of cycles at 50%DOD per cycle)	Self-discharge
Lead acid	~ 60%	~ 40 - 100	~150 – 200	~400 cycles	~20% per month
Li-ion	~90%	~ 530	~ 400 – 700	~5000 cycles	~10% per month

Table 1: Comparison between battery technologies

2.7.2.2 Model description

In this section is presented a model to determine the evolution in time of the available energy in a battery. This model is based on [26] but this case considers distinct charge and discharge efficiencies.

$$SOC_{(k+1)} = SOC_{(k)} + 100 \cdot \frac{\Delta t}{Q_{nom}} (\eta \cdot P_{batt_{(k)}} - P_{sd}) \tag{2.29}$$

$$\eta = \begin{cases} \eta_c & if\ P_{batt_{(k)}} \geq 0 \quad (charge\ mode) \\ 1/\eta_d & if\ P_{batt_{(k)}} < 0 \quad (discharge\ mode) \end{cases} \tag{2.30}$$

$SOC_{(k)}$is the percentage of energy available in the battery at certain time instant k where 100 represents the case when the battery is fully charged and 0 when it is fully discharged, $Q_{nom}$is the nominal capacity of a battery and it is expressed in kWh, η_c, η_d refer to the charging and discharging efficiencies respectively and range between 0 and 1, $P_{batt_{(k)}}$ is the power exchanged with the battery and depending on its sign it can be absorbed or produced energy by the battery and it is expressed in kW; and P_{sd} is a constant term that represents the self-discharge effect on batteries, and it is expressed in kW.

Chapter 3 Numerical optimization

1.1 Introduction

In a general way, an optimization problem is formulated as follows:

$$\min_{z} f(z) \quad (3.1)$$

$$\textit{subject to:}$$

$$z \in S \subseteq Z$$

The objective of the problem is to find the optimization variable z that minimizes the cost function f(z). The minimization is subjected to the constraint that z must belong to a set S which is known as feasible set and S in turn should be included in Z which is the domain of the decision variable. If the set S is empty the problem is called unfeasible while if S = Z the problem is said to be unconstrained.

In the literature is common to use the word program to refer to an optimization problem. Optimization problems can be classified depending on the form of the cost function and the constraints.

In this chapter the following will be discussed:

- Fundamentals of a type of optimization problem called Mixed integer linear programming characterized by involving continuous and discrete variables.
- Hints to model desired features as mixed integer linear programs
- Description of the branch and bound algorithm which is the most used technique to solve mixed integer linear programs

3.1 Mixed integer linear programming (MILP)

It is an optimization problem where the cost function and the constraints are linear combinations of the optimization variables which can be continuous and discrete. The general form of this kind of optimization problem takes the following form:

$$\min_{u,\delta} f^T \begin{bmatrix} u \\ \delta \end{bmatrix} \quad (3.2)$$

$$\textit{subject to:}$$

$$A \begin{bmatrix} u \\ \delta \end{bmatrix} = b$$

$$C \begin{bmatrix} u \\ \delta \end{bmatrix} \leq d$$

where:

$f \in \mathbb{R}^{1 \times (m+n)}$, $u \in \mathbb{R}^m$, $\delta \in \mathbb{N}^n$, $A \in \mathbb{R}^{p \times (m+n)}$, $b \in \mathbb{R}^p$, $C \in \mathbb{R}^{q \times (m+n)}$, $d \in \mathbb{R}^q$

and m is the number of continuous variables, n is the number of discrete variables, p is the number of equality constraints and q is the number of inequality constraints.

3.2 Branch and bound algorithm

This section explains in a simple way the branch and bound algorithm and the influence of the modelling of the problem in the performance. The information presented in this section was obtained from [27], so this work should be consulted for more details. An optimization problem with only continuous variables is known as linear program and has the advantage that the optimal solution has to occur at a vertex of the feasible region, i.e. the solution relies on points that cannot be written as linear combination of other points of the feasible region. The inclusion of discrete variables complicates the optimization problem because the solution does not have to occur in a vertex anymore, so the whole feasible region has to be examined. This makes the problem NP-hard which means that there is not any algorithm that can guarantee the solution of the problem in a time that is polynomial function of the size of the problem. At first glance, a straightforward way to solve this kind of problems may be to solve the LP-relaxation which consists in considering the integer variables as they were continuous, solve the problem as a linear program and then round the solution to the nearest integer. However, it is shown in [27] that this approach leads to suboptimal solutions. Another tempting approach is to solve the problem for each possible combination of the discrete variables and then find the optimal value among all these solutions; however, the number of combinations grows exponentially with the number of discrete variables. For instance, with this approach a problem with 20 binary variables implies to solve 2^{20},equivalent to 1048576, linear programs. In this context, other approaches are needed and the most used technique to solve these problems is known as branch &

bound methods [28]. The main characteristic of this algorithm is that when a solution is found it can be guaranteed that it is globally optimal. However, due to NP-completeness of mixed integer programs the time needed to find the solution is not bounded.

The main idea of this algorithm is to divide the original problem into smaller subproblems and then solve them relaxing the integer conditions to find regions that do not contain the optimal solution and to find candidate solutions, then when the whole feasible region is examined the best solution is picked. The following steps describe this algorithm for a minimization problem:

1. Initialization:

   1.1. Solve the LP-relaxation of the original MILP problem:

   - If the relaxed problem is unfeasible, stop the algorithm because the MILP is also unfeasible
   - If the relaxed variables have an integer solution, then stop because the solution of the MILP is found
   - Otherwise, the solution of the LP-relaxation is the best solution so far and is also the lower bound of the optimal solution of the MILP. Then, add the original MILP problem to the list of candidate problems to be divided

2. Branching:

   - Select a candidate subproblem to divide
   - Divide the subproblem by branching on an integer variable that does not have an integer value in the LP-relaxation solution, and add the divided subproblems to the list of candidates

3. Bounding:

   3.1. Solve the LP-relaxation for each of the divided problems

   3.2. For each subproblem:

   - If the subproblem is not feasible then it does not contain the optimal solution of the original MILP and is not further divided.
   - If the solution of a divided subproblem is greater than the best solution obtained so far, then this node is not required to be further divided because the solutions of further divisions will not be better.
   - If the solution presents integer solutions, then further branching is not needed. If the best solution obtained so far is greater than the solution, then it is updated. It also becomes the upper bound of the optimal solution of the MILP

- If the previous conditions are not satisfied, then add this subproblem to the list of candidates to be further divided. The solution of this subproblem becomes the lower bound of the optimal solution

4. Optimality test: If there are not more candidate problems to be divided then the best solution obtained so far is the optimal solution of the original MILP problem. If there are still more problems to divide, then go to step 2

The branch & bound methods differ between them in the way how they decide which subproblem should be further divided, and once a problem is chosen, the way how to decide which integer variable use to branch. There are several methods to perform these decisions but there is not any that works better for all cases, so it needs to be determined empirically. The main factor that affects the computational efficiency is how close the solutions of the LP-relaxations are to integer values, if the solution is not integer but very close, the solution can be accepted as integer. Additionally, the convergence towards an optimal solution also depends on the number of discrete variables because it influences in the number of possible branches. In this sense, it is generally preferable to reduce the number of discrete variables although it may not always be truth because the speed depends more on the closeness of the LP-relaxations to integer solutions.

3.3 MILP modelling

The inclusion of discrete variables allows to model logical conditions or discontinuities that otherwise could not be included directly in an optimization problem. In the following sections, modelling techniques are introduced.

3.3.1 Continuous variable taking discontinuous values

If in a certain optimization problem, a continuous variable presents discontinuity, as in the following expression:

$$u = 0 \; or \; L \leq \; u \leq U \tag{3.3}$$

Then binary auxiliary variables can be used to model this situation as indicated in [29]. Consider the binary variable δ defined as:

$$\delta = \begin{cases} 0 & for \; u = 0 \\ 1 & for \; L \leq \; u \leq U \end{cases} \tag{3.4}$$

Then the following inequality model the discontinuity:

$$L\delta \leq u \leq U\delta \tag{3.5}$$

From equation (3.5), it can be seen that if δ=0 then x=0 and if δ=1 then L ≤ u ≤ U

3.3.2 Modelling of piecewise affine (PWA) function

This part follows the approach detailed in [30]. Consider the following piecewise affine function:

$$y = \begin{cases} ax & for\ x \geq 0 \\ bx & for\ x < 0 \end{cases} \tag{3.6}$$

If an auxiliary variable δ is introduced such that:

$$x \geq 0 \iff \delta = 1 \tag{3.7}$$

Then the piecewise affine function can be written as:

$$y = bx + \delta x(a - b) \tag{3.8}$$

These expressions cannot be included in that form in a linear optimization problem since the definition of δ implies a logical statement and the expression (3.8) depends on the product of a continuous and binary variable. However, these expressions are equivalent to linear inequalities.

In particular, the conditional statement below:

$$x \geq 0 \iff \delta = 1 \tag{3.9}$$

is equivalent to the following linear inequalities:

$$-m\delta \leq x - L \tag{3.10}$$

$$-(U + \varepsilon)\delta \leq -x - \varepsilon \tag{3.11}$$

where:

$$U = \ max(x) \qquad (3.12)$$
$$L = \ min(x)$$

Regarding the product of variables, consider the following

$$g = \ x_1 \delta_1 \qquad (3.13)$$

where x_1 is continuous and δ_1 is binary. Then, the equivalent linear inequalities are:

$$\begin{aligned} g &\leq \ M\delta_1 \\ g &\geq \ m\delta_1 \\ g &\leq \ x_1 - m(1-\delta_1) \\ g &\geq \ x_1 - M(1-\delta_1) \end{aligned} \qquad (3.14)$$

where:

$$M_g = \ max(x_1) \qquad (3.15)$$
$$m_g = \ min(x_1)$$

Then using these inequalities in expression (3.8), the following is obtained:

$$\begin{aligned} y &\leq \ M\delta + ax \\ -y &\geq \ m\delta - bx \\ y &\leq \ ax - m(1-\delta) \\ -y &\geq \ -bx + M(1-\delta) \end{aligned} \qquad (3.16)$$

where:

$$M = \ max(a,b) \cdot U \qquad (3.17)$$
$$m = \ max(a,b) \cdot L$$

The inequalities corresponding to the conditional statement and the product of variables can be written in the following compact form:

$$\underbrace{\begin{bmatrix} -L \\ -(U+\varepsilon) \\ -M \\ m \\ -m \\ M \end{bmatrix}}_{E_2}\delta + \underbrace{\begin{bmatrix} 0 \\ 0 \\ 1 \\ -1 \\ 1 \\ -1 \end{bmatrix}}_{E_3} y \leq \underbrace{\begin{bmatrix} 1 \\ -1 \\ b \\ -b \\ a \\ -a \end{bmatrix}}_{E_1} x + \underbrace{\begin{bmatrix} -L \\ -\varepsilon \\ 0 \\ 0 \\ -m \\ M \end{bmatrix}}_{E_5} \tag{3.18}$$

Note that if a and b change over time then these inequalities are time variant

3.3.3 Piecewise affine linearization

There are times where a nonlinear term appears in the optimization problem either in the cost function or in the constraints, but it can be approximated by a piecewise affine linear function. This approximation of a nonlinear function allows to solve the problem as a linear program.

Consider a general nonlinear function f(x) where x is within $[a_0, a_m]$ and a_k (k=0 … m) are the breakpoints of f(x) as it is shown in the Fig. 3.1 taken from [31]:

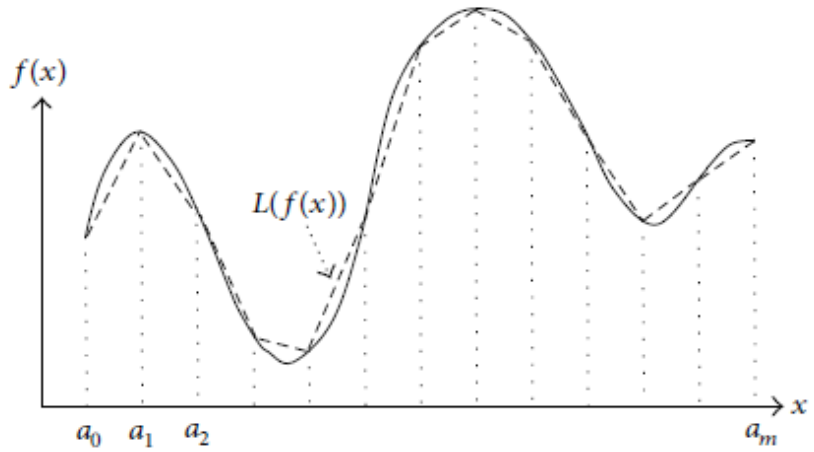

Fig. 3.1: piecewise linearization of non-linear function

In Fig. 3.1. f(x) is approximated with L(f(x)) which is a combination of m linear functions. There are several methods to perform this approximation, two of them will be discussed in this section. The first one uses $\log_2 m$ binary variables to perform the approximation and is indicated in [31] whereas the second method presented in [32] does not use binary variables but the function needs to be fully convex or concave

a) Method 1:

To describe this method, it is needed to introduce some notation first

Consider P=$\{0, 1, 2, \dots, m\}$ and p ∈ P, where m is the number of breakpoints. Then a function B is defined as:

$B(p) = (u_1, u_2, \dots, u_{\log_2 m}) \quad \forall u_k \in \{0, 1\}$, k = 1, 2, ..., $\log_2 m$

Also by definition:

B(p) and B(p+1) differ in at most one component $\forall p \in \{1, 2, \dots, m\}$

and $B(0) = B(1)$

Also consider the following sets:

$S^+(k) = \{p \mid \forall B(p) \wedge B(p+1)\ u_k = 1, p = (1, 2, \dots, m-1)\ \} \cup \{p \mid \forall B(p)\ u_k = 1, p = (0, m)\ \}$

$S^-(k) = \{p \mid \forall B(p) \wedge B(p+1)\ u_k = 0, p = (1, 2, \dots, m-1)\ \} \cup \{p \mid \forall B(p)\ u_k = 0, p = (0, m)\ \}$

Then, the approximation can be expressed mathematically as:

$$
\begin{aligned}
L\big(f(x)\big) &= \sum_{p=1}^{m} f(a_p) t_p \\
x &= \sum_{p=1}^{m} a_p t_p \\
&\sum_{p=0}^{m} t_p = 1 \\
&\sum_{p \in S^+(k)} t_p \leq u_k \\
&\sum_{p \in S^-(k)} t_p \leq 1 - u_k
\end{aligned}
\tag{3.19}
$$

where $t_p \in \mathbb{R}^+$

The previous equations can be described as:

- t_p can be seen as weights
- the sum of all weights is 1
- the linear combination of the weights and the breakpoints gives x
- the approximation of f(x) is the linear combination of the weights and f(a_p) which are known
- $\log_2 m$ binary variables are needed while in the previous method m binary variables were needed.
- $3+2 * \log_2 m$ constraints are needed in this case while in the previous case m+5 constraints were needed.

b) Method 2: No use of binary variables

The previous method made use of binary variables to approximate the nonlinear function. However, with this method it will be shown that binary variables are not needed if the nonlinear function is either fully convex or concave.

Considering a convex nonlinear function C(x) as shown in Fig. 3.2 obtained from [32]:

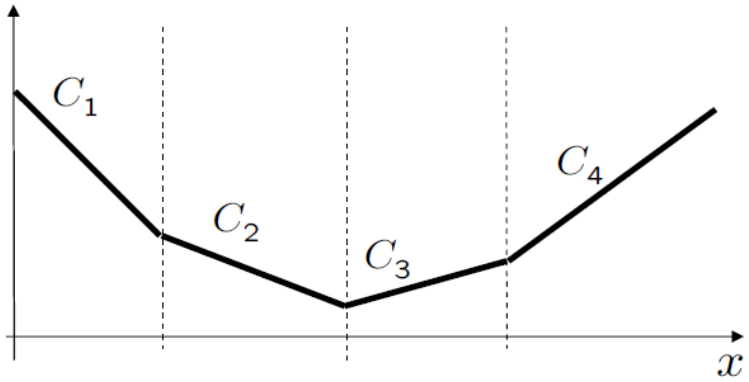

Fig. 3.2: Non-linear convex function

Then this function can be approximated without binary variables

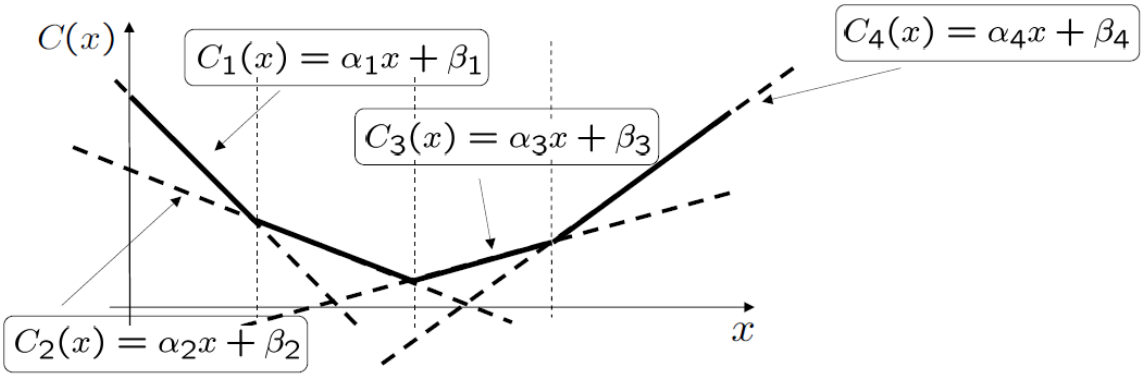

Fig. 3.3: Piecewise linear approximation of convex non-linear function

From Fig. 3.3 is clear to see that:

$$C_{(x)} = max\{C_{1(x)}, C_{2(x)}, C_{3(x)}, C_{4(x)}\} \tag{3.20}$$

where $C_{1(x)}, C_{2(x)}, C_{3(x)}, C_{4(x)}$ are linear functions of x

Considering a general nonlinear function that is fully convex and considering m breakpoints, equation(3.20) can be expressed as a linear program:

$$\begin{aligned} &min(s) \\ &subject\ to: \\ &C_{k(x)} \leq s \qquad \forall\, k = 1, 2, \dots, m \end{aligned} \tag{3.21}$$

For the concave case, the approach is similar; however, in this case the minimum is used instead of the maximum:

$$C_{(x)} = min\{C_{1(x)}, C_{2(x)}, C_{3(x)}, C_{4(x)}\} \tag{3.22}$$

Also, considering a general nonlinear function that is fully concave with m breakpoints, equation (3.22) can be expressed as a linear program:

$$\begin{aligned} &min(-s) \\ &subject\ to: \\ &C_{k(x)} \geq s \qquad \forall\, k = 1, 2, \dots, m \end{aligned} \tag{3.23}$$

Chapter 4 Model predictive control (MPC)

Model predictive control (MPC) [33] refers to a control technique that uses the mathematical model of a system to predict its future evolution and produces the control signal that generates a desired behaviour by solving an optimization problem at each time instant. Nowadays, it is a very popular technique due to the following reasons:

- It can manage multiple inputs and multiple outputs
- The produced control law is optimal with respect to a certain optimization objective
- Performance features can be included easily since they are expressed as numerical constraints in an optimization problem
- It can manage not only linear time-invariant systems but also those that are nonlinear and time-variant.
- It compensates unpredictable disturbances naturally

Although, it also has some drawbacks:

- It is not suitable for processes with fast dynamics since an optimization problem must be solved at each time instant, which is time consuming
- The performance of this algorithm is related with the accuracy of the model.

4.1 MPC formulation

At each time instant an optimization problem is formulated where the cost function penalizes undesired conditions. This cost function depends on the future evolution of the system which is predicted using the model of the system and the current known conditions. In the optimization problem equality and inequality constraints can be included accounting for performance features. The most used constraints are bounds

on the inputs, states, and outputs of the system. Then, after solving the optimization problem a sequence of control inputs is generated. However, models are not perfect and there are always unknown disturbances in the process therefore predictions will not match the real evolution of the system. For this reason, the receding horizon principle is used according to which only the first value of the control sequence is applied to the system and in the next time instant the evolution of the system is measured or estimated and then the optimization problem is run again. This methodology repeats at each instant. This is an open technique in the sense that the cost function and the constraints can be freely chosen in the design. The type of systems that can be controlled is also not restricted, so MPC can manage linear, nonlinear, continuous-time, discrete-time models. However, discrete-time models are mostly used because most of the times the controller consists of a digital computer that acquires and send signals at discrete time instants.

Considering the general discrete-time dynamics of a system:

$$x_{(k+1)} = f_{(x_{(k)},u_{(k)})} \tag{4.1}$$

where $x_{(k)} \in \mathbb{R}^n$ represents the n states of the system and $u_{(k)} \in \mathbb{R}^m$ represents the m inputs of the system

Then at each time instant k, the mathematical formulation of MPC is:

$$\min_{\{u_{(k/k)},u_{(k+1/k)},\dots u_{(k+N-1/k)}\}} \sum_{i=0}^{N-1} l(x_{(k+i/k)}, u_{(k+i/k)}) + l_N(x_{(k+N/k)}) \tag{4.2}$$

subject to:

$$x_{(k+i+1/k)} = f_{(x_{(k+i/k)},u_{(k+i/k)})} \qquad i = 0, \dots, N-1 \tag{4.3}$$

$$x_{(k/k)} = x_{(k)} \tag{4.4}$$

$$u_{(k+i/k)} \in S_u \qquad i = 0, \dots, N-1 \tag{4.5}$$

$$x_{(k+i/k)} \in S_x \qquad i = 1, \dots, N \tag{4.6}$$

where $x_{(k+i/k)}$ and $u_{(k+i/k)}$ represent the states at a future time k+i predicted at time k and $u_{(k+i/k)}$ is the control input at future time k+i predicted at time k

As it can be seen, equation v allows to predict the future by starting from an initial condition expressed by equation (4.4). This initial state can be obtained by

measurements or estimated by an external algorithm if the state is unmeasurable. Inequalities (4.5) and (4.6) can be included in the optimization problem to model operational restrictions. It is important to mention that equation (4.3) is not explicitly included as constraint in the optimization problem, instead it is implicitly embedded in the cost function and the constraints. The minimization problem is represented by equation (4.2) where a sequence of inputs is generated. Note that in the cost function the term $l_N(x_{(k+N/k)})$ is included to penalize a function depending on the final state. This is usually used to assure stability by penalizing divergence of the final state. Finally, only the first input of the sequence is applied to the system as shown in the following equation:

$$x_{(k+1)} = f_{(x_{(0)},u_{(k/k)})} \tag{4.7}$$

The dynamics of the system, the cost function and the constraints presented before have a general structure therefore a nonlinear optimization technique should be used to solve the optimization problem which may take long computation times. However, these times can be improved if the type of problem is restricted. In this thesis the problem is restricted to linear systems, linear cost function, linear constraints, and continuous and discrete decision variables.

4.2 MPC of linear systems

Consider the following linear time-invariant system

$$x_{(k+1)} = Ax_{(k)} + Bu_{(k)} \tag{4.8}$$

where $x \in \mathbb{R}^n$, $u \in \mathbb{R}^m$

And the following cost function:

$$J_{(x_0,k)} = \sum_{i=1}^{N-1} \left\| Qx_{(k+i/k)} \right\|_\infty + \sum_{i=0}^{N-1} \left\| Ru_{(k+i/k)} \right\|_\infty + \left\| Px_{(k+N/k)} \right\|_\infty \tag{4.9}$$

where the cost function is defined for a certain time instant k, and the weighting matrices Q, R and P can have arbitrary number of rows, so $Q \in \mathbb{R}^{a\,x\,n}$, $R \in \mathbb{R}^{b\,x\,m}$, $P \in \mathbb{R}^{c\,x\,n}$

The cost function $J_{(x_0,k)}$can be expressed linearly by using auxiliary variables as follows:

$$J_{(x_0,k)} = \sum_{i=1}^{N-1} \varepsilon_{(i)}^{x} + \sum_{i=0}^{N-1} \varepsilon_{(i)}^{u} + \varepsilon_{(N)}^{x} \tag{4.10}$$

where:

$$\underbrace{[-1 \dots -1]}_{a}^{T} \varepsilon_{(i)}^{x} \leq Qx_{(k+i/k)} \leq \underbrace{[1 \dots 1]}_{a}^{T} \varepsilon_{(i)}^{x} \qquad i = 1, 2, \dots, N-1 \tag{4.11}$$

$$\underbrace{[-1 \dots -1]}_{\mathrm{b}}^{\mathrm{T}} \varepsilon_{(\mathrm{i})}^{\mathrm{u}} \leq \mathrm{R}u_{(\mathrm{k+i/k})} \leq \underbrace{[1 \dots 1]}_{\mathrm{b}}^{\mathrm{T}} \varepsilon_{(\mathrm{i})}^{\mathrm{u}} \qquad i = 0, 1, \dots, N-1 \tag{4.12}$$

$$\underbrace{[-1 \dots -1]}_{c}^{T} \varepsilon_{(N)}^{\mathrm{x}} \leq P\mathrm{x}_{(k+\mathrm{N/k})} \leq \underbrace{[1 \dots 1]}_{b}^{T} \varepsilon_{(N)}^{\mathrm{x}} \tag{4.13}$$

So the optimal control problem with infinity norm at each time instant k is:

$$\min_{U,\varepsilon_x,\varepsilon_u} J_{(x_0,k,U)} = \min_{U,\varepsilon} \left(\sum_{i=1}^{N-1} \varepsilon_{(i)}^{x} + \sum_{i=0}^{N-1} \varepsilon_{(i)}^{u} + \varepsilon_{(N)}^{x} \right) \tag{4.14}$$

subject to:

$$\mathrm{x}_{(\mathrm{k+i+1/k})} = \mathrm{A}\mathrm{x}_{(\mathrm{k+i/k})} + \mathrm{B}\mathrm{u}_{(\mathrm{k+i/k})}$$

$$\mathrm{x}_{(\mathrm{k/k})} = \mathrm{x}_{(0)}$$

$$\underbrace{[-1 \dots -1]}_{a} \varepsilon_{(i)}^{x} \leq Qx_{(k+i/k)} \leq \underbrace{[1 \dots 1]}_{a} \varepsilon_{(i)}^{x} \qquad i = 1, 2, \dots, N-1$$

$$\underbrace{[-1 \dots -1]}_{\mathrm{b}} \varepsilon_{(\mathrm{i})}^{\mathrm{u}} \leq \mathrm{R}u_{(\mathrm{k+i/k})} \leq \underbrace{[1 \dots 1]}_{\mathrm{b}} \varepsilon_{(\mathrm{i})}^{\mathrm{u}} \qquad \mathrm{i} = 0,1, \dots, \mathrm{N}-1$$

$$\underbrace{[-1 \dots -1]}_{\mathrm{c}} \varepsilon_{(\mathrm{N})}^{\mathrm{x}} \leq \mathrm{P}\mathrm{x}_{(\mathrm{k+N/k})} \leq \underbrace{[1 \dots 1]}_{\mathrm{c}} \varepsilon_{(\mathrm{N})}^{\mathrm{x}}$$

where $\mathrm{U} = [u_{(k/k)}, u_{(k+1/k)}, \ \dots \ u_{(k+N-1/k)}]$
and $\varepsilon_{\mathrm{x}} = [\varepsilon_{(1)}^{x}, \varepsilon_{(2)}^{x}, \dots, \varepsilon_{(\mathrm{N})}^{x}], \varepsilon_{\mathrm{u}} = [\varepsilon_{(0)}^{u}, \varepsilon_{(1)}^{u}, \varepsilon_{(2)}^{u}, \dots, \varepsilon_{(\mathrm{N}-1)}^{u}]$

In the case of a cost defined as shown below:

$$J_{(x_0,k,U)} = \sum_{i=1}^{N-1} \left\| Q x_{(k+i/k)} \right\|_1 + \sum_{i=0}^{N-1} \left\| R u_{(k+i/k)} \right\|_1 + \left\| P x_{(k+N/k)} \right\|_1 \tag{4.15}$$

The cost function $J_{(x_0,k,U)}$ can be expressed linearly by using auxiliary variables:

$$J_{(x_0,k,U)} = \sum_{i=1}^{N-1} \sum_{j=1}^{a} \varepsilon_{(i)}^{x,j} + \sum_{i=0}^{N-1} \sum_{j=1}^{b} \varepsilon_{(i)}^{u,j} + \sum_{j=1}^{c} \varepsilon_{(N)}^{x,j} \tag{4.16}$$

where:

$$-\varepsilon_{(i)}^{x,j} \le Q^j x_{(i)} \le \varepsilon_{(i)}^{x,j} \qquad \begin{matrix} i = 1,2,\dots,N-1 \\ j = 1,2,\dots,a \end{matrix} \tag{4.17}$$

$$-\varepsilon_{(i)}^{u,i} \le R^j u_{(i)} \le \varepsilon_{(i)}^{u,j} \qquad \begin{matrix} i = 0,1,\dots,N-1 \\ j = 1,2,\dots,b \end{matrix} \tag{4.18}$$

$$-\varepsilon_{(N)}^{x} \le P^j x_{(k)} \le \varepsilon_{(N)}^{x} \tag{4.19}$$

where the suffix j represents the j-th row of a matrix

So the optimal control problem with 1-norm at each time instant k is:

$$\min_{U,\varepsilon_x,\varepsilon_u} J_{(x_0,k,U)} = \sum_{i=1}^{N-1} \sum_{j=1}^{a} \varepsilon_{(i)}^{x,j} + \sum_{i=0}^{N-1} \sum_{j=1}^{b} \varepsilon_{(i)}^{u,j} + \sum_{j=1}^{c} \varepsilon_{(N)}^{x,j} \tag{4.20}$$

subject to:

$$x_{(k+i+1/k)} = Ax_{(k+i/k)} + Bu_{(k+i/k)}$$
$$x_{(k/k)} = x_{(0)}$$

$$-\varepsilon_{(i)}^{x,j} \le Q^j x_{(k+i/k)} \le \varepsilon_{(k)}^{x,j} \qquad \begin{matrix} i = 1,2,\dots,N-1 \\ j = 1,2,\dots,a \end{matrix}$$

$$-\varepsilon_{(i)}^{u,j} \le R^j u_{(k+i/k)} \le \varepsilon_{(k)}^{x,j} \qquad \begin{matrix} i = 0,1,\dots,N-1 \\ j = 1,2,\dots,b \end{matrix}$$

$$-\varepsilon_{(N)}^{x,j} \leq P^j x_{(k+N/k)} \leq \varepsilon_{(N)}^{x,j} \qquad j = 1,2,\dots,c$$

where $U = [u_{(k/k)}, u_{(k+1/k)}, \dots u_{(k+N-1/k)}]$

$\varepsilon_x = [\varepsilon_{(1)}^{x,1}, \varepsilon_{(1)}^{x,2}, \dots, \varepsilon_{(1)}^{x,a}, \varepsilon_{(2)}^{x,1}, \varepsilon_{(2)}^{x,2}, \dots, \varepsilon_{(2)}^{x,a}, \dots, \varepsilon_{(N-1)}^{x,1}, \varepsilon_{(N-1)}^{x,2}, \dots, \varepsilon_{(N-1)}^{x,a}, \varepsilon_{(N)}^{x,1}, \varepsilon_{(N)}^{x,2}, \dots, \varepsilon_{(N)}^{x,c}]$,

and $\varepsilon_u = [\varepsilon_{(0)}^{u,1}, \varepsilon_{(0)}^{u,2}, \dots, \varepsilon_{(0)}^{u,b}, \varepsilon_{(1)}^{u,1}, \varepsilon_{(1)}^{u,2}, \dots, \varepsilon_{(1)}^{u,b}, \dots, \varepsilon_{(N-1)}^{u,1}, \varepsilon_{(N-1)}^{u,2}, \dots, \varepsilon_{(N-1)}^{u,b}]$

The first cost function may be seen as a function with 1-norm over time and ∞-norm over space whereas the second case represents a function with 1-norm over time and space. Any other combination of 1-norm and ∞-norm can be represented as a linear program following the procedures presented.

The previous approaches allow to include the cost function in a LP program, however, note that in both cases the optimal control problem is restricted to $x_{(k+i+1/k)} = Ax_{(k+i/k)} + Bu_{(k+i/k)}$. The following procedure allows to embed this restriction into a linear program

Consider the initial linear time-invariant system

$$x_{(k+1)} = Ax_{(k)} + Bu_{(k)} \tag{4.21}$$

where $x \in \mathbb{R}^n$, $u \in \mathbb{R}^m$

From the previous equation, the state at time i can be determined as:

$$x_{(k+i/k)} = A^i x_{(k)} + \sum_{j=0}^{i-1} A^{i-j-1} B u_{(k+j/k)} \qquad \forall i = 1,2,\dots,N \tag{4.22}$$

where N is the prediction horizon

In a compact form the previous equation can be expressed as:

$$\underbrace{\begin{bmatrix} x_{(k+1/k)} \\ x_{(k+2/k)} \\ \cdots \\ x_{(k+N-1/k)} \\ x_{(k+N/k)} \end{bmatrix}}_{X_{(k)}} = \underbrace{\begin{bmatrix} A^1 \\ A^2 \\ \cdots \\ A^{N-1} \\ A^N \end{bmatrix}}_{A_x} x_{(k/k)} + \underbrace{\begin{bmatrix} B & 0 & 0 & \cdots & 0 & 0 \\ AB & B & 0 & \cdots & 0 & 0 \\ \cdots & \cdots & \cdots & \cdots & \cdots & \cdots \\ A^{N-2}B & A^{N-3}B & A^{N-4}B & \cdots & AB & A^{N-2}B \\ A^{N-1}B & A^{N-1}B & A^{N-1}B & \cdots & A^{N-1}B & A^{N-1}B \end{bmatrix}}_{B_x} \underbrace{\begin{bmatrix} u_{(k/k)} \\ u_{(k+1/k)} \\ \cdots \\ u_{(k+N-2/k)} \\ u_{(k+N-1/k)} \end{bmatrix}}_{U_{(k)}} \tag{4.23}$$

Using this expression, the optimal control problem for both costs at each time instant k, is:

$$\min_{U,\varepsilon_x,\varepsilon_u} J_{(x_0,k,U)} = \underbrace{[1,1,\ldots,1]}_{n_{\varepsilon x}+n_{\varepsilon u}} \begin{bmatrix} \varepsilon_x \\ \varepsilon_u \end{bmatrix} \tag{4.24}$$

subject to:

$$x_{(k/k)} = x_{(0)}$$

$$-\varepsilon_x \leq \begin{bmatrix} Q \\ P \end{bmatrix} X_{(k)} \leq \varepsilon_x$$

$$-\varepsilon_u \leq RU_{(k)} \leq \varepsilon_u$$

where $n_{\varepsilon x}$ and $n_{\varepsilon u}$ are the lengths of the vector that contain the auxiliary variables

Contribution

Chapter 5 System description and control strategy

In this thesis an MPC strategy is used to manage a microgrid by controlling its storage system and its interaction with the utility grid. The management of the microgrid aims to achieve different objectives. On the one hand, it is desired to minimize the energy exchange with the microgrid and thus reduce the stress in the utility grid. This objective can be considered as a technical benefit because energy losses are reduced due to fewer power flows in the distribution grid. On the other hand, it is also desired to obtain economic benefits with the operation of the microgrid. This objective is desired by the owner of the microgrid. Both objectives cannot be achieved at the same time because the first one minimizes the acquisition of energy from the grid and the sale of energy to the grid; whereas to obtain economic benefits the import of energy is minimized but the export of energy is encouraged. Additionally, photovoltaic generation and electrical demand are largely variable which has negative impact in the grid, so their variability can be absorbed by the storage system and thus the interaction with the grid is less variable. This objective can be achieved together with other goals previously described. This thesis is based on simulations and two different microgrids are studied where the main difference relies on the storage system used. The first case considers a regenerative hydrogen fuel cell as storage whereas the second case uses a battery and both systems have equivalent storage capacity. In this chapter the microgrids components and the management strategy are described.

5.1 Systems description

The main difference in both microgrids considered in this thesis is the type of storage. Apart from that, both systems consider non-controllable loads and photovoltaic generation which is also non-controllable. So, the balance of energy is achieved by controlling the storage and deciding the amount of energy exchanged with the grid.

5.1.1 Microgrid with regenerative hydrogen fuel cell

Fig.5.1 depicts the microgrid that uses hydrogen to store energy.

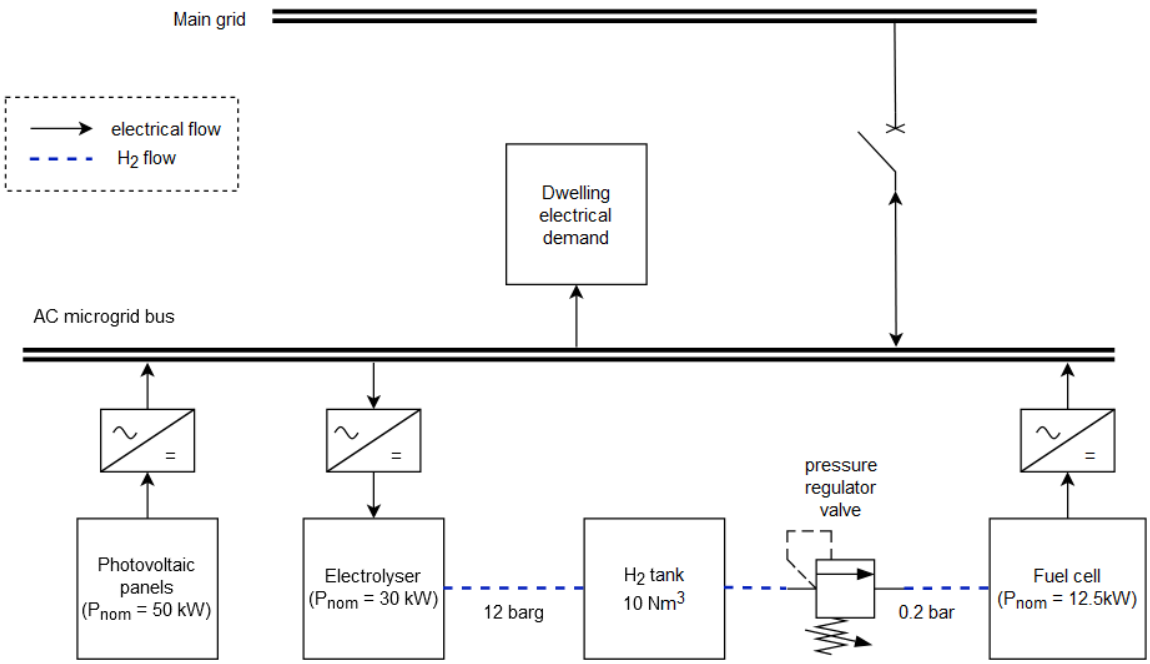

Fig. 5.1: Scheme of microgrid with RHFC considered in the simulations

The electrolyser produces H_2 at 12 barg which is then delivered to the tank without further compression. The tank can store 10 Nm^3 of hydrogen (equivalent to 0.9 kg). Since the pressure of the tank depends on the amount of hydrogen inside, a pressure regulator valve at the output supplies hydrogen at constant pressure to the fuel cell. The PV panels, the electrolyser and fuel cell work with DC power so AC-DC converters are used to connect them to the microgrid bus. There is a circuit breaker that connects the microgrid with the utility grid to buy or sell energy. The power balance is achieved by controlling the electrolyser and the fuel cell since the PV panels and the electrical demand are uncontrollable. The control system should assure that the electrolyser and fuel cell do not operate simultaneously since it would imply losses of energy.

5.1.2 Microgrid with battery

The microgrid with a battery as storage system is illustrated in Fig. 5.2:

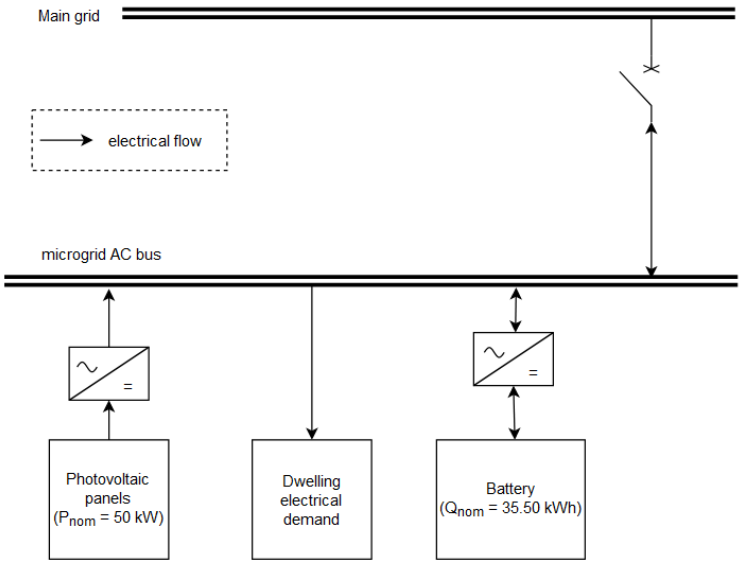

Fig. 5.2: Scheme of microgrid with battery considered in the simulations

As mentioned before, this microgrid is similar to the one previous presented, however, in this case a battery is considered. To compare the performance of both systems the capacity of the storage systems is chosen to be similar, in fact 10 Nm^3 is approximately equivalent to 35.50 kWh considering the HHV of hydrogen [34].

5.2 Control architecture

The control system proposed in this work consists in a prior planification and a MPC controller to schedule the operation of the microgrid. Due to the computational load of MPC this control system does not act directly on the components of the microgrid but give power references to the local controllers which are simpler and operate in a faster timeframe. The following graph illustrates this structure:

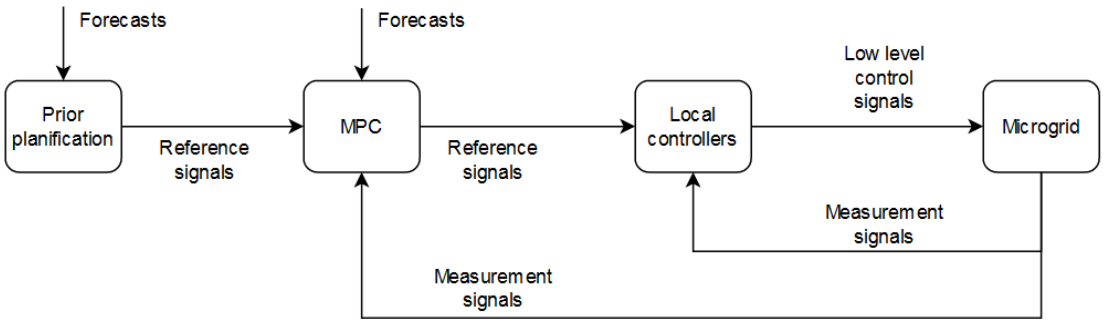

Fig. 5.3: General control architecture

The prior planification consists of an open loop optimization problem and uses forecasts of photovoltaic generation and demand to estimate the optimal values of exchanged power with the grid and profile of energy in the storage for the next day. The main objective of this optimization routine is to obtain a profile of the energy level in the storage and a profile of power exchanged with the grid. The first output should consider similar levels of energy at the beginning and at the end of the day. Whereas the second output is used to emulate what occurs in a conventional grid where power exchanged with the grid is declared priorly to the grid operator. These signals are sent as references to be followed by the MPC controller. Since forecasts and the model of the system for the optimization are never perfect the MPC controller compensate these errors by receiving feedback at each time instant. The open loop prior scheduling and the optimization problems of MPC consist of mixed integer linear programs. For the simulations in this thesis, the models used in the optimization problems and the models that represent the real equipment are slightly different because the models are simplified when they are used in optimization. This consideration is reasonable because mathematical models never match exactly reality so in this way this mismatch is simulated. Furthermore, is better for optimization to use simplified models to cope with high computational loads.

5.2.1 Hydrogen based microgrid

The control architecture for the microgrid based on hydrogen is displayed in Fig. 5.4:

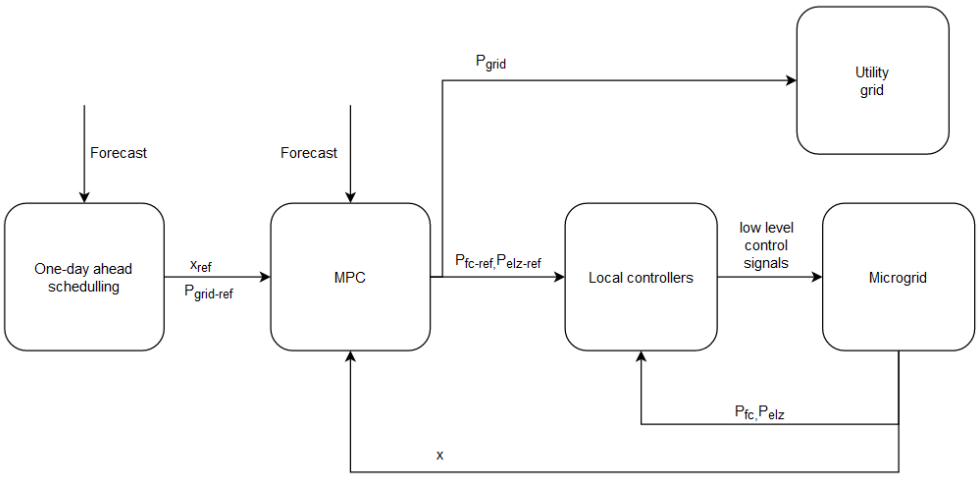

Fig. 5.4: Control architecture for system with storage based on hydrogen

The optimal control inputs produced by MPC are the power references to the fuel cell, electrolyser and power exchanged with the grid whereas the feedback signal is the amount of hydrogen in the tank.

For the electrolyser, the dynamics of the model is given by the variations of temperature, so the model used in optimization assumes constant temperature

whereas the real device is represented by the complete model which considers variations of temperature. For the fuel cell, the complete model is non-linear and static, so the model used in the optimization is a linearization of the complete model.

5.2.2 Battery based microgrid

The control architecture for the microgrid based on hydrogen is displayed in Fig. 5.5:

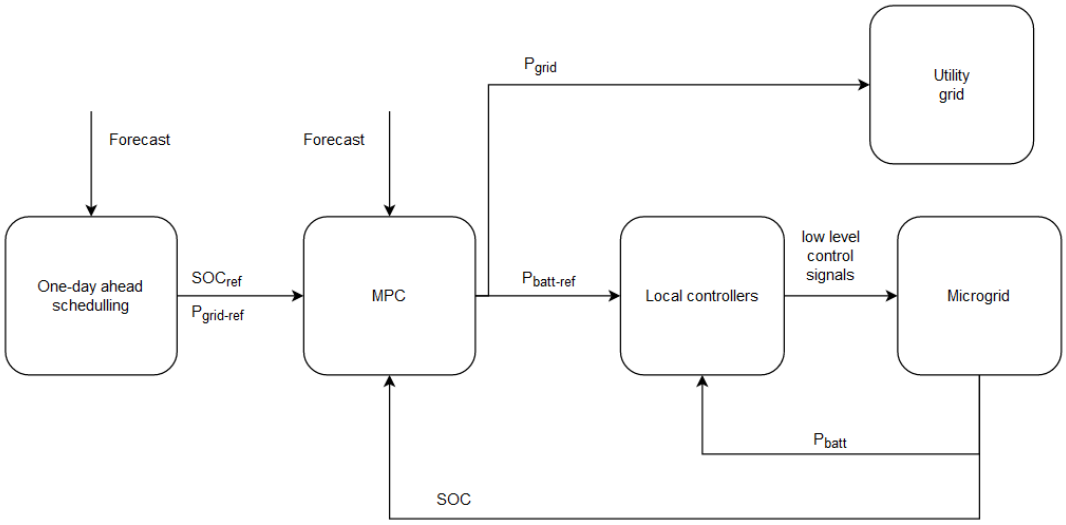

Fig. 5.5: Control architecture for system with storage based on batteries

The optimal control inputs produced by MPC are the power reference to the battery and the power exchanged with the grid, whereas the feedback signal is the SOC of the battery. The power exchanged with the battery can take positive values when charging and negative values when discharging differently from the case of storage with hydrogen where the references towards the electrolyser and fuel can only take positive values. Regarding the mismatch between models, in this case it is given by slightly different charge and discharge efficiencies.

5.3 System modelling for RHFC

5.3.1 Alkaline electrolyser

According to equation (2.8) presented in chapter 2, a voltage should be applied to let electrolysis happen. Also, the production of H_2 is directly proportional to the current fed to the electrolyser. These equations show that voltage changes depending on the current therefore the power demand also depends on the current. Since the electrolyser operates DC electricity an AC-DC converter is usually used as interface between the electrolyser and the bus. Note that production of hydrogen, voltage and

power depend on the current, so a local controller should be able to control the converter to obtain a desired current at the input of electrolyser. In the system considered in this thesis, the MPC controller sends power setpoints to the electrolyser system, so this local controller should receive these setpoints and control the converter as it is shown in Fig. 5.6:

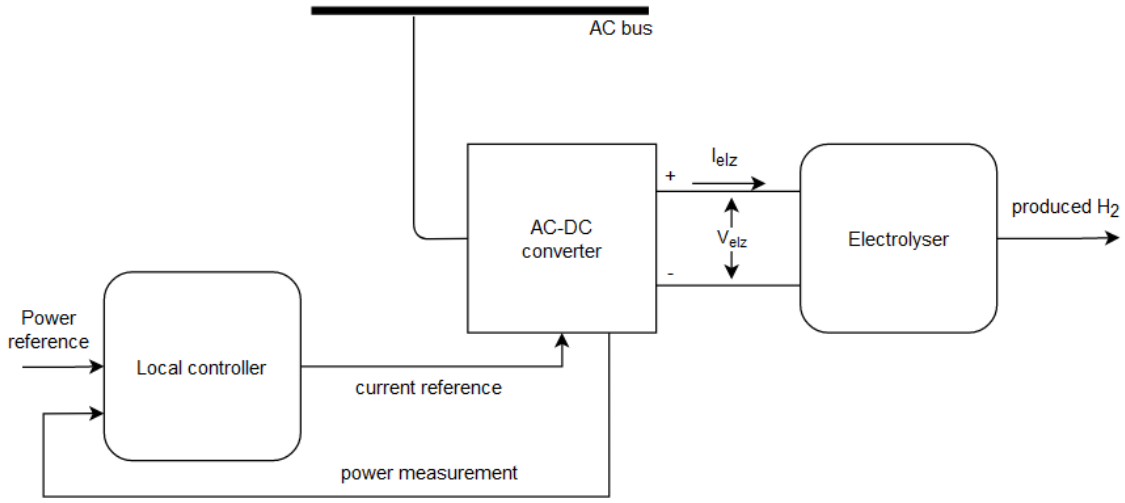

Fig. 5.6: Scheme of local operation of an electrolyser

The equations presented in chapter 2 allow to develop a model as shown in Fig. 5.7:

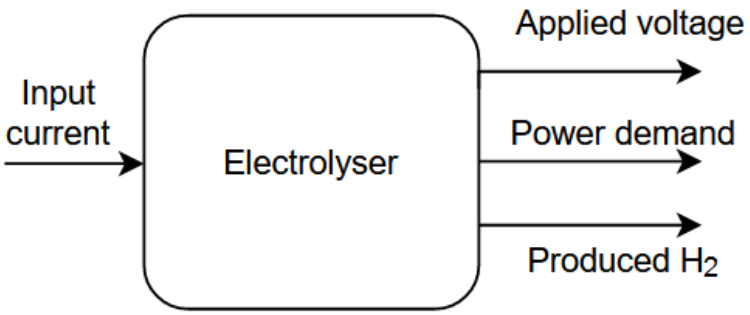

Fig. 5.7: Scheme of inputs and output of the electrolyser model

The electrolyser analysed in [11] and the empirical parameters presented there, will be used for the simulations in this thesis. Table 2 contains the technical specifications of this electrolyser:

Characteristic	Value	Unit
Rated power	30	kW
Voltage operation range	240 - 420	V
Current operation range	25 – 71	A
Operation range	20 - 100	%
Rated pressure	12	Barg
Rated operation temperature	80	°C
Rated production of hydrogen (at 80°C)	5.33	Nm^3/h
	88.83	slpm
Number of cells	180	-
Active cell area	0.06	m^2

Table 2: Technical specification of the alkaline electrolyser

And the empirical parameters are the following:

Parameter	Value
r_0	$0.004747\ VA^{-1}m^{-2}$
r_1	$-1.367 \cdot 10^{-5}\ VA^{-1}{}^{\circ}C^{-1}m^{-2}$
s	0.35 V
t_0	$49.31\ A^{-1}m^{-2}$
t_1	$-0.3065\ A^{-1}{}^{\circ}C^{-1}m^{-2}$
t_2	$0.0004782\ A^{-1}{}^{\circ}C^{-2}m^{-2}$
f_1	$20000\ A^2m^{-4}$
f_2	0.93
C_T	$1.6824 \cdot 10^5\ JK^{-1}$
R_T	$0.4441\ WK^{-1}$
h_n	$6\ WK^{-1}$
h_c	$30\ WK^{-1}$

Table 3: Empirical parameters considered in the electrolyser model

It is assumed that the converter provides the current requested by the controller. Since the local controller transforms the power setpoints into current references the relationship between power and current is analysed. For this purpose, the following

graphs are obtained considering the operation of the electrolyser at rated temperature, i.e. 80°C

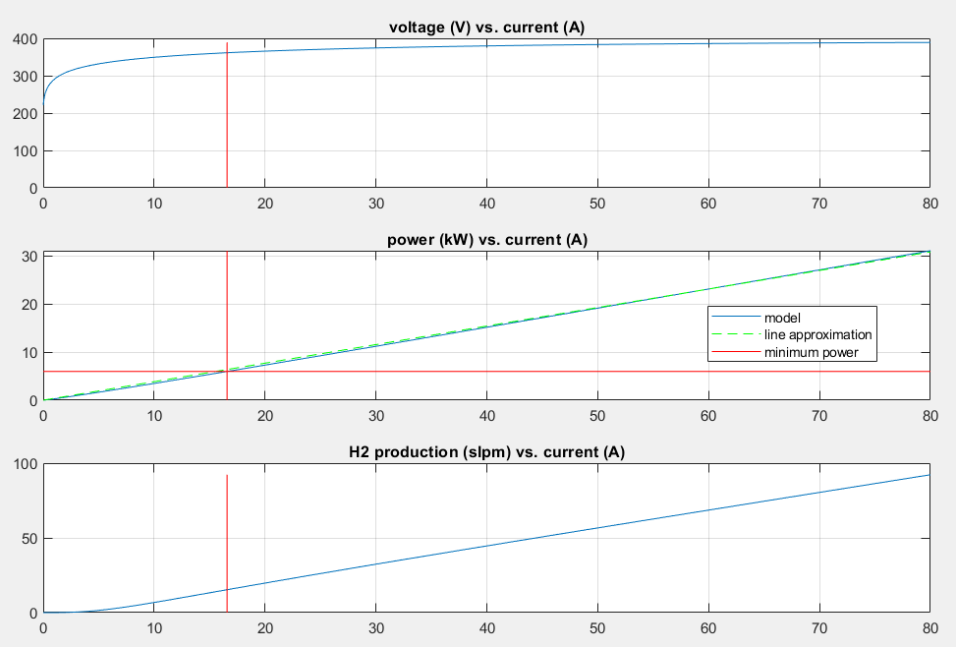

Fig. 5.8: Simulation of the fuel cell model

According to the specifications, the electrolyser should operate with power higher than 20% of the nominal power, i.e. 6kW. It can be seen that above this value the relationship between power and current it is almost linear. The following graphs show this relationship at different temperatures.

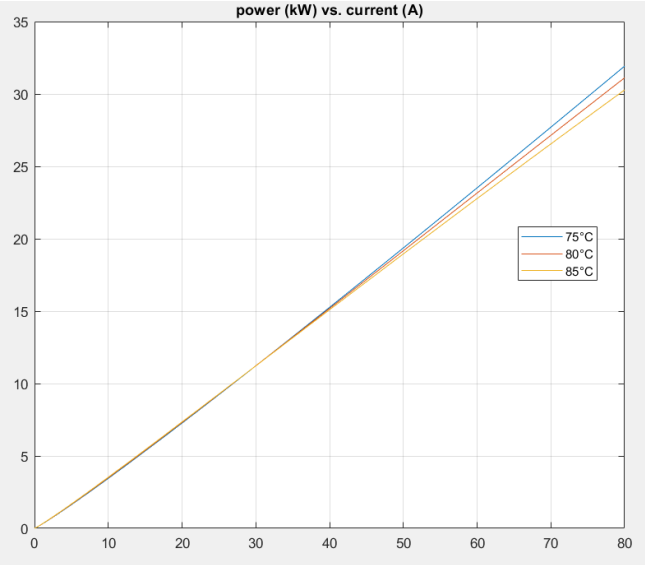

Fig. 5.9: Variations of power due to changes of temperature - electrolyser

Since power is affected by both current and temperature, for simplicity in this work the local controller consists of a lookup table with power reference and temperature as inputs and current as output. This current is then applied to the model of the electrolyser. The table below describes the values of the lookup table:

	T=75°C	T=75°C	T=75°C
Power =0 kW	0 A	0 A	0 A
Power =10 kW	26.9870 A	26.9069 A	26.9069 A
Power =15 kW	36.3994 A	39.5596 A	39.7998 A
Power =20 kW	51.5716 A	52.1321 A	52.7728 A
Power =25 kW	63.5035 A	64.6246 A	65.9059 A
Power =30 kW	75.4354 A	77.1972 A	79.2793 A

Table 4: Lookup table to transform power references into current for the electrolyser

The complete model that represent the real electrolyser is shown in the following scheme:

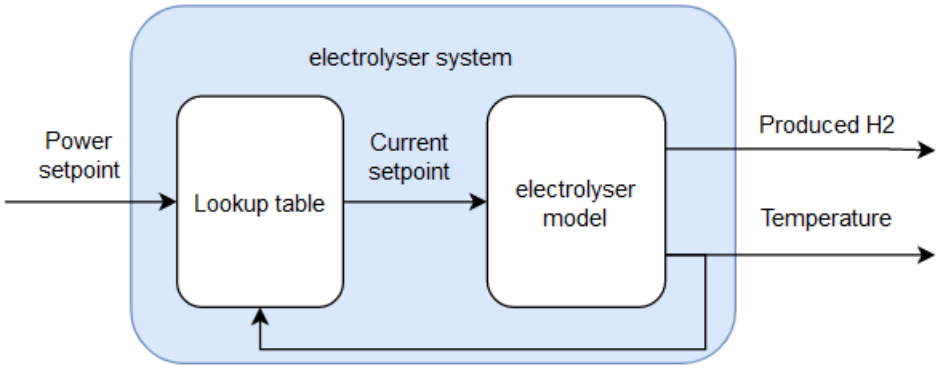

Fig. 5.10: Scheme of the complete model for the electrolyser

However, for the model user by the optimization routines further simplifications can be made. In fact, it is show in equation (2.10) ($\dot{m}_{H_2} = \eta_f \frac{n_c I}{zF}$) that the production of H_2 is dependent on current, but also on the Faraday efficiency η_f. The following graph depicts the influence of current on this efficiency at 80°C:

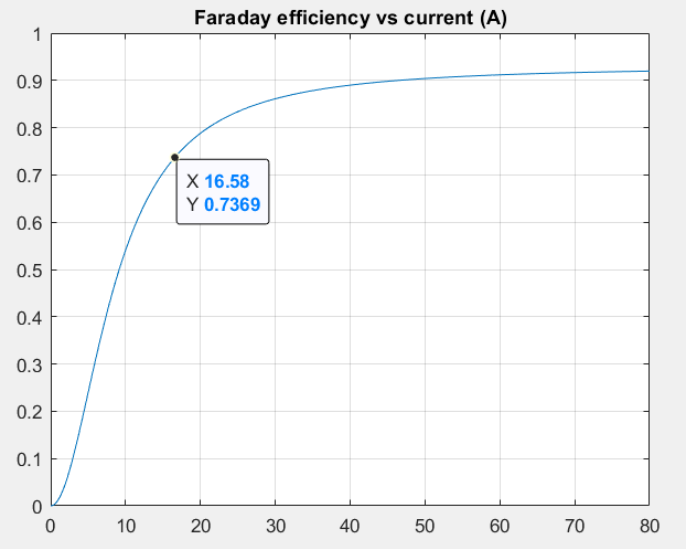

Fig. 5.11: Relationship between Faraday efficiency and current for the electrolyser

It can be seen that with values of current higher than the minimum limit the efficiency does not change too much. Hence the main variable that influences on the production of H_2 is the current. As previously seen, the relation between current and power is almost linear, therefore the relationship between power and production of H_2 presents a similar behaviour:

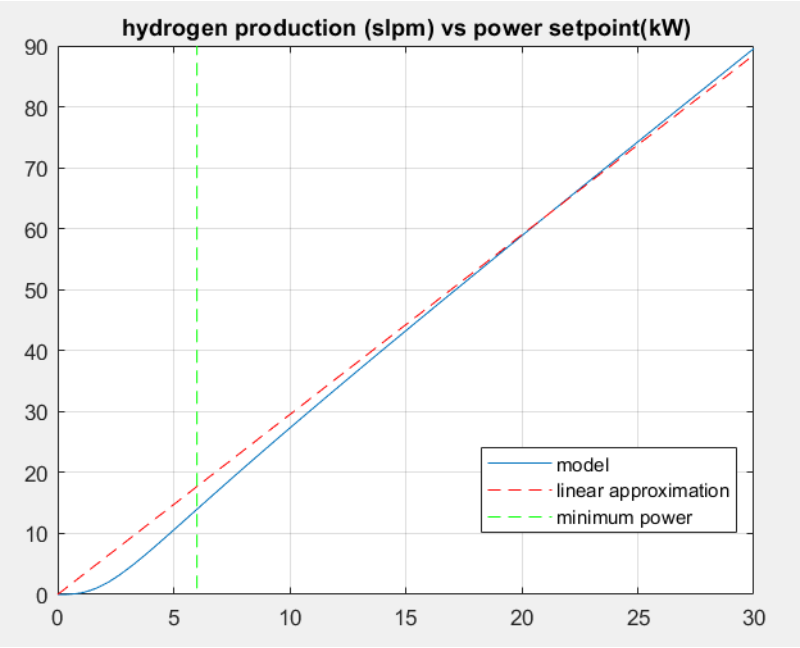

Fig. 5.12: Linear relationship between power setpoints and production of hydrogen

The approximation is not good at low values of power due to the efficiency term but at high values the approximation is better. Since the electrolyser should operate above

6kW the relation between power and production of hydrogen can be approximated linearly. The model of the electrolyser system used for the optimization problems is:

$$\dot{m}_{ely\,(k)} = P_{ely\,(k)} * 2.95 \tag{5.1}$$

5.3.2 PEM fuel cell

The following diagram depicts the functioning of a PEM fuel cell:

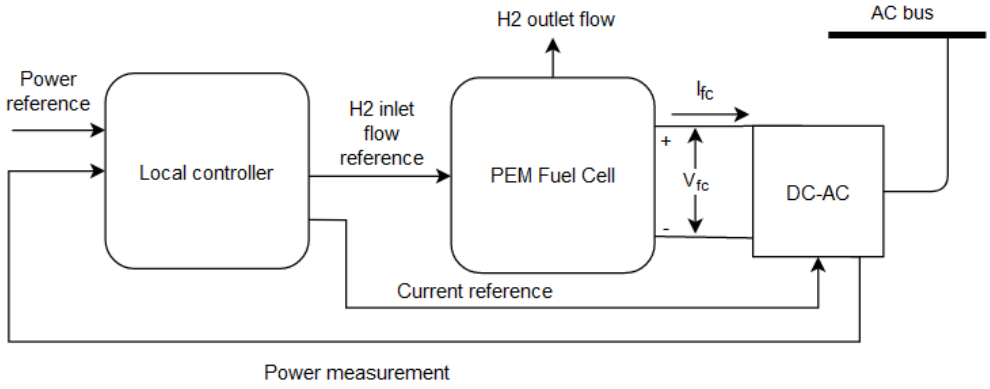

Fig. 5.13: Scheme of local operation of a PEM fuel cell

There is an inlet flow of H_2 that produces a voltage at the terminals of the fuel cell and when a load is connected to the terminals then current flows through the fuel cell. Due to Faraday's law, the consumption of H_2 depends on the flow of current, so the consumption of hydrogen depends on the power consumed by the load. Note that the consumption of hydrogen is independent of the inlet flow, so what usually happens is that not all hydrogen fed is used and there is an outlet flow of unutilized hydrogen. It is common practice to reuse the unutilized hydrogen by making it recirculate and to avoid large amount of unutilized hydrogen, the inlet flow is usually regulated depending on the current. For simplicity, in thesis is assumed that the utilization rate is constant. On the other hand, the power output of the fuel cell is DC, so a DC-AC converter is used to connect the fuel cell to the AC bus of the microgrid. As mentioned above, the power output of the fuel cell depends on the load connected to it, so to regulate the power of the fuel cell the current that passes through the converter is controlled. Therefore, the local controller should output a current reference to control the power of the fuel cell and an inlet flow reference to maintain constant the utilization percentage.

The model presented in chapter 2 allow to compute voltage, power and consumed flow of hydrogen given the current the circulates through the fuel cell as represented by the diagram below:

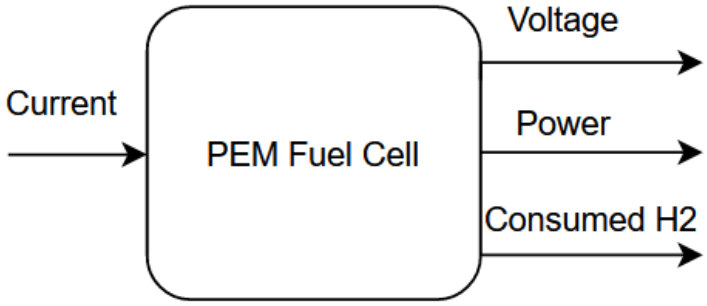

Fig. 5.14: Input and outputs of the PEM fuel cell model

This model is validated using experimental data provided by a third party which performed an experiment in a laboratory [35]. The validation consists of using the same current used in the experiment and compare the outputs of the model against the measurements of the experiment. The PEM fuel cell used in the experiments has the following specifications:

Characteristic	Value	Unit
Power	12.5	kW
Nominal voltage	83.7	V
Nominal current	150	A
Maximum current	170	A
Number of cells	110	-

Table 5: Technical specification of PEM fuel cell

The experiment was carried out under the follow conditions:

Characteristic	Value	Unit
Pressure of H2	0.2	Bar
Pressure of O2	1	Bar
Concentration of H2	59	%
Concentration of O2	40	%
Temperature of experiment	60	°C
Utilization rate	95	%

Table 6: Conditions of the experiment for validation of the PEM fuel cell model

The empirical parameters used in the model where found in the literature [36], and are presented in the table below:

Parameter	Value
ξ_1	-0.948
ξ_3	$7.22 \cdot 10^{-5}$
ξ_4	$-1.0615 \cdot 10^{-4}$
λ	14
B	0.016
R_c	0.0003

Table 7: Empirical parameters considered in the PEM fuel cell model

For the experiment, the current shown in Fig. 5.15 was used:

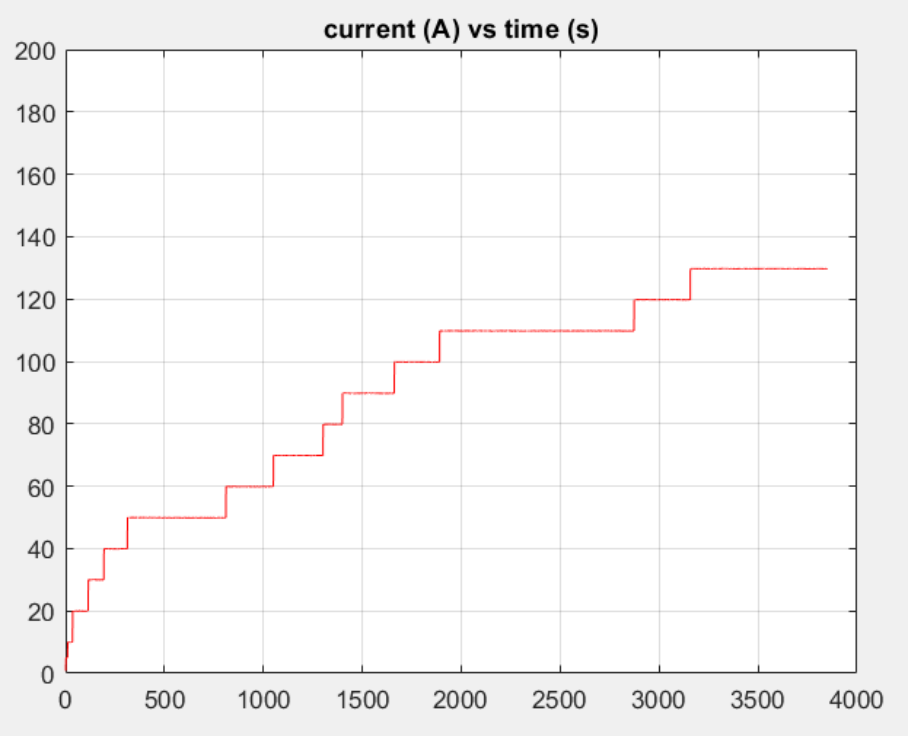

Fig. 5.15: Current input for PEM fuel cell model validation

And the results are the following:

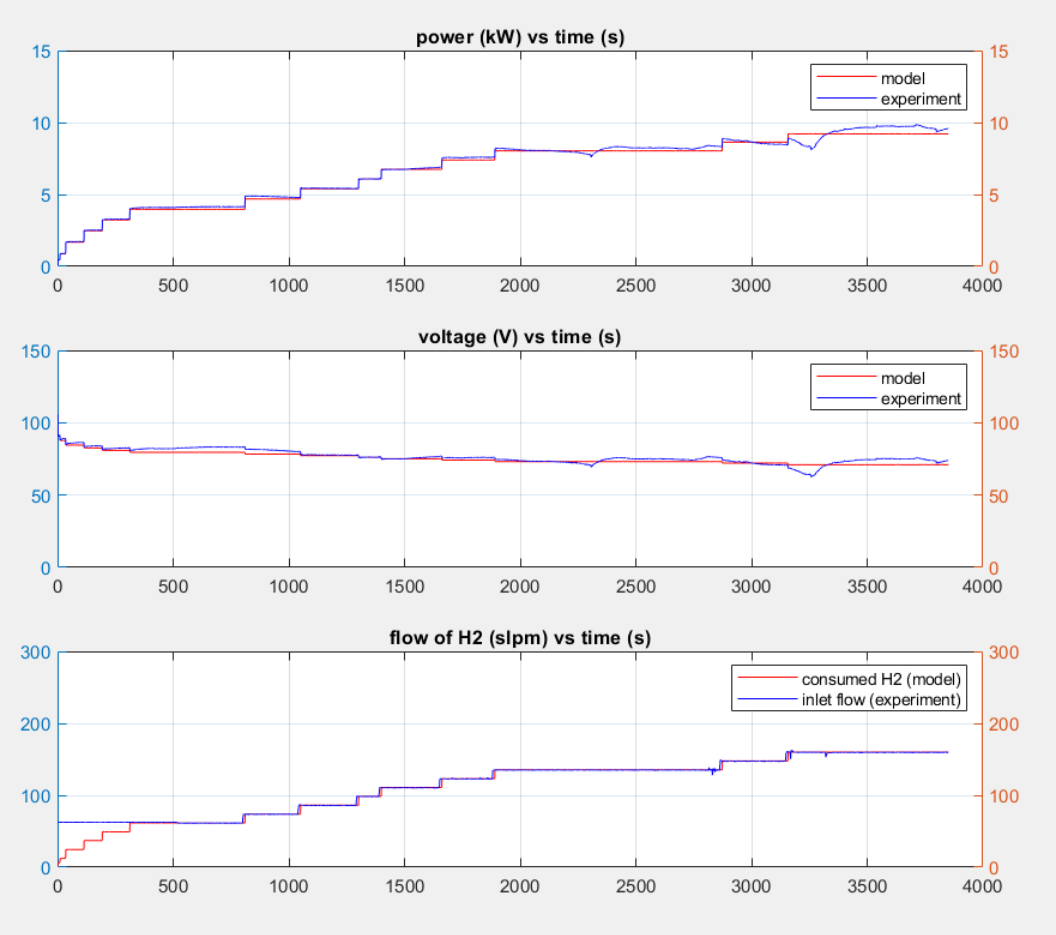

Fig. 5.16: Result of PEM fuel cell model validation

As it can be seen, the outputs of the model match the data obtained from experiments. At the beginning of the experiment there is a mismatch between the flow of the experiment and the model. This difference is because there is a flow of hydrogen, but the load was not consuming energy so there was an outlet flow of hydrogen not used.

Note that the experiment was carried out at certain conditions of pressure and concentration of the gases. However, these conditions change during the operation of the fuel cell as part of the storage system. In fact, in this case hydrogen is obtained from the tank which is considered pure as it is produced by the electrolyser whereas in the experiment the concentration of hydrogen was of 59%. Henceforth, the same conditions of the experiment will be considered except by the fact that the fuel cell uses pure hydrogen, i.e. concentration of hydrogen is 100%.

The following graph illustrates the dependence of power as function of current:

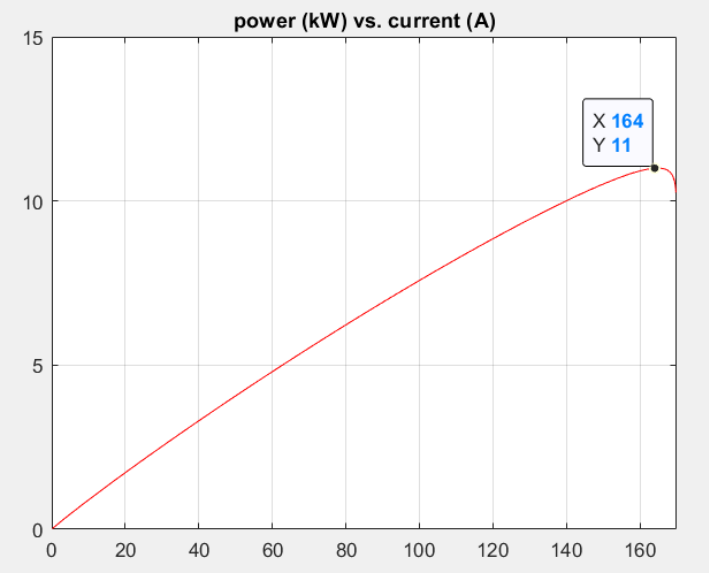

Fig. 5.17: relation between power and current - PEM fuel cell model

It can be seen that an increase of the current corresponds to a continuous increase of power until around 164 A where there is an abrupt decrease of power. This represents the maximum power that can be delivered by the fuel cell. In this thesis power values above 11kW are avoided to exploit the linear behaviour. The change of power near the limit is because the current gets closer to its maximum admissible value what causes an abrupt change of concentration voltage which in turn reduces the total voltage of the cell. Fig 5.18 shows the change of concentration voltage when the current approaches to its limit:

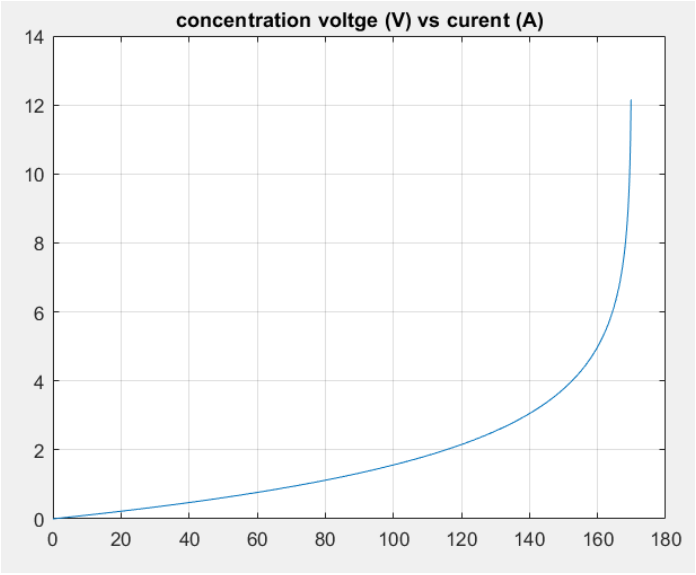

Fig. 5.18: Relation between concentration cell voltage and current - PEM fuel cell model

The local controller is needed to transform the power setpoints into current signals. To perform this transformation a lookup table is used. Fig. 5.19 shows the curve current vs power obtained from the model, the breakpoints that conform the lookup table and the linear approximation with the table:

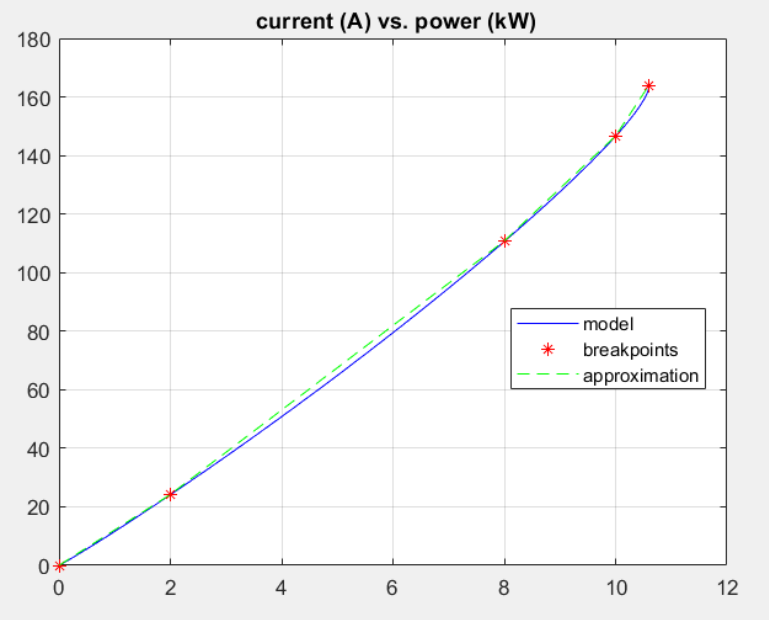

Fig. 5.19: Linearity of current as function of power - PEM fuel cell model

Therefore the controller consists of a lookup table that transforms the power references into current references. The tablet below shows the breakpoints of the lookup table:

Power (kW)	*Current* (A)
0	0.0
2	24.2
8	110.8
10	146.7
10.6	164.0

Table 8: Lookup table to transform power references into current for the fuel cell

Then the fuel cell system it is shown in Fig. 5.20:

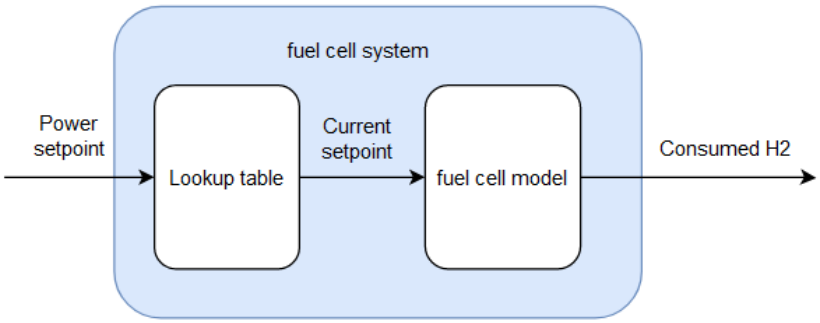

Fig. 5.20: Scheme of the complete model for the PEM fuel cell

As mentioned before, the MPC uses a simplified model where the electrolyser is seen as an actuator which receives power setpoints and consumes hydrogen. Hence, the function that makes this transformation is obtained from the model and is represented in Fig 5.21.

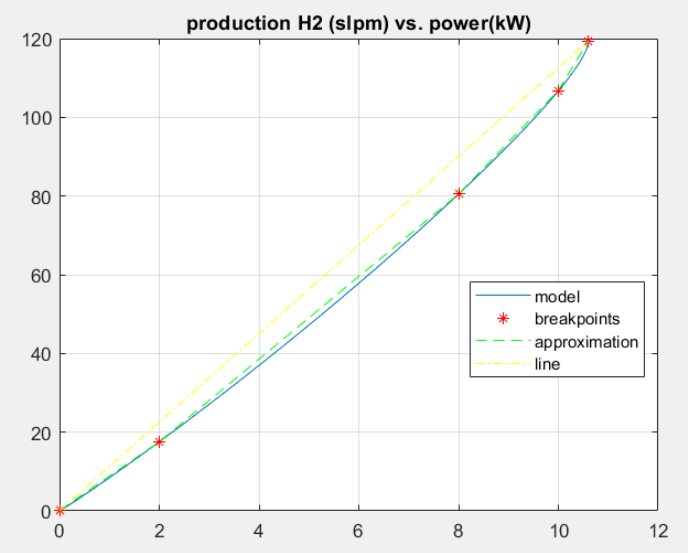

Fig. 5.21: Relationship between production of hydrogen and power - PEM fuel cell model

It can be seen that the whole fuel cell system can be approximated by a piecewise linear function. The function of the fuel cell is expressed as:

$$\dot{m}_{fc\,(k)} = f_{(P_{fc\,(k)})} \tag{5.2}$$

where $f_{(x)}$ is a piecewise linear function with the breakpoints shown in Table 9

Power(kW)	H_2 consumption(slpm)
0	0
2	17.56
8	80.53
10	106.82
10.6	119.36

Table 9: Breakpoints for the piecewise linearization of fuel cell function

Note that the original function is fully convex since the entire function is always lower than a line between two points, so according to the technique for linearization explained in chapter 3, the approximation can be made without binary variables, so:

$$f_{(\ P_{fc\,(k)})} = max\left(A_i \cdot\ P_{fc\,(k)} + b_i\right) \qquad i = 1,2,3,4 \tag{5.3}$$

where each pair A_i and b_i represent the polynomial coefficients of each line and since there are 5 breakpoints there are 4 lines. These coefficients are:

i	A_i	b_i
1	8.78	0
2	10.4950	-3.43
3	13.1450	-24.63
4	20.5574	-98.7540

Table 10: Polynomial coefficients for the piecewise linearization of fuel cell function

The previous equation can be written in a compact form as:

$$f_{(\ P_{fc\,(k)})} = \left\|A \cdot P_{fc\,(k)} + b\right\|_{\infty} \tag{5.4}$$

where $A=\begin{bmatrix} 8.78 \\ 10.4950 \\ 13.1450 \\ 20.5574 \end{bmatrix}$ and $b=\begin{bmatrix} 0 \\ -3.43 \\ -24.63 \\ -98.7540 \end{bmatrix}$

The equation (5.4) can be expressed in linear form as follows:

$$\dot{m}_{fc(k)} = f_{(\ P_{fc\,(k)})} = \ \varepsilon_{(k)}^{PWA} \tag{5.5}$$

where $\varepsilon_{(k)}^{PWA}$ is the minimum value that satisfies the following inequality:

$$\varepsilon_{(k)}^{PWA} \geq \ A \cdot P_{fc_{(k)}} + b \tag{5.6}$$

Although the previous expression is enough to represent the infinity norm, it has been seen in practice that adding the following constraint allows to compute $\varepsilon_{(k)}^{PWA}$ faster when $\varepsilon_{(k)}^{PWA}$ is part of a bigger optimization problem:

$$\varepsilon_{(k)}^{PWA} \leq S \cdot P_{fc_{(k)}} \tag{5.7}$$

where S is the slope of a line which is always greater than the nonlinear function. In this case, using the points from table 9, a line that joins the extreme points of the nonlinear function, i.e. (0,0) and (10.6,119.36) has a slope S of 11.26.

5.3.3 System equation

The storage dynamics is given by equation (2.28) which was presented in chapter 2 and it is shown below:

$$x_{(k+1)} = x_{(k)} + \frac{100 \cdot \Delta t}{Q_{max}} \cdot (\dot{m}_{ely} - \ \dot{m}_{fc}) \tag{5.8}$$

From the equations (5.1), (5.5), (5.6) and (5.7), both $\dot{m}_{ely}$ and $\dot{m}_{ely}$ can be expressed as functions of power. Also, since the sampling time is one minute the previous equation becomes:

$$x_{(k+1)} = x_{(k)} + \frac{100}{Q_{max}} \cdot (2.95 \cdot P_{ely(k)} - \left\| A \cdot P_{fc\,(k)} + b \right\|_{\infty}) \tag{5.9}$$

The max term due to the piecewise linearization can be replaced by an auxiliary variable ε^{PWA}. Then the previous equation becomes:

$$x_{(k+1)} = x_{(k)} + \frac{100}{Q_{max}} \cdot 2.95 \cdot P_{ely_{(k)}} - \frac{100}{Q_{max}} \varepsilon_{(k)}^{PWA} \tag{5.10}$$

subjected to:

$$\varepsilon_{(k)}^{PWA} \geq A \cdot P_{fc_{(k)}} + b$$

$$\varepsilon_{(k)}^{PWA} \leq S \cdot P_{fc_{(k)}}$$

Hereafter the following will be considered for compactness:

$$\mathrm{b}_1 = \frac{100}{\mathrm{Q_{max}}} \cdot 2.95$$

$$\mathrm{b}_2 = \frac{100}{\mathrm{Q_{max}}} \cdot -1$$

Note that the previous equations do not restrict simultaneous operation of the fuel cell and electrolyser which should not occur. The following procedure will assure that only one of them runs at a time.

Consider two binary variables $\delta_{(k)}^1, \delta_{(k)}^2$ defined as follows:

$$\delta_{(k)}^1 = \begin{cases} 0 & for\ P_{ely_{(k)}} = 0 \\ 1 & for\ P_{min}^{ely} \leq P_{ely_{(k)}} \leq P_{max}^{ely} \end{cases} \tag{5.11}$$

$$\delta_{(k)}^2 = \begin{cases} 0 & for\ P_{fc_{(k)}} = 0 \\ 1 & for\ P_{min}^{fc} \leq P_{fc_{(k)}} \leq P_{max}^{ely} \end{cases} \tag{5.12}$$

$$\delta_{(k)}^1 + \delta_{(k)}^2 \leq 1 \tag{5.13}$$

The introduction of these auxiliary variables and the inequalities now restrict the simultaneous activation of the electrolyser and fuel cell. These variables $\delta_{(k)}^1$and $\delta_{(k)}^2$

serve as enablers for the electrolyser and fuel cell respectively and inequality (5.13) only allows one device enabled at the same time. Note that the definition of the binary variables also imposes the range of operation of the fuel cell and the electrolyser. Although the simultaneous operation is now restricted, the expressions (5.11) and (5.12) represent logical conditions which cannot be written directly in linear form. However, according to the techniques described in chapter 3, these expressions are equivalent to linear inequalities:

$$P_{ely-min}\delta^1_{(k)} \leq P_{ely_{(k)}} \leq P_{ely-max}\delta^1_{(k)} \tag{5.14}$$

$$P_{fc-min}\delta^2_{(k)} \leq P_{fc_{(k)}} \leq P_{fc-max}\delta^2_{(k)}$$

Recapitulating, the dynamical equation of the storage system is:

$$x_{(k+1)} = x_{(k)} + b_1 P_{ely_{(k)}} + b_2 \varepsilon^{PWA}_{(k)} \tag{5.15}$$

subjected to:

$$\begin{gathered} \varepsilon^{PWA}_{(k)} \geq A \cdot P_{fc_{(k)}} + b \\ \varepsilon^{PWA}_{(k)} \leq S \cdot P_{fc_{(k)}} \\ P_{ely-min}\delta^1_{(k)} \leq P_{ely_{(k)}} \leq P_{ely-max}\delta^1_{(k)} \\ P_{fc-min}\delta^2_{(k)} \leq P_{fc_{(k)}} \leq P_{fc-max}\delta^2_{(k)} \\ \delta^1_{(k)} + \delta^2_{(k)} \leq 1 \end{gathered} \tag{5.16}$$

Equation (5.15) represents the model of the storage considered for MPC and hereafter, inequalities (5.16)will be referred as hydrogen model inequalities

5.4 System modelling for battery

5.4.1 System equation

The equations (2.29)– (2.30) presented in chapter 2 represent the dynamical model for the battery:

$$SOC_{(k+1)} = SOC_{(k)} + 100 \cdot \frac{\Delta t}{Q_{nom}} (\eta \cdot P_{batt_{(k)}} - P_{sd}) \tag{2.25}$$

and

$$\eta = \begin{cases} \eta_c & if\ P_{batt_{(k)}} \geq 0 \quad (charge\ mode) \\ 1/\eta_d & if\ P_{batt_{(k)}} < 0 \quad (discharge\ mode) \end{cases} \tag{2.26}$$

To express this equations in a single expression, consider the following auxiliary variables: $P_{(k)}^{char}$ and $P_{(k)}^{dis}$ which are continuous and $\delta_{(k)}^{b1}$ and $\delta_{(k)}^{b2}$ which are binary

$$\delta_{(k)}^{b1} = \begin{cases} 0 & for\ P_{(k)}^{char} = 0 \\ 1 & for\ P_{min}^{char} \leq P_{(k)}^{char} \leq P_{max}^{char} \end{cases} \tag{5.17}$$

$$\delta_{(k)}^{b2} = \begin{cases} 0 & for\ P_{(k)}^{dis} = 0 \\ 1 & for\ P_{min}^{dis} \leq P_{(k)}^{dis} \leq P_{max}^{dis} \end{cases} \tag{5.18}$$

$$\delta_{(k)}^{b1} + \delta_{(k)}^{b2} \leq 1 \tag{5.19}$$

$$P_{batt_{(k)}} = P_{(k)}^{char} - P_{(k)}^{dis} \tag{5.20}$$

Then considering a sample time of one minute and that the capacity of batteries is expressed in kWh, the equation of the battery becomes:

$$SOC_{(k+1)} = SOC_{(k)} + \frac{100}{Q_{nom} \cdot 60} \cdot \left(\eta_c P_{(k)}^{char} - \frac{1}{\eta_d} P_{(k)}^{dis} - P_{sd} \right) \tag{5.21}$$

It can be seen that inequalities (5.17) and (5.18) depend on the maximum and minimum values that $P_{(k)}^{char}$ and $P_{(k)}^{dis}$ can assume, so implicitly these inequalities also define the limits of operation of these variables. The expressions (5.17) and (5.18) represent logical conditions which cannot be included directly in a linear optimization problem. However, according to the techniques described in chapter 3, these expressions are equivalent to linear inequalities:

$$P_{min}^{char} \delta_{(k)}^{1} \leq P_{(k)}^{char} \leq P_{max}^{char} \delta_{(k)}^{b1} \tag{5.22}$$

$$P_{min}^{dis} \delta_{(k)}^{b2} \leq P_{(k)}^{dis} \leq P_{max}^{dis} \delta_{(k)}^{b2} \tag{5.23}$$

The following is defined for compactness:

$$b_1 = \frac{100}{Q_{nom} \cdot 60} \cdot \eta_c$$

$$b_2 = \frac{100}{Q_{nom} \cdot 60} \cdot \frac{-1}{\eta_d}$$

$$b_3 = \frac{100}{Q_{nom} \cdot 60} \cdot -P_{sd}$$

The equation of the system is:

$$SOC_{(k+1)} = SOC_{(k)} + b_1 z^b_{(k)} + b_2 P_{batt_{(k)}} + b_3 P_{sd} \tag{5.24}$$

subject to:

$$P^{char}_{min} \delta^1_{(k)} \leq P^{char}_{(k)} \leq P^{char}_{max} \delta^{b1}_{(k)}$$

$$P^{dis}_{min} \delta^{b2}_{(k)} \leq P^{dis}_{(k)} \leq P^{dis}_{max} \delta^{b2}_{(k)} \tag{5.25}$$

$$\delta^{b1}_{(k)} + \delta^{b2}_{(k)} \leq 1$$

Equation (5.24) represents the dynamical equation of the storage system based on battery and hereafter, inequalities (5.25) will be referred as battery model inequalities

Note that expression (5.20) is not included in the previous expressions. This is because $P_{batt_{(k)}}$ is a linear combination of $P^{char}_{(k)}$ and $P^{dis}_{(k)}$, so it is not necessary to include it in the optimization problems.

5.5 Energy exchange with the grid

5.5.1 Balance of energy

The balance of energy should be achieved at every time instant.

For the system with storage based on hydrogen:

$$P_{ely_{(k)}} - P_{fc_{(k)}} - P_{grid_{(k)}} - P_{PV_{(k)}} + D_{(k)} = 0 \tag{5.26}$$

For the system with battery:

$$P_{(k)}^{char} - P_{(k)}^{dis} - P_{grid_{(k)}} - P_{PV_{(k)}} + D_{(k)} = 0 \tag{5.27}$$

$P_{grid_{(k)}}$ is the power exchange with the grid and it is considered positive if energy enters the microgrid and negative if the microgrid delivers energy to the main grid

$P_{PV_{(k)}}$ and $D_{(k)}$ are the photovoltaic power and electrical demand respectively and are uncontrollable

Inequalities (5.26) and (5.27) will be referred as balance of energy constraints

5.5.2 Purchase and sale of energy

When the microgrid is connected to the utility grid, it can sell or purchase energy. The price of energy can be represented as:

$$C_{(k)}^{g} = \begin{cases} \dfrac{c_{(k)}^{p} P_{grid_{(k)}}}{60} & for\ P_{grid_{(k)}} \geq 0 \\ \dfrac{c_{(k)}^{s} P_{grid_{(k)}}}{60} & for\ P_{grid_{(k)}} < 0 \end{cases} \tag{5.28}$$

where $c_{(k)}^{p}$ and $c_{(k)}^{s}$ are the purchasing and selling energy prices respectively and are expressed in $€/kWh$.

This expression assumes that the given prices $c_{(k)}^{p}$ and $c_{(k)}^{s}$ are positive. However, note that if the values of $c_{(k)}^{p}$ and $c_{(k)}^{s}$ are 60 and -60 respectively then $C_{(k)}^{g}$ represents the absolute value of $P_{grid_{(k)}}$ which can be used to minimize the energy exchange with the utility grid. To include expression (5.28) in a linear program, a binary variable $\delta_{(k)}^{g}$ is introduced such that:

$$\delta_{(k)}^{g} = 1 \Leftrightarrow P_{grid_{(k)}} \geq 0 \tag{5.29}$$

Then the previous expression is equivalent to:

$$C_{(k)}^{g} = c_{(k)}^{p} P_{grid_{(k)}} \delta_{(k)}^{g} + c_{(k)}^{s} P_{grid_{(k)}} (1 - \delta_{(k)}^{g}) \tag{5.30}$$

The logical condition (5.29) and equation (5.30) cannot be expressed linearly in a direct way because they represent a logical condition and product of variables. However, according to the procedure presented chapter 3, these expressions are equivalent to the following linear inequalities

$$E_2^g \delta_{(k)}^g + E_3^g C_{(k)}^g \leq E_1^g P_{grid_{(k)}} + E_5^g \tag{5.31}$$

where:

$$\mathrm{E}_{2_{(k)}}^{\mathrm{g}} = \begin{bmatrix} -P_{min}^{grid} \\ -(P_{max}^{grid} + \varepsilon) \\ -M_{g_{(k)}} \\ m_{g_{(k)}} \\ -m_{g_{(k)}} \\ M_{g_{(k)}} \end{bmatrix}, \quad \mathrm{E}_{3_{(k)}}^{\mathrm{g}} = \begin{bmatrix} 0 \\ 0 \\ 1 \\ -1 \\ 1 \\ -1 \end{bmatrix}, \quad \mathrm{E}_{1_{(k)}}^{\mathrm{g}} = \begin{bmatrix} 1 \\ -1 \\ c_{(k)}^{s} \\ -c_{(k)}^{s} \\ c_{(k)}^{p} \\ -c_{(k)}^{p} \end{bmatrix}, \quad \mathrm{E}_{5_{(k)}}^{\mathrm{g}} = \begin{bmatrix} -P_{min}^{grid} \\ -\varepsilon \\ 0 \\ 0 \\ -m_{g_{(k)}} \\ M_{g_{(k)}} \end{bmatrix}$$

$$M_{g_{(k)}} = \max\left(\left(c_{(k)}^{p} - c_{(k)}^{s}\right) \cdot P_{max}^{grid}, \left(c_{(k)}^{p} - c_{(k)}^{s}\right) \cdot P_{min}^{grid}\right)$$

$$m_{g_{(k)}} = \min\left(\left(c_{(k)}^{p} - c_{(k)}^{s}\right) \cdot P_{max}^{grid}, \left(c_{(k)}^{p} - c_{(k)}^{s}\right) \cdot P_{min}^{grid}\right)$$

Note that these inequalities depend on the selling and purchasing prices of energy which are time variant, so these inequalities also change over time. These matrices also depend on the maximum and minimum power exchanged with the grid, so this variable is implicitly bounded. The inequalities (5.31) will be referred from now on as purchase and sale of energy inequalities.

5.5.3 Prices of energy

The prices considered for the simulations in this thesis were obtained from [37] for a certain day and are shown in Fig. 5.22:

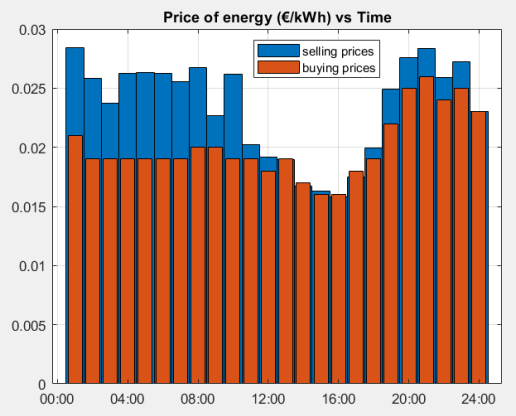

Fig. 5.22: Energy prices over 24 hours

5.6 Constraints

5.6.1 Storage bounds

For both types of storage systems the capacity of storage is defined in terms of percentage and ranges from 0% to 100%. The following constraints represent the physical bounds of the storage.

Hydrogen system:

For the tank, the amount of hydrogen must be between $x_{min} = 10\%$ and $x_{max} = 90\%$

A security band is left to prevent the tank from complete emptying or filling.

$$x_{min} \leq x_{(k)} \leq x_{max} \qquad k = 1, 2, \dots, N-1 \tag{5.32}$$

Battery system:

In the case of batteries, their lifetime is inversely proportional to the depth of discharge, so smaller discharge cycles are preferred to avoid shortening their lifetime. The bounds chosen for this case are $SOC_{min} = 30\%$ and $SOC_{max} = 90\%$

$$SOC_{min} \leq SOC_{(k)} \leq SOC_{max} \qquad k = 1, 2, \dots, N-1 \tag{5.33}$$

In the case of the planification one-day ahead a terminal condition is added:

$$x_0 - 5 \leq x_{(N)} \leq x_0 + 5 \tag{5.34}$$

$$SOC_0 - 5 \leq SOC_{(k)} \leq SOC_0 + 5 \tag{5.35}$$

Whereas in the case of MPC, the terminal value needs to be within a band around the reference:

$$x_{(N)}^{ref} - 1 \leq x_{(N)} \leq x_{(N)}^{ref} + 1 \tag{5.36}$$

$$SOC_{(N)}^{ref} - 1 \leq SOC_{(N)} \leq SOC_{(N)}^{ref} + 1 \tag{5.37}$$

5.6.2 Ramp rate

The alkaline electrolyser due to its nature cannot change its power absorption by more than 20% of its rated power per minute [11]. The nominal power of the electrolyser is 30kW, so its power variation limit is set to 6kW. The fuel cell is PEM, so in a minute it can change its power in the full range, so the limit is only imposed to the electrolyser.

$$-\Delta P_{ely}^{max} \leq P_{ely_{(k)}} - P_{ely_{(k-1)}} \leq \Delta P_{ely}^{max} \qquad k = 1, 2, \dots, N \tag{5.38}$$

Similarly, batteries can also stand variations of power in the full range, so this constraint is not applied in this case

5.6.3 Interaction with the grid logical constraints

A situation that should be avoided is discharging the storage to sell energy or buying energy to charge the storage. The following inequalities will restrict these situations:

<u>Hydrogen system:</u>

$$\delta_{(k)}^{g} + \delta_{(k)}^{1} \leq 1 \qquad k = 1, 2, \dots, N \tag{5.39}$$

$$-\delta_{(k)}^{g} + \delta_{(k)}^{2} \leq 0 \qquad k = 1, 2, \dots, N \tag{5.40}$$

<u>Battery system:</u>

$$\delta_{(k)}^{g} + \delta_{(k)}^{b1} \leq 1 \qquad k = 1, 2, \dots, N \tag{5.41}$$

$$-\delta_{(k)}^{g} + \delta_{(k)}^{b2} \leq 0 \qquad k = 1, 2, \dots, N \tag{5.42}$$

Since the models considered by MPC do not match exactly the real equipment, the energy level in the storage may diverge from the reference; hence it may be needed to buy energy to charge the storage or sell energy to discharge the battery to satisfy the terminal constraint regarding the energy level in the storage. So to guarantee feasibility and stability, these constraints are not considered by the optimization problems of MPC.

5.6.4 Start up and shutdown

Hydrogen system:

A problem with alkaline electrolysers is that they need long times to start. Hence, to avoid frequent activation and deactivation the term $\left|\delta^1_{(k)} - \delta^1_{(k-1)}\right|$ should be penalized in the cost function. Although, PEM fuel cells do not have this problem, frequent switching is also penalized but more importance is given to the electrolyser in the optimization problem. To this end, the weight of the fuel cell is lower than the weight of the electrolyser. The following inequalities allow to represent the absolute value in the cost function

$$-SU^{ely}_{(k)} \leq c^{SU}_{ely}\left(\delta^1_{(k)} - \delta^1_{(k-1)}\right) \leq SU^{ely}_{(k)} \qquad k = 1, 2, \dots, N \tag{5.43}$$

$$-SU^{fc}_{(k)} \leq c^{SU}_{fc}\left(\delta^2_{(k)} - \delta^2_{(k-1)}\right) \leq SU^{fc}_{(k)} \qquad k = 1, 2, \dots, N \tag{5.44}$$

$$SU^{ely}_{(k)} \geq 0 \qquad k = 1, 2, \dots, N \tag{5.45}$$

$$SU^{fc}_{(k)} \geq 0 \qquad k = 1, 2, \dots, N \tag{5.46}$$

Battery system:

The lifetime of batteries is limited by the number of discharge and charge cycles. Therefore, the switching from charging to discharging and vice versa is restricted to not reduce the lifetime of the battery.

$$-SU^{char}_{(k)} \leq c^{SU}_{char}(\delta^{b1}_{(k)} - \delta^{b1}_{(k-1)}) \leq SU^{char}_{(k)} \qquad k = 1, 2, \dots, N \tag{5.47}$$

$$-SU^{dis}_{(k)} \leq c^{SD}_{dis}(\delta^{b2}_{(k)} - \delta^{b1}_{(k-1)}) \leq SU^{dis}_{(k)} \qquad k = 1, 2, \dots, N \tag{5.48}$$

$$SU^{char}_{(k)} \geq 0 \qquad k = 1, 2, \dots, N \tag{5.49}$$

$$SU^{dis}_{(k)} \geq 0 \qquad k = 1, 2, \dots, N \tag{5.50}$$

The auxiliary variables should be minimized in the cost function to reduce the frequency of switching.

5.6.5 Variation of power exchanged with the grid

A desirable feature is to minimize the variability of the power exchanged with the grid. This feature can be considered in the optimization by including the term $\sum_{i=1}^{N-1}\left|P_{grid_{(k)}} - P_{grid_{(k-1)}}\right|$ in the cost function. To include this expression in a linear program the following inequality can be used:

$$-\varepsilon_{(k)}^{\Delta grid} \leq P_{grid_{(k)}} - P_{grid_{(k+1)}} \leq \varepsilon_{(k)}^{\Delta grid} \qquad k = 1, 2, \dots, N \tag{5.51}$$

where $\varepsilon_{(k)}^{\Delta grid}$ is an auxiliary variable that should be included in the cost function. In this way, the optimization problem would minimize $\varepsilon_{(k)}^{\Delta grid}$ and therefore the variation of power is also minimized.

5.6.6 Tracking the reference of energy level in the storage

As described before, the MPC controller should regulate the energy level in the storage to follow the reference given by the planification one-day ahead. This feature can be considered in the optimization problem by including the term $\sum_{i=0}^{N-1} \left| x_{(k+i)} - x_{(k+i)}^{ref} \right|$ in the cost function, in this way the error is penalized. To include this expression in a linear program the following inequality can be used

For the storage system based on hydrogen:

$$-\varepsilon_{level(k)}^{track} \leq x_{(k)} - x_{(k)}^{ref} \leq \varepsilon_{level(k)}^{track} \qquad k = 1, 2, \dots, N \tag{5.52}$$

For the storage system based on batteries:

$$-\varepsilon_{\mathrm{level(k)}}^{\mathrm{track}} \leq \mathrm{SOC_{(k)}} - SOC_{\mathrm{(k)}}^{\mathrm{ref}} \leq \varepsilon_{\mathrm{level(k)}}^{\mathrm{track}} \qquad \mathrm{k} = 1, 2, \dots, \mathrm{N} \tag{5.53}$$

where $\varepsilon_{level(k)}^{track}$ is an auxiliary variable that should be included in the cost function. In this way, the optimization problem would minimize $\varepsilon_{level(k)}^{track}$ and therefore the level would follow the reference.

Additionally, to improve the tracking the auxiliary variables are also restricted such that the difference between the energy level in the storage in its reference is limited:

$$0 \leq \varepsilon_{level(k)}^{track} \leq 10 \qquad k = 1, 2, \dots, N \tag{5.54}$$

5.6.7 Tracking the reference of power exchanged with the grid

Similarly to the previous case, the power exchanged with the grid obtained by the MPC controller should be similar to what was indicated by the prior scheduling. This is achieved by including the term $\sum_{i=1}^{N-1}\left|P_{grid_{(k)}} - P_{grid(k)}^{ref}\right|$ in the cost function. To include this expression in a linear program the following inequality can be used

$$-\varepsilon_{grid}^{track} \leq P_{grid_{(k)}} - P_{grid(k)}^{ref} \leq \varepsilon_{grid}^{track} \qquad k = 1, 2, \dots, N \tag{5.55}$$

where $\varepsilon_{grid}^{track}$ is an auxiliary variable that should be included in the cost function. In this way, the optimization problem would minimize $\varepsilon_{grid}^{track}$ and therefore $P_{grid_{(k)}}$would follow its reference.

Differently from the previous case, in this case the auxiliary variable is not restricted because is desired to minimize the error, but this variable should be able to take very different variables if needed.

5.7 One day-ahead scheduling

A prior scheduling is performed for the following reasons:

- It is advantageous to obtain similar levels of energy in the storage system at the beginning and at end of the day. Thus, if during the night there is a blackout there is energy left in the storage to satisfy essential needs.
- In the main grid, generators indicate anticipately the amount of energy they will produce to the grid coordinator. To emulate this behaviour a prior planification is needed to obtain an expected profile of exchanged power with the grid. This profile is obtained by solving an optimization problem which considers 1-day forecasts of photovoltaic generation and demand to produce the power references that would satisfy the energy balance. Since these forecasts are not perfectly met, the MPC controller produces power references different to what was given by the prior optimization. To fulfil what was declared to the grid coordinator the MPC controller should try to produce an output similar to the reference.

The optimization problem evaluates the whole day considering a resolution of one minute and it produces power references of energy exchange with the grid and with the storage system. Then, it is possible to use the model of the storage and the solution produced by the optimization problem to obtain a storage level profile. The reference

of power exchange with the grid and level profile are sent to the MPC which should follow these references.

In a general way, for both types of storage systems the one-day ahead scheduling consists of solving the following mixed-integer linear program:

$$\min_{U} J_{(U,x_0)} \tag{5.56}$$

$$\textit{subject to:}$$

$$\textit{model constraints}$$

$$\textit{storage limits constraints}$$

$$\textit{ramp rate constraints}$$

$$\textit{price of energy constraints}$$

$$\textit{start up and shutdown constraints}$$

$$\textit{interaction with the grid logical constraints}$$

$$\textit{variation of energy exchange with the grid constraints}$$

$$\textit{balance of energy constraints}$$

where U is the vector of decision variables, x_0 is the initial energy level in the storage and $J_{(U,x_0)}$ is the cost function of the optimization problem.

The cost function used for both types of storage systems are similar but present slight differences because they use different decision variables. In the next sections, the cost functions are described by making use of the variables already presented until now. However, the following notation is introduced first since it will be used for both systems.

The symbol $(\cdot)^*$ in a vector refers to: $a^* = \underbrace{[a_{(0)}, a_{(1)}, \dots, a_{(N-1)}]}_{N}$

5.7.1 Cost function for system based on hydrogen

The following vector of decision variables is considered:

$$\mathrm{U}_{\mathrm{H}_2} = \left[P^*_{ely}, P^*_{fc}, \delta^{1*}, \delta^{2*}, \varepsilon^{PWA*}, P^*_{grid}, \delta^{g*}, C^{g*}, SU^{ely*}, SU^{fc*}, \varepsilon^{\Delta grid*}\right]^T$$

Then the proposed cost function is the following:

$$J_{(U_{H_2})} = \sum_{k=0}^{1439} w_1 C^g_{(k)} + w_2\left|\delta^1_{(k)} - \delta^1_{(k-1)}\right| + w_3\left|\delta^2_{(k)} - \delta^2_{(k-1)}\right| + w_4\varepsilon^{PWA}_{(k)} + w_5\left|P_{grid_{(k)}} - P_{grid_{(k-1)}}\right| \quad (5.57)$$

The first term corresponds to the energy exchange with the grid and there are two cases. On the one hand, for minimization of energy exchange, the terms $c^p_{(k)}$and $c^s_{(k)}$ should be 60 and -60 respectively, in this way $C^g_{(k)}$represents the absolute value of the energy exchange so both import and export of energy are penalized. On the other hand, to obtain economic benefits the terms $c^p_{(k)}$and $c^s_{(k)}$ should take the values of the purchasing and selling prices, thus when importing energy the term $C^g_{(k)}$ is positive so it is penalized, whereas when selling energy the term $C^g_{(k)}$ is negative so exporting energy is encouraged. The second and third terms penalize the on/off switching of the electrolyser and fuel cell, respectively. The term $\varepsilon^{PWA}_{(k)}$ corresponds to the piecewise approximation of the fuel cell function. Finally, the last term penalizes the variability of energy exchange with grid. The summatory of terms with absolute value can be replaced by auxiliary variables and linear inequalities as shown below:

$$J_{H_2(U)} = \sum_{k=0}^{1439} w_1 C^g_{(k)} + SU^{ely}_{(k)} + SU^{fc}_{(k)} + w_4\varepsilon^{PWA}_{(k)} + w_5\varepsilon^{\Delta grid}_{(k)} \quad (5.58)$$

where the auxiliary variables $SU^{ely}_{(k)}$, $SU^{fc}_{(k)}$, $\varepsilon^{\Delta grid}_{(k)}$ were introduced in the constraints section.

5.7.2 Cost function for system based on battery

The following vector of decision variables is considered:

$$\mathrm{U}_{batt} = \left[P^{char*}, P^{dis*}, \delta^{b1*}, \delta^{b2*}, P^*_{grid}, \delta^{g*}, C^{g*}, SU^{char*}, SU^{dis*}, \varepsilon^{\Delta grid*}, \varepsilon^{track*}_{level}, \varepsilon^{track*}_{grid}\right]^T$$

Then the proposed cost function is the following:

$$J_{(k)} = \sum_{k=0}^{1439} C_{(k)}^{g} + w_2\left|\delta_{(k)}^{b1} - \delta_{(k-1)}^{b1}\right| + w_3\left|\delta_{(k)}^{b2} - \delta_{(k-1)}^{b2}\right| + w_4\left|P_{grid_{(k)}} - P_{grid_{(k-1)}}\right| \tag{5.59}$$

Similarly to the previous case, $c_{(k)}^{p}$and $c_{(k)}^{s}$ should take suitable values to achieve minimization of energy exchange or to obtain economic benefits. The second and third terms penalize constant switching between charging and discharging. The last term penalizes variations of power exchanged to the grid. As explained in the previous case, the absolute value can be replaced by auxiliary variables and linear inequalities presented in the constraints section:

$$J_{batt(U)} = \sum_{k=0}^{1439} w_1 C_{(k)}^{g} + SU_{(k)}^{char} + SD_{(k)}^{char} + SU_{(k)}^{dis} + SD_{(k)}^{dis} + w_4 \varepsilon_{(k)}^{\Delta grid} \tag{5.60}$$

5.8 MPC control problem

In this section the MPC optimization problem is formulated. This problem attempts to find an optimal sequence of inputs that produce a desired behaviour of the system in a future horizon. At each time instant, only the first input of the sequence is applied and in the next time instant a new optimization problem is stated using new measured information. In this way, it compensates for inaccuracies of the model and possible disturbances.

In a general way, for both systems the MPC algorithm consists of the following steps at each time instant:

1. The actual energy level in the storage is measured and a forecast of the following N values of generation and consumption is performed. The foreseen data allows to state the balance of energy constraints which will be used in the following step.

2. Solve the following optimization problem

$$\min_{U_{(k)}} J_{(k,x_0,U_{(k)})} \tag{5.61}$$

subject to:

model constraints

storage limits constraints

ramp rates constraints

price of energy constraints

start up and shutdown constraints

variation of energy exchange with the grid constraints

balance of energy constraints

tracking energy level reference constraints

tracking grid reference constraints

where U is the vector of decision variables, x_0 is the initial energy level in the storage, k is the time instant and $J_{(k,U,x_0)}$ is the cost function of the optimization problem.

3. After solving the problem is produced a sequence of N values for each decision variable. From this sequence only the first values are applied to the real system represented in this thesis by the complete models. In the case of the storage based on hydrogen, $P_{ely(0)}$, $P_{fc(0)}$ and $P_{grid(0)}$are applied whereas in the case of the battery-based system, $P_{ely(0)}$, $P_{fc(0)}$ and $P_{grid(0)}$ .Furthermore, it is considered that forecast of the next N values of generation and consumption is perfect thus $P_{ely(0)}$, $P_{fc(0)}$ and $P_{grid(0)}$ perfectly satisfy the energy balance.

In this case the cost function depends on the index k which means that there is a different cost function at each time instant k whereas in the scheduling one-day ahead there was only a single cost function for the whole simulation. The cost function used in MPC is similar to the cost function in the scheduling one-day ahead although in this case two additional terms are added. These terms allow the system to follow the references given by the prior scheduling.

The MPC formulation is presented in the following sections for both types of storage systems.

5.8.1 Cost function for system based on hydrogen

Consider the following vector of decision variables:

$$\mathrm{U}_{\mathrm{H}_2(k)} = \left[P^*_{ely}, P^*_{fc}, \delta^{1*}, \delta^{2*}, \varepsilon^{PWA*}, P^*_{grid}, \delta^{g*}, C^{g*}, SU^{ely*}, \; SU^{fc*}, \varepsilon^{\Delta grid*}, \varepsilon^{track*}_{level}, \varepsilon^{track*}_{grid}\right]^T$$

The cost function considered is the following:

$$\begin{aligned} J_{H_2(k,x_0,U_{H_2(k)})} = & \sum_{i=0}^{N-1} w_1 C^g_{(k+i)} + w_2 \left\| \delta^1_{(k+i)} - \delta^1_{(k+i-1)} \right\|_1 \\ & + w_3 \left\| \delta^2_{(k+i)} - \delta^2_{(k+i-1)} \right\|_1 + w_4 \varepsilon^{PWA}_{(k+i)} \\ & + w_5 \left\| P_{grid_{(k+i)}} - P_{grid_{(k+i-1)}} \right\|_1 + w_6 \left\| x_{(k+i)} - x^{ref}_{(k+i)} \right\|_1 \\ & + w_7 \left\| P_{grid_{(k+i)}} - P^{ref}_{grid(k+i)} \right\|_1 \end{aligned} \tag{5.62}$$

Similarly to the prior scheduling case, this cost function can be included in a linear program by using the auxiliary variables introduced in the constraints section, then:

$$\begin{aligned} J_{H_2(k,x_0,U_{H_2(k)})} = & \sum_{i=0}^{N-1} w_1 C^g_{(k+i)} + SU^{char}_{(k)} + SU^{dis}_{(k)} + \varepsilon^{PWA}_{(k+i)} + w_4 \varepsilon^{\Delta grid}_{(k+i)} \\ & + w_5 \varepsilon^{track}_{level(k+i)} + w_6 \varepsilon^{track}_{grid(k+i)} \end{aligned} \tag{5.63}$$

5.8.2 Cost function for system based on battery

Consider the following vector of decision variables:

$$\mathrm{U}_{batt} = \left[P^{char*}, P^{dis*}, \delta^{b1*}, \delta^{b2*}, P^*_{grid}, \delta^{g*}, C^{g*}, SU^{char*}, SD^{char*}, SU^{dis*}, SD^{dis*}, \varepsilon^{\Delta grid*}, \varepsilon^{track*}_{level}, \varepsilon^{track*}_{grid}\right]^T$$

The cost function considered is the following:

$$J_{H_2(k,x_0,U_{H_2(k)})} = \sum_{i=0}^{N-1} w_1 C^g_{(k+i)} + w_2 \left\| \delta^{b1}_{(k+i)} - \delta^{b1}_{(k+i-1)} \right\|_1 + w_3 \left\| \delta^{b2}_{(k+i)} - \delta^{b2}_{(k+i-1)} \right\|_1 + w_4 \varepsilon^{PWA}_{(k+i)} + w_5 \left\| P_{grid_{(k+i)}} - P_{grid_{(k+i-1)}} \right\|_1 + w_6 \left\| x_{(k+i)} - x^{ref}_{(k+i)} \right\|_1 + w_7 \left\| P_{grid_{(k+i)}} - P^{ref}_{grid(k+i)} \right\|_1 \quad (5.64)$$

Similarly to the prior scheduling case, this cost function can be included in a linear program by using the auxiliary variables introduced in the constraints section, then:

$$J_{H_2(k,x_0,U_{H_2(k)})} = \sum_{i=0}^{N-1} w_1 C^g_{(k+i)} + SU^{char}_{(k)} + SU^{dis}_{(k)} + \varepsilon^{PWA}_{(k+i)} + w_4 \varepsilon^{\Delta grid}_{(k+i)} + w_5 \varepsilon^{track}_{level(k+i)} + w_6 \varepsilon^{track}_{grid(k+i)} \quad (5.65)$$

5.9 Generation of photovoltaic generation data

As seen in chapter 2, the power generation by photovoltaic panels depends on solar irradiance. So for the simulations of this thesis solar irradiance data is obtained from a model called “Bright Solar Model” [38] [39] [40] [41] [42] which generates stochastic data of irradiance with resolution of one minute. The information it needs to produce the data is: start and final dates, geographical coordinates, height above sea level, pressure of the location, wind speed of the place and orientation of the panels. The selected location for the simulations is Milan and the geographical coordinates and height above sea level were obtained from [43] while the pressure and speed of wind were obtained from [44]. In [45] is considered that for places located in the Northern Hemisphere the panels should face due south, so the azimuth angle is 0 according to the user instructions of the model. Regarding the pitch angle, in [46] is mentioned that the optimal value for Italy is 30 degrees. The parameters shown in table 11 were used to generate the data:

Parameter	Value
Latitude	45.4642
Longitude	9.1825
Height above sea level	127
Tilt angle	30
Azimuth angle	0

Table 11: Parameters used in the BRIGHT model to produce irradiance data

Then the obtained irradiance data is used in the equations (2.1), (2.2) and (2.3) presented in chapter 2 to compute power:

$$T_C = T_a + \frac{NOCT}{800} \cdot G \tag{2.1}$$

$$\eta_{th} = 1 - \alpha_{th} \cdot (T_c - 25) \tag{2.2}$$

$$\frac{P_{AC}}{P_{nom}} = \eta_{DC-AC} \cdot \frac{G}{1000} \cdot \eta_{th} \tag{2.3}$$

The nominal power P_{nom} is 50kW and the parameters take the following values as reported in [8]:

Parameter	Description	Value
NOCT	Nominal operating cell temperature	45.0°C
α_{th}	Loss coefficient due to temperature	0.45%
η_{DC-AC}	Efficiency due to cables, connections, and inverter	0.828

Table 12: Parameters to transform irradiance into power

Note that to calculate power the temperature of the air is also required, which was retrieved from [44]. Fig. 5.23 shows the obtained power profiles:

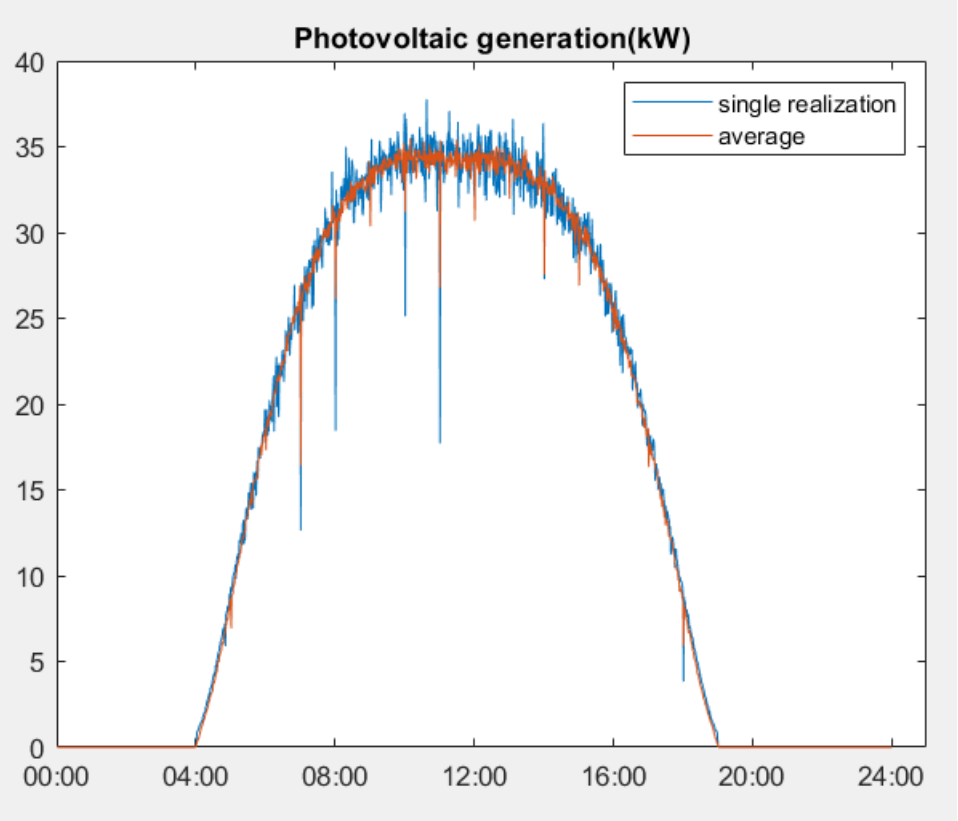

Fig. 5.23: Photovoltaic generation data produced by the BRIGHT model

Note that the maximum power achieved is less than 50 kW because of the losses. There were obtained 9 different realizations, one of them is used for MPC and the heuristic algorithm. The other 8 realization are averaged and then used by the planification one-day ahead.

5.10 Generation of electrical demand data

The electrical demand data considered in this thesis is obtained by using a stochastic generator of electrical demand called CREST Demand Model [47]. This model is open in the sense that modifications can be made freely. It produces one-minute resolution data of photovoltaic generation, electrical and thermal domestic demand for a group of dwellings, although only the electrical demand is used in this thesis. Fig. 5.24 depicts the architecture of the electrical demand model [47]:

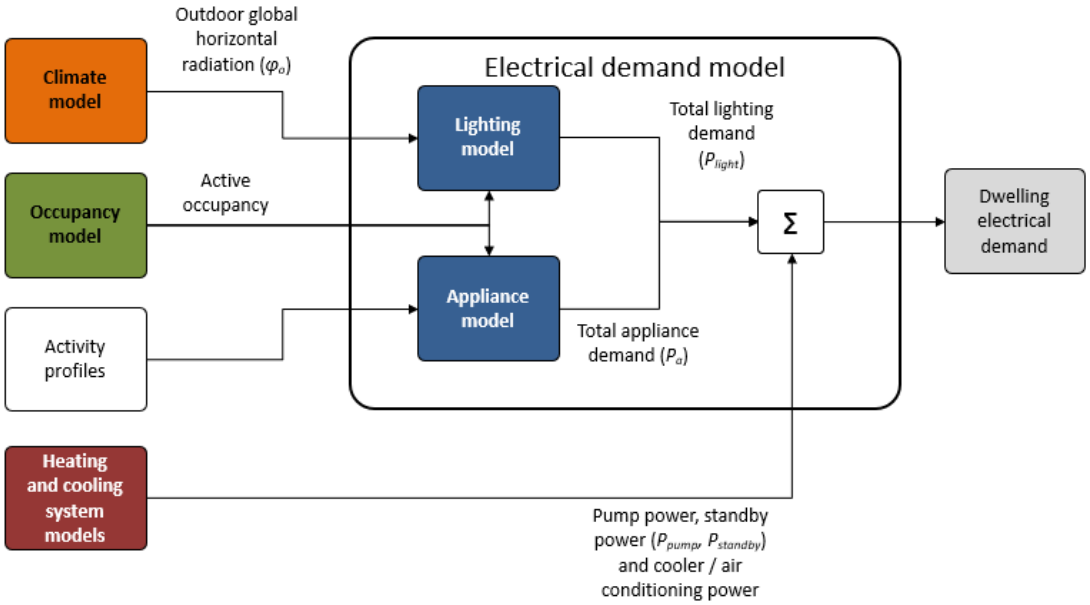

Fig. 5.24: Architecture considered by the CREST model to generate electrical demand data

This model considers the electrical consumption of lighting, domestic appliances, and thermal equipment to compute the total electrical demand. It uses weather and occupancy data to determine the necessity of lighting. The climate data is generated from historical monthly temperatures and geographical coordinates for a predefined location. Also, activity profiles and occupancy data determine the appliance demand. The activity profile refers to the probability of residents performing certain activities throughout the day and the occupancy consists of stochastic data that determines if a resident is at home and if is active or asleep. The occupancy and activity information are based on historical data for the UK. Additionally, since thermal equipment also consume electrical energy the necessity of heat is computed and depends on climate data. Regarding this data, the original model only had location and weather information from UK and Indian cities; so this information corresponding to Milan was also included, which was retrieved from [44]. This model is based on Excel VBA and its user interface is the following:

1	**CREST Demand Model v2.2**													
2														
3														
4		**Simulation inputs**												
5														
6		1. Specify the date:	**Enter day of month:**	**26**	**Enter month of year:**	**6**	(Specify a number for the month e.g. for January enter '1')							
7		2. Specify if this is a weekday (wd) or weekend (we):		**wd**	(Specify 'wd' or 'we')									
8		3. Specify the location for solar:	**Latitude (°):**	**45.5**	**Longitude (°):**	**9.2**	**Local standard time meridian (°):**					**15**	(0 for England	
9		4. Specify the location for temperature:		**Milano**	(Specify 'England' or a city e.g. 'N Delhi'. List, plus latitude & longitude in ClimateData)								82.5 for India)	
10		5. Specify country and year for appliance ownership		**Italy**	(India or UK)	**2020**	(2006 to 2031)	**Urban**	(Urban or Rural)					
11		6. Country uses daylight saving time (summer time)?		☑	(Yes in UK/Italy, not in India)									
12		7. Specify the number of dwellings to simulate in this run:		**20**										
13		8. Stochastically assign dwelling parameters?		☑	If not, then specify the dwelling parameters manually in the "Dwellings" worksheet									
14		9. Include high-resolution dynamic output?		☑										
15		10. Include daily demand totals for each dwelling?		☑										
16		11. Overwrite existing data?		☑										
17		12. PV included as an option?		☐										
18		13. Run or stop the model by clicking the buttons to the right:		Run simulation	Stop simulation		Stopped							
19														
20														

Fig. 5.25: Main interface of CREST demand model

From this model one-minute resolution data was obtained for 20 dwellings. There were obtained 9 different realizations, one of them is used for MPC and the heuristic algorithm. The other 8 realization are averaged and then used by the planification one-day ahead. The electrical demand profiles obtained are the following:

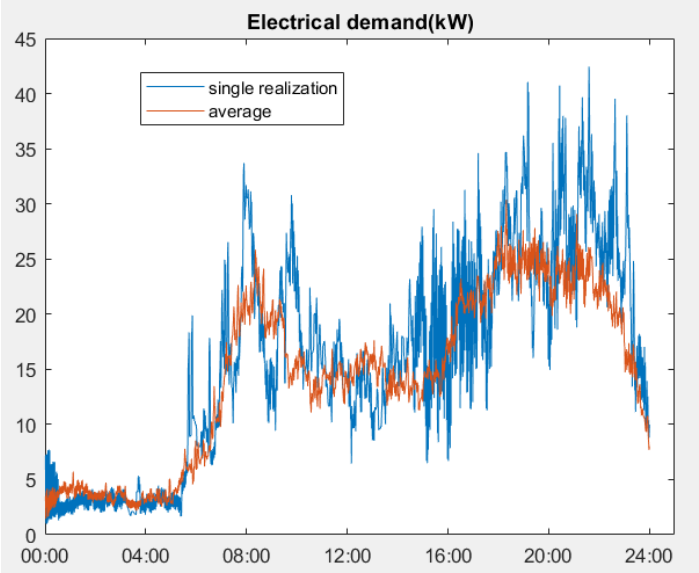

Fig. 5.26: Electrical demand data produced by the CREST demand model

5.11 Alternative management algorithm

An alternative control algorithm is proposed to compare the results obtained with the MPC strategy. The algorithm consists of fixed logical rules to determine the amount of energy to exchange with the grid and the storage system. To make the comparison between control strategies, this algorithm also receives the references from the planification one-day ahead to assure that energy level in the storage at the beginning and at the end of the day are similar.

This algorithm consists of tracking the energy level profile using a hysteresis band to avoid continuous switching.

For the case of the system based on batteries, Fig. 5.27 contains the flowchart represents this algorithm.

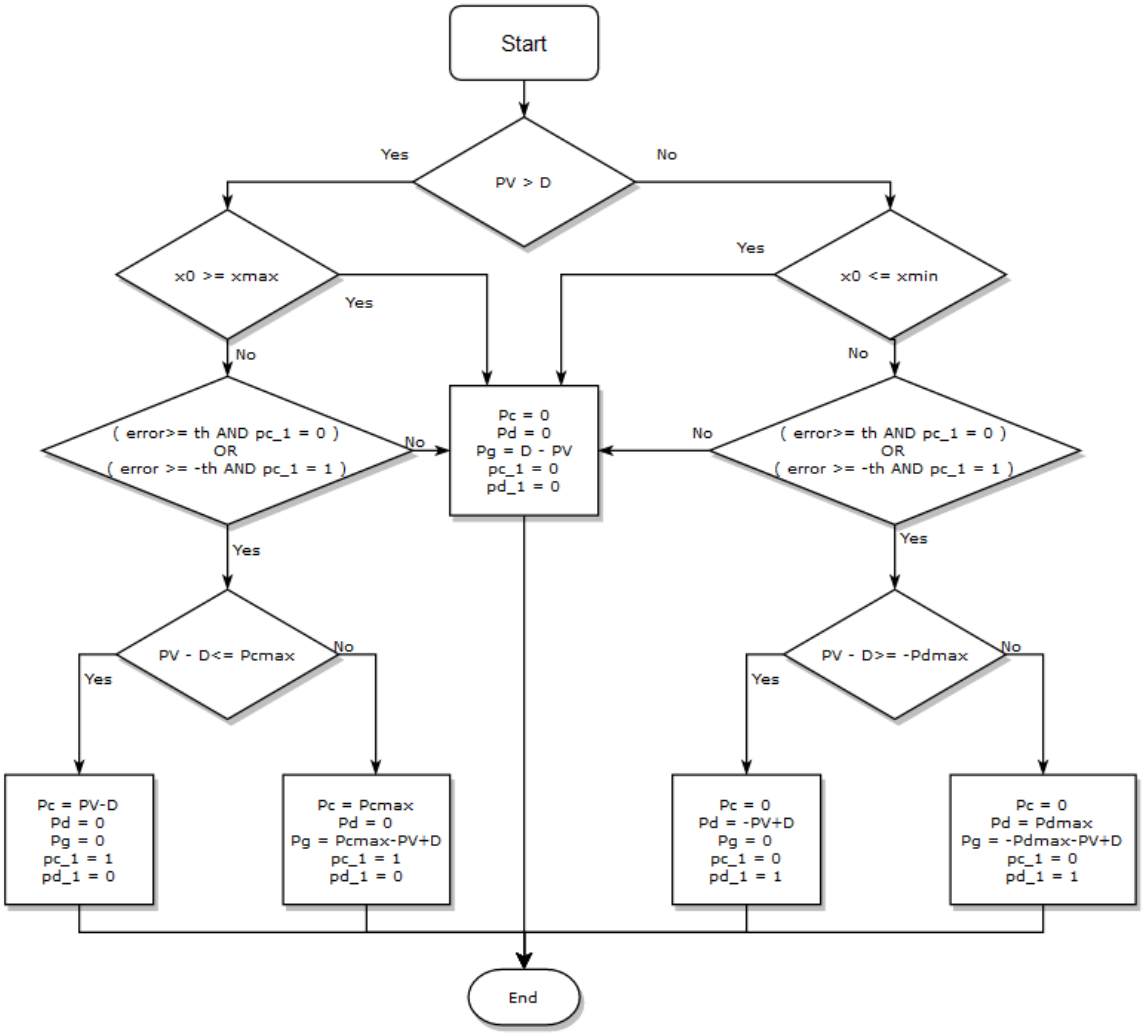

Fig. 5.27: Flow chart of the heuristic algorithm for the storage system based on battery

For the case of the system based on hydrogen, the following chart flow represents this algorithm.

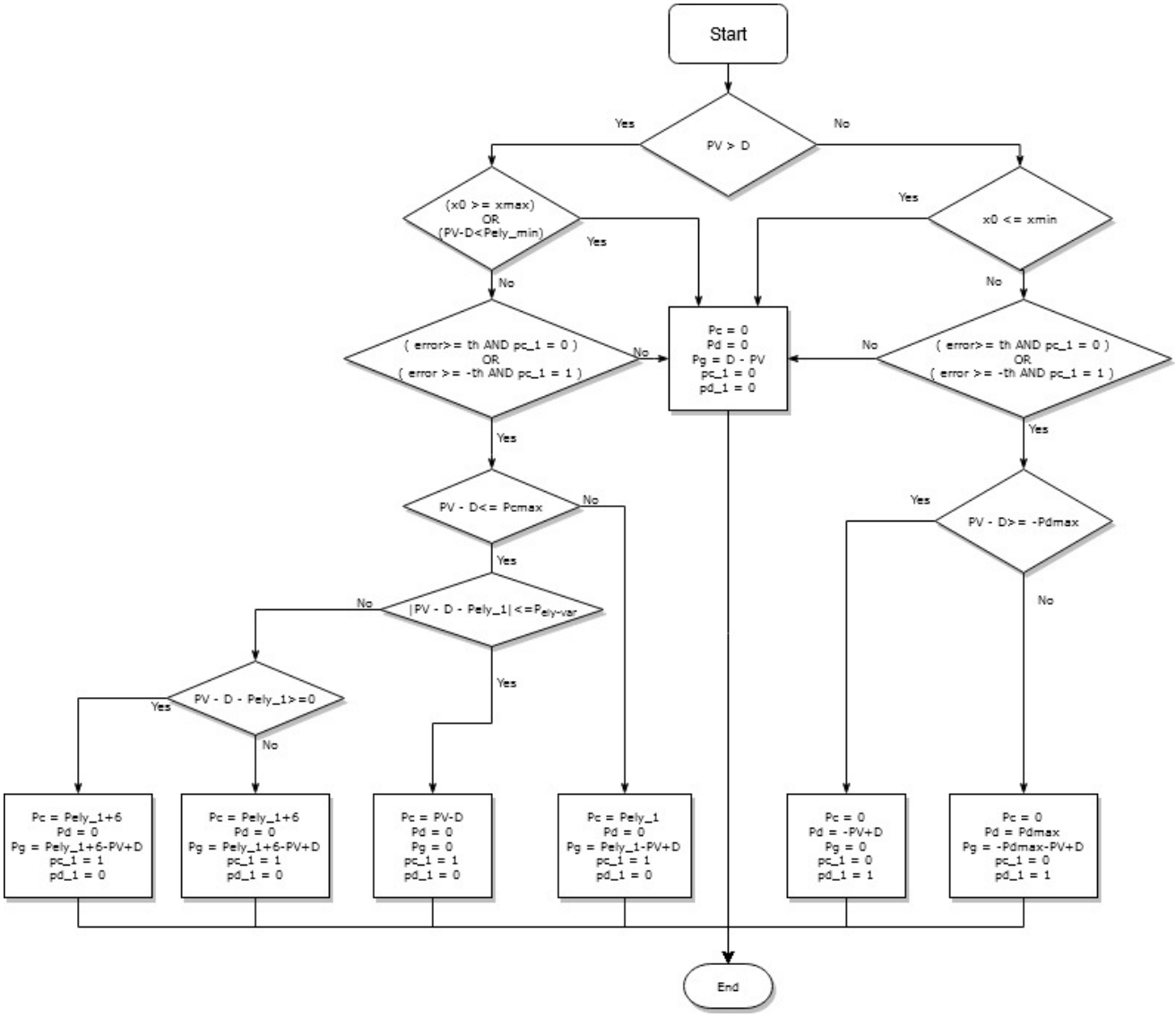

Fig. 5.28: Flow chart of the heuristic algorithm for the storage system based on hydrogen

This chart flow is similar to the one considered for the system with batteries but in this case, it is also considered the ramp rate limitation of the alkaline electrolyser

Chapter 6 Simulations and results

In this section, the results of the simulations are presented. As explained before, the control system attempts to achieve two mutually exclusive objectives: minimization of energy exchange with the grid and reduction of energy costs. Hence, the results of these problems are presented for the two types of microgrids presented before. Also, the performance of the proposed control system is compared with the performance of the heuristic algorithm that consists of conditional rules which was presented in the previous chapter. It is important to mention that the one-day ahead planification gives signal references not only to the MPC algorithm but also to the heuristic algorithm. Otherwise the algorithms could not be compared proper\ly because it may occur that the heuristics achieve better performance but at the expense of obtaining an empty storage at the end of the day. Regarding the types of storage of the microgrids, it is important to mention that the capacity for both storages are 10 Nm^3 of hydrogen and 35.49 kWh for the batteries. These quantities are equivalent since 11.1 Nm^3 of hydrogen is equivalent to 39.4 kWh when the HHV of hydrogen is used [34].

The simulations were carried out in Matlab, and the solver IBM® ILOG® CPLEX® was used for the optimization tasks.

6.1 Comparison criteria

In this section evaluation criteria are stablished to compare the performance of the control strategies. It can be noted that the criteria presented below are similar to those presented in the cost function considered for MPC

6.1.1 Energy exchange with the grid

In this case is considered the total energy exchanged with the grid through 24 hours. This can be expressed mathematically as:

$$J_{\text{ex}} = \frac{\sum_{k=1}^{1439} \left| P_{grid_{(k)}} \right|}{60} \tag{6.1}$$

where J_{ex} is expressed in kWh

6.1.2 Energy costs

In this case is considered the cost of energy that the user must pay. This criterion can be expressed as:

$$J_{bill} = \sum_{k=1}^{1439} P_{grid_{(k)}} \cdot Cost^{g}_{(k)} \tag{6.2}$$

$$Cost^{g}_{(k)} = \begin{cases} \dfrac{c^{p}_{(k)}}{60} & for\ P_{grid_{(k)}} \geq 0 \\ \dfrac{c^{s}_{(k)}}{60} & for\ P_{grid_{(k)}} < 0 \end{cases}$$

Where $c^{p}_{(k)}$ and $c^{s}_{(k)}$are the purchasing and selling prices expressed in kWh

6.1.3 Grid power variation

In this case is considered the variations of the energy exchanged with the grid. This criterion can be expressed as:

$$J_{grid-var} = \sum_{k=2}^{1439} \left| P_{grid_{(k)}} - P_{grid_{(k-1)}} \right| \tag{6.3}$$

6.2 Minimization of energy exchange with the grid

Both control strategies, MPC and heuristic algorithm, are applied to both types of microgrid (storage based on hydrogen and storage consisting of batteries). In this section, the graphs of the simulations are presented and then the results are compared.

6.2.1 Microgrid with storage based on hydrogen

6.2.1.1 Planification one-day ahead

Fig. 6.1 shows the evolution in time of the amount of hydrogen in the tank produced by the prior scheduling:

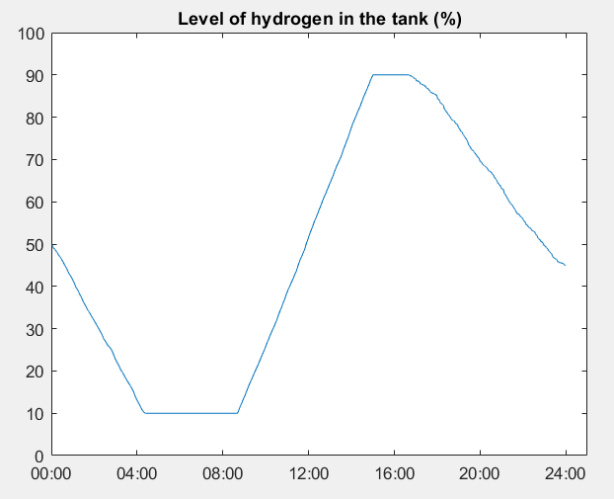

Fig. 6.1: Percentage of hydrogen in the tank according to planification one-day ahead for minimization of energy exchange with the grid

It can be seen that the one-day ahead planification produces a profile that is within 10% and 90%. This profile is later used as reference for both control strategies

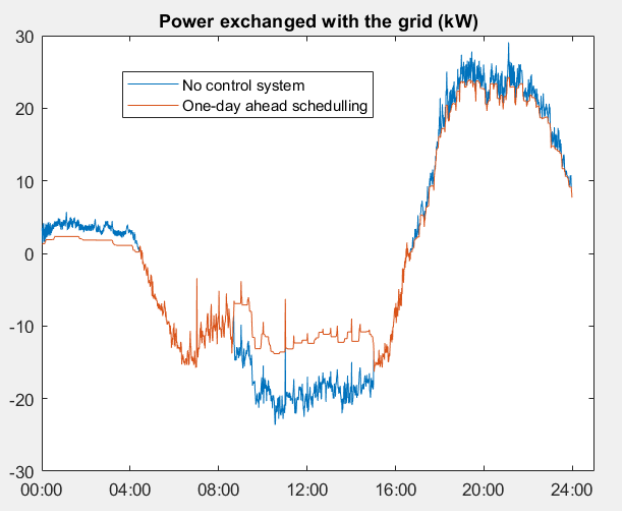

Fig. 6.2: Profile of power exchanged with the grid produced by prior planification for minimization of energy exchange with the grid

It can be seen from Fig. 6.2 that to minimize the energy exchange with the grid, the prior scheduling discharges the storage when there is excess of energy and charges the storage when there is surplus of energy.

6.2.1.2 MPC

The outputs produced by the optimization of the MPC are sent to the complete models which are different from the simplified model used by the MPC. Then, Fig.6.3 shows the results produced:

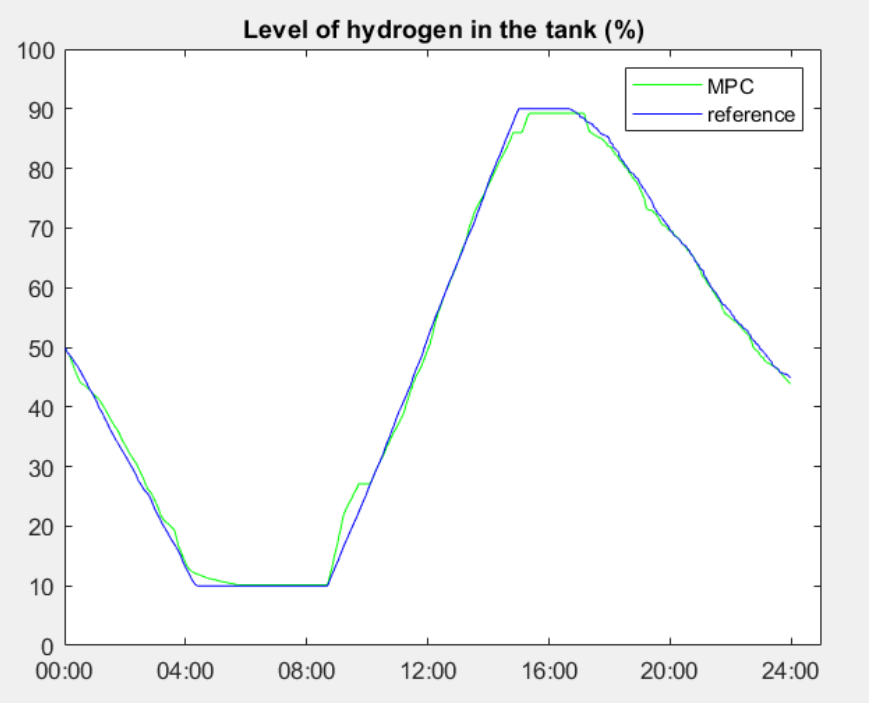

Fig. 6.3: Evolution of the amount of hydrogen in the tank when using the MPC on the microgrid for minimization of energy exchange with the grid

It can be seen that the MPC controller follows properly its reference. Since the prior scheduling already produces a profile where the level of hydrogen at the end of the day is in a range of +/- 5% of the initial state, the MPC controller is set to follow its reference with a range of +/- 1%

The power exchanged with the grid also follows its corresponding reference although as it was showed in the cost function section, in this case the deviation from the reference is penalized but is not constrained, so it may occur that it takes very different values with respect to the reference

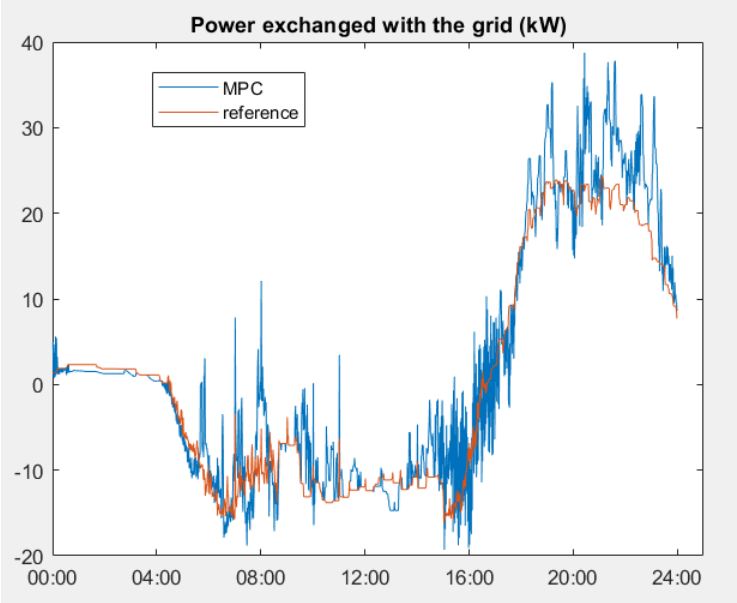

Fig. 6.4 Power exchanged with the grid when using the MPC for minimization of exchange with the grid

Looking at Fig. 6.5, it is clear that the MPC controller is reducing the energy exchange with the grid when comparing this result to the curve produced if the control system were not used. In fact at 12:00, part of the surplus of energy is used to charge the battery.

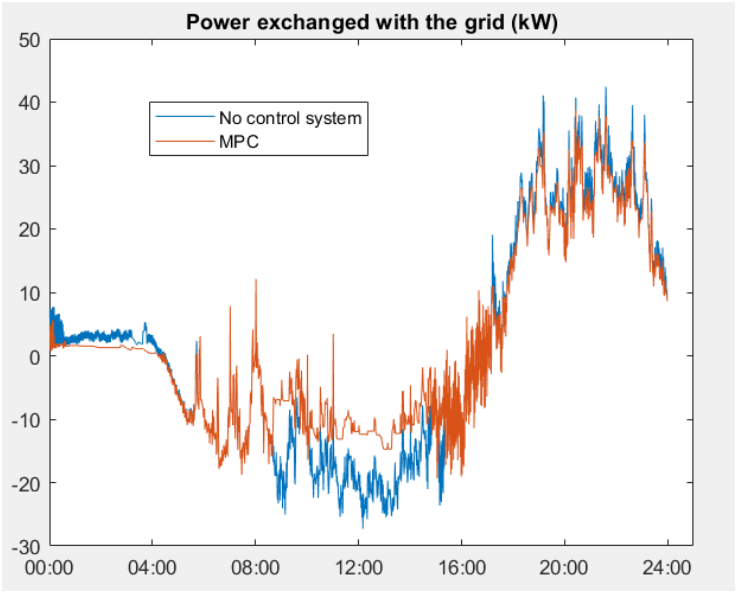

Fig. 6.5: Comparison between power exchanged with the grid when using MPC for minimization of energy exchange and not using any storage

Finally, in Fig. 6.6 it is shown the exchanged power with the storage system. It is important to note that the power consumed by the electrolyser respects the restriction of the minimum power which is characteristic of alkaline electrolysers.

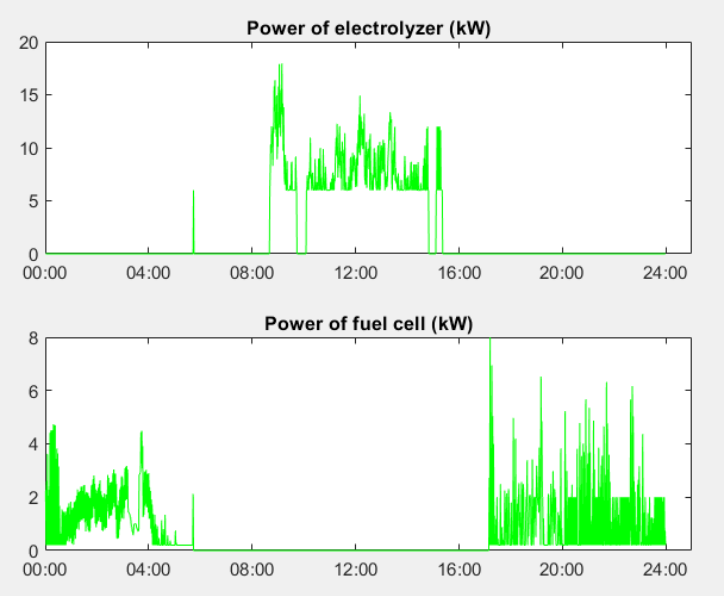

Fig. 6.6: Power references for the electrolyser and fuel cell produced when using MPC for minimization of energy exchange with the grid

6.2.1.3 Heuristic algorithm

As explained in the previous chapter, the heuristic algorithm consists of follow the energy level reference and respecting the restrictions of the electrolyser of maximum ramp rate and minimum power. In Fig. 6.7 is shown the evolution of the levels of hydrogen in the storage when the heuristic algorithm is used.

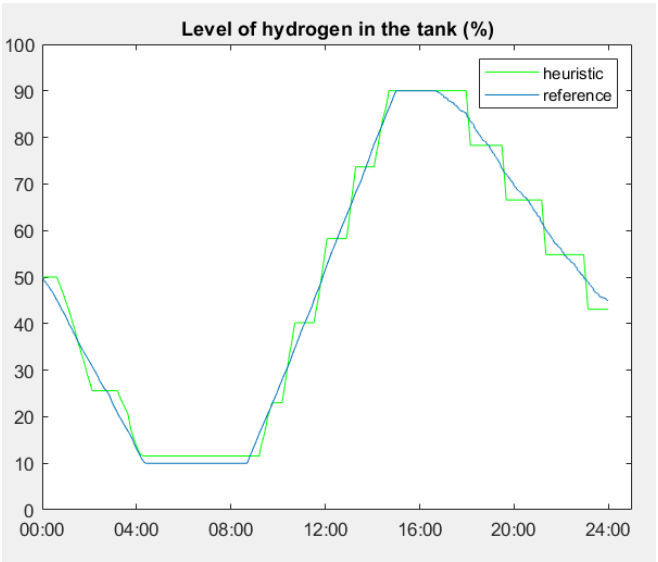

Fig. 6.7 Evolution of the amount of hydrogen in the tank when using the heuristic algorithm for minimization of energy exchange

It can be noted from Fig. 6.7 the continuous switching due to hysteresis.

In Fig. 6.8 is shown the exchanged power with the storage system.

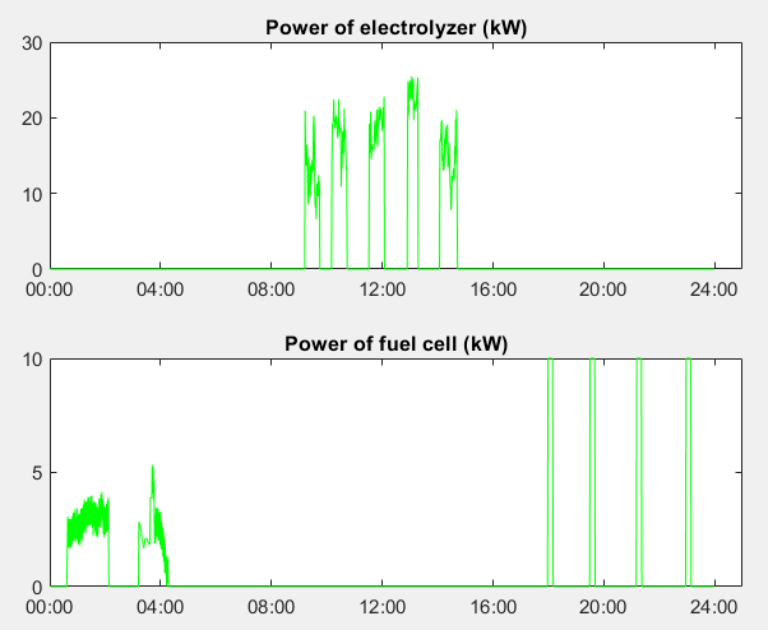

Fig. 6.8: Power references for the electrolyser and fuel cell when using the heuristic algorithm for minimization of energy exchange with the grid

It can be seen that also in this case the minimum power of the electrolyser is respected. However, the switching behaviour of hysteresis also introduces a switching pattern in the power exchanged with the grid as shown in Fig. 6.9:

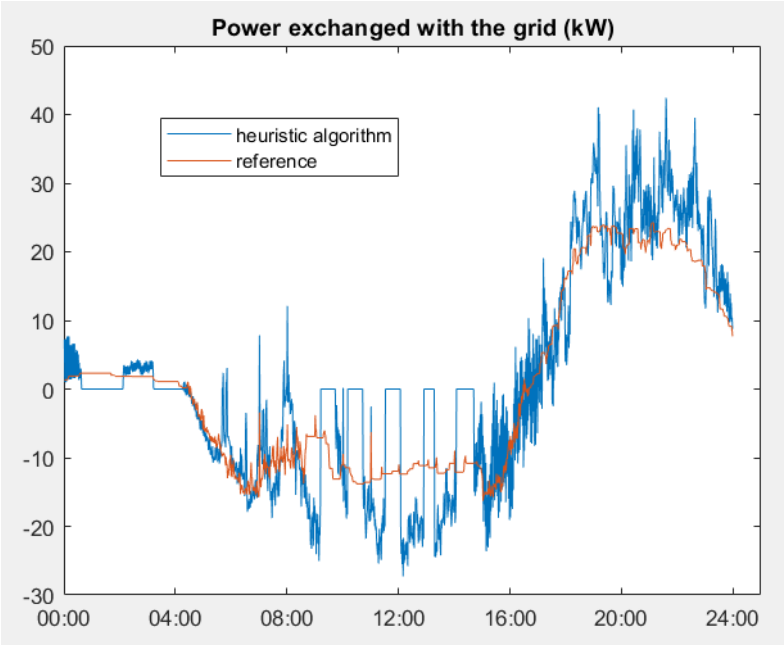

Fig. 6.9: Power exchanged with the grid when using the heuristic algorithm for storage based on hydrogen for minimization of energy exchange

6.2.2 Microgrid with storage based on batteries

6.2.2.1 Planification one-day ahead

The profile of energy level in the battery is obtained:

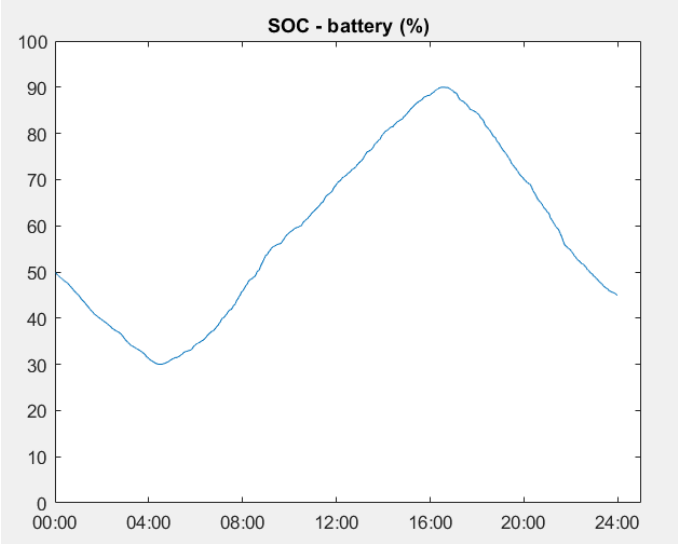

Fig. 6.10: SOC evolution produced by one-day ahead planification for minimization of energy exchange

It can be seen that the maximum and minimum bounds of energy stored in the battery are respected. Differently from the case of the system based on hydrogen, in this case the lower bound is 30% and not 10%. This is because deep discharge cycles seriously affect their lifetime. In Fig. 6.11 the energy exchange produced by the prior planification is shown. It is also shown what would be the profile if no storage and control system were used.

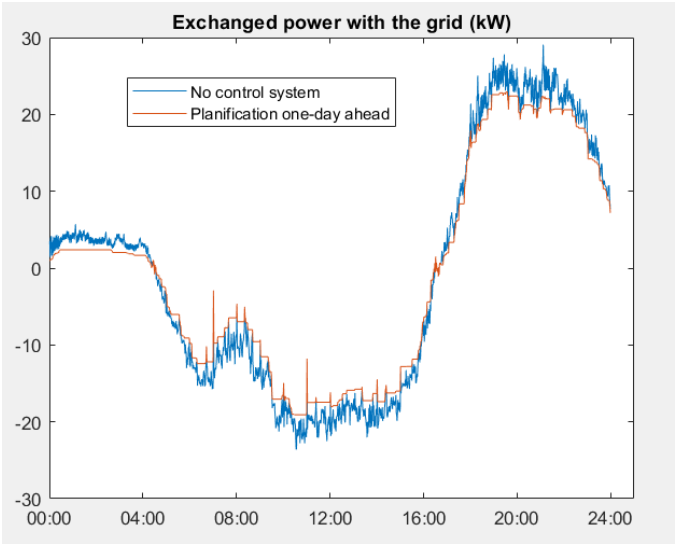

Fig. 6.11: Power exchanged with the grid profile produced by one-day ahead planification for minimization of energy exchange

6.2.2.1.1 MPC

The outputs produced by the optimization of MPC are sent to the complete models which are different from the simplified model that use MPC. Then the following graphs are produced:

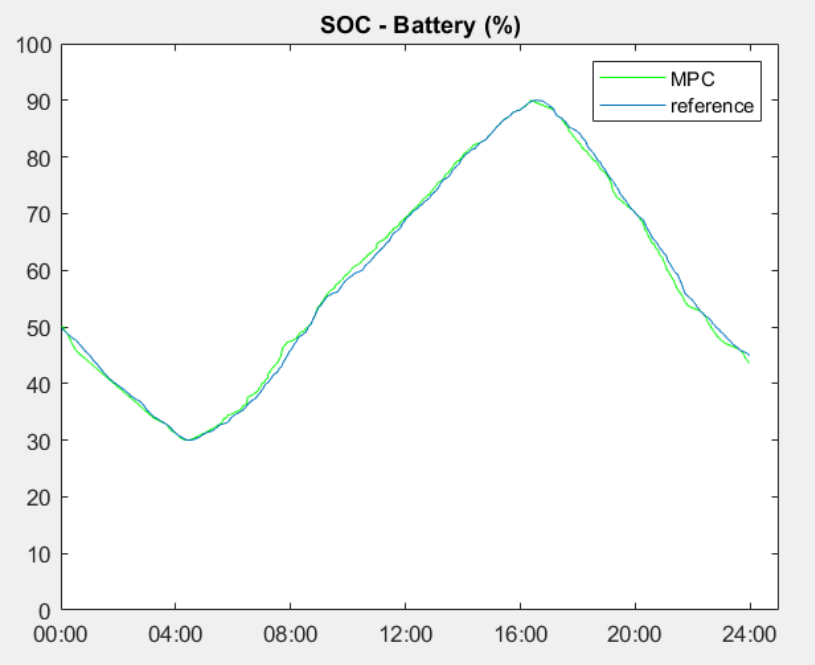

Fig. 6.12: SOC evolution when using the MPC for minimization of energy exchange

In Fig. 6.12, it can be seen that the state of charge of the battery follow its reference properly. Similarly, in Fig. 6.13 is shown that the power exchange also follows its reference properly

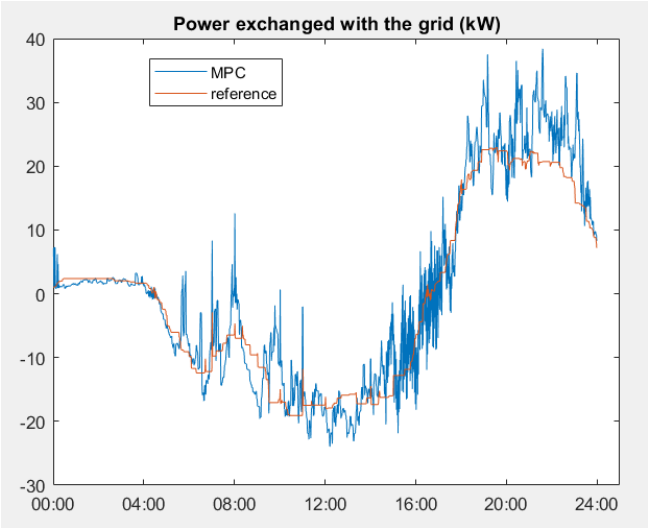

Fig. 6.13: Power exchanged with grid when using MPC for minimization of energy exchange

In Fig. 6.14, it can be seen that the use of MPC helps to reduce the variability of power exchanged with the grid. Moreover, when this figure is compared to Fig. 6.5 that corresponds to the microgrid based on hydrogen, it can be seen that in the case of microgrid with batteries, the storage absorbs less energy due to the reduced range of operation

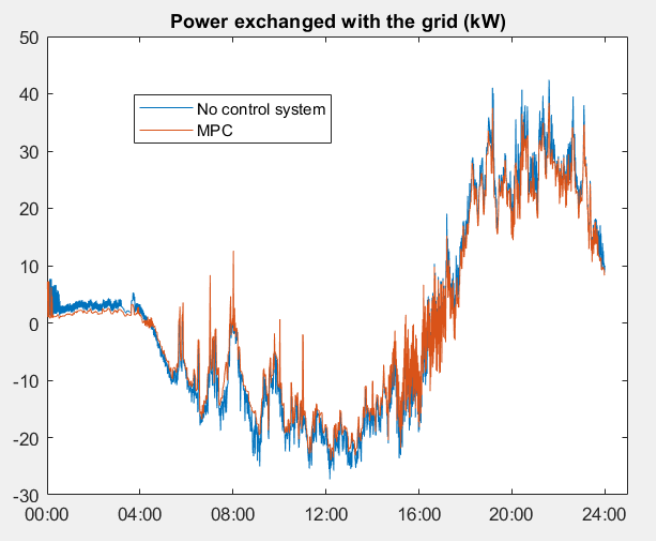

Fig. 6.14: Comparison between power exchanged with the grid when using MPC for minimization of energy exchange and not using any storage

It is important to note in Fig. 6.15 that there are few transitions between charging and discharging states, thus the lifetime of the batteries is not affected.

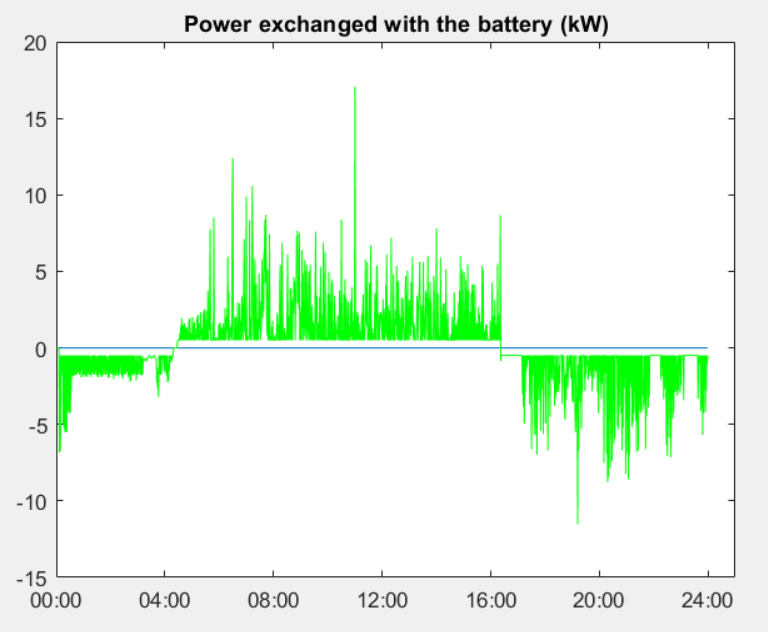

Fig. 6.15: Power reference for the battery when using MPC for minimization of energy exchange

6.2.2.2 Heuristic algorithm

Similarly to the case based on hydrogen, the SOC reference is followed with a hysteresis.

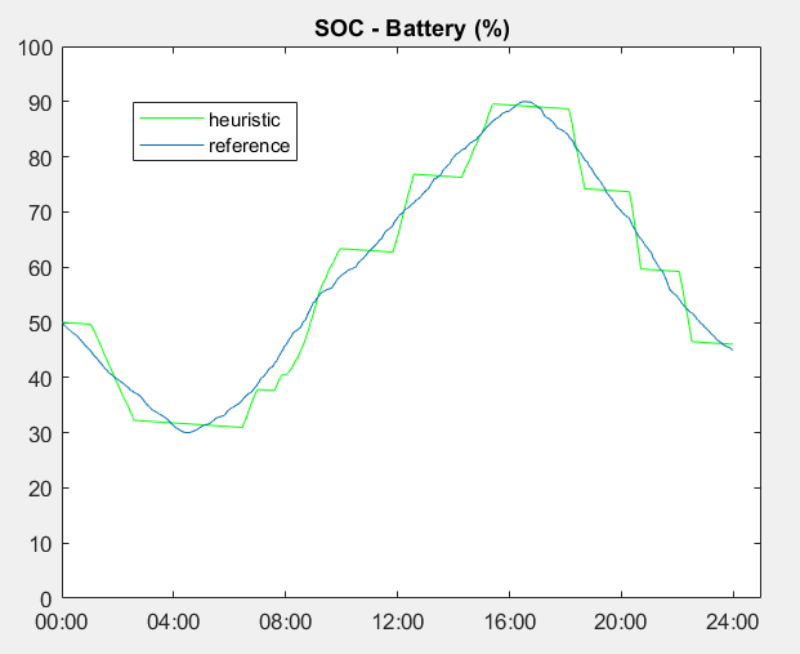

Fig. 6.16: Evolution of the SOC of the battery when using the heuristic algorithm for minimization of energy exchange

However, the switching of hysteresis also causes switching values in the power exchanged with the grid.

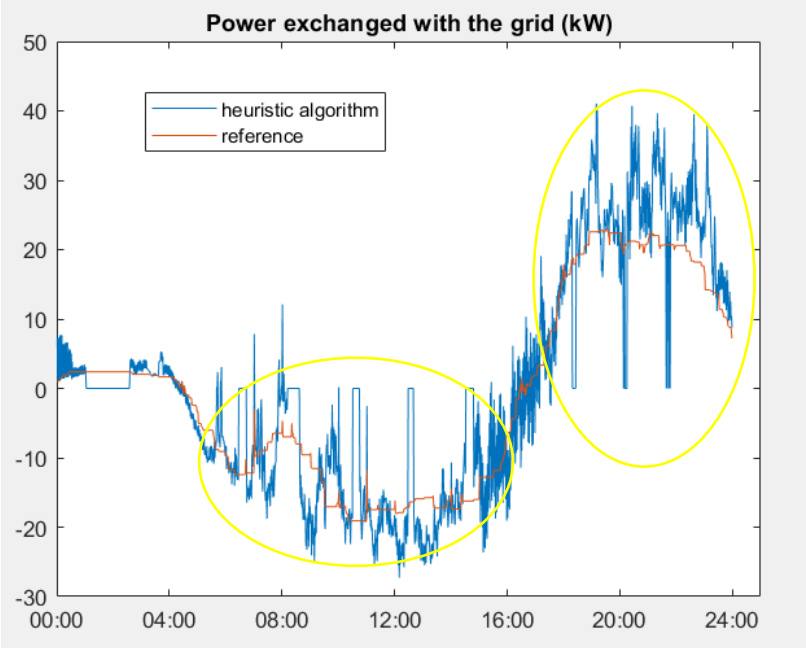

Fig. 6.17: Power exchanged with the grid when using the heuristic algorithm for battery for minimization of energy exchange

Additionally, due to the simplicity of this algorithm, the nominal power is used to regulate the charge of the battery. This causes intermittent peaks in the power exchanged with the grid.

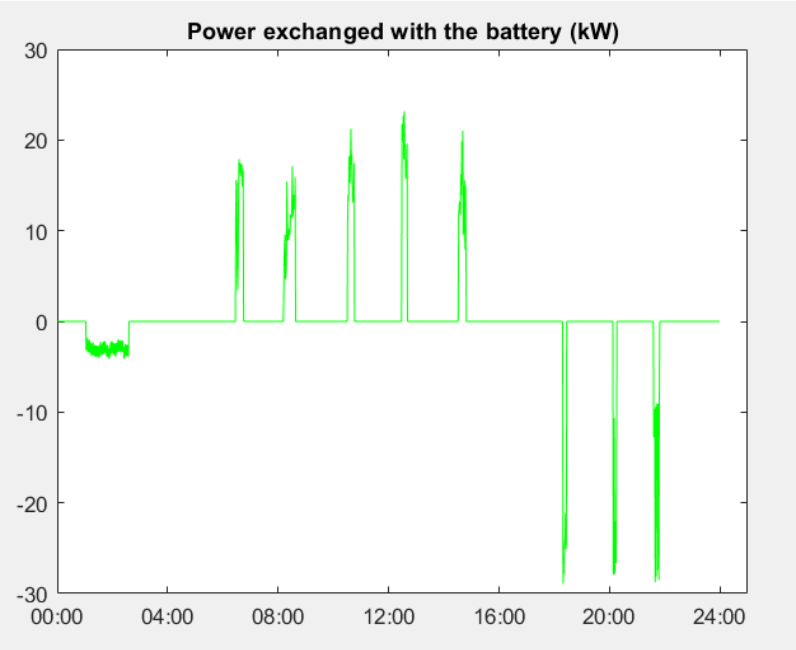

Fig. 6.18: Power references for the battery when using the heuristic algorithm for minimization of energy exchange

6.2.3 Comparison

The criteria presented in equations 6.1 and 6.3 are used to compare the performance of the different control strategies applied to both types of microgrids. Additionally, these criteria are also used to compare the performance of the control strategies with the case of no using any storage in the microgrid. The results are presented in table 13:

	Battery storage		Hydrogen storage		No control system
	MPC	Heuristic	MPC	Heuristic	
Energy exchange (kWh)	298.99	300.30	273.57	278.03	337.30
Grid variation (kW)	2888.84	4530.24	3289.12	4634.08	4923.90

Table 13: Quantitative comparison for the case of energy exchange minimization

From these results the following can be stated:

- In all the cases it is always better to use a storage system
- MPC has better performance than the heuristic algorithm. For both types of storage, MPC achieves lower exchanged energy with the grid and less variability.
- Regarding the type of storage, it can be seen that the storage based on hydrogen is better to minimize the energy exchange with the grid although the energy exchanged by the system with batteries is less variable. The main reason is that the system with batteries has less range of operation, from 30-90% when this range is 10-100% for batteries, so it absorbs less power when there is surplus of energy

6.3 Reduction of energy costs

6.3.1 Microgrid with storage based on hydrogen

6.3.1.1 Planification one-day ahead

When using the planification one-day ahead to obtain economic benefits, the result of optimization is to not use the storage system.

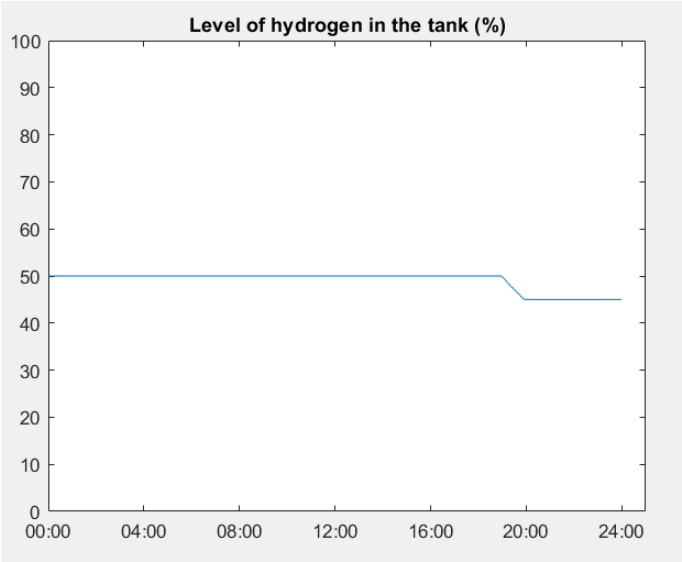

Fig. 6.19: Energy level of the tank when using the prior planification for reduction of energy costs

6.3.1.2 MPC

When the MPC is used to follow this reference, the energy stored is slightly reduced.

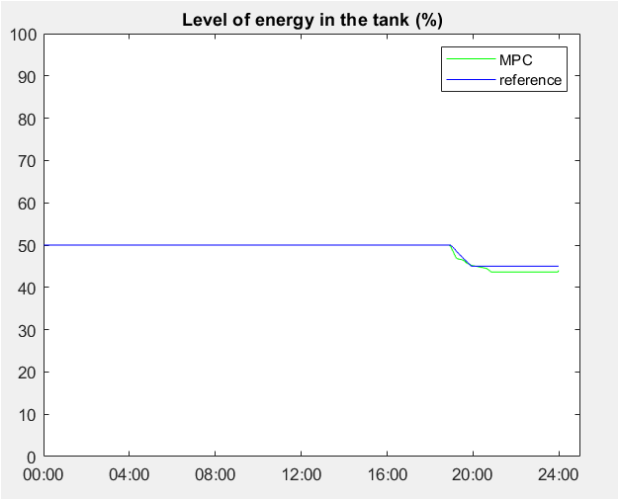

Fig. 6.20: Energy level in the tank when using the MPC for reduction of energy costs

The little reduction near the end of the day is because in this way it can absorb a little amount of power and also the energy level at the end of the day is close to the initial value.

6.3.1.3 Heuristic algorithm

When the heuristic algorithm receives the reference it does not use the storage at all because the little variation of the reference is less than the minimum change defined in the hysteresis for an activation to happen

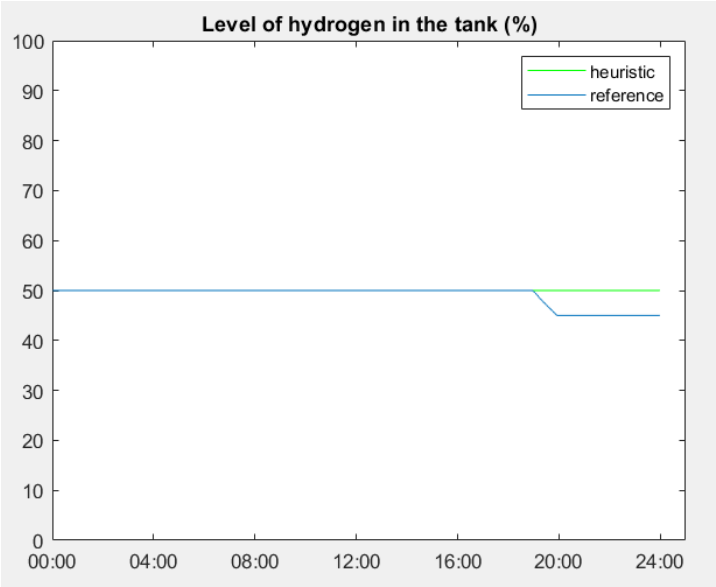

Fig. 6.21: Energy level in the tank when using the heuristic algorithm for reduction of energy costs

6.3.2 Microgrid with storage based on batteries

6.3.2.1 Planification one-day ahead

Differently from the previous case, there is usage of the storage when it is desired to obtain economic benefits as shown in Fig 6.22:

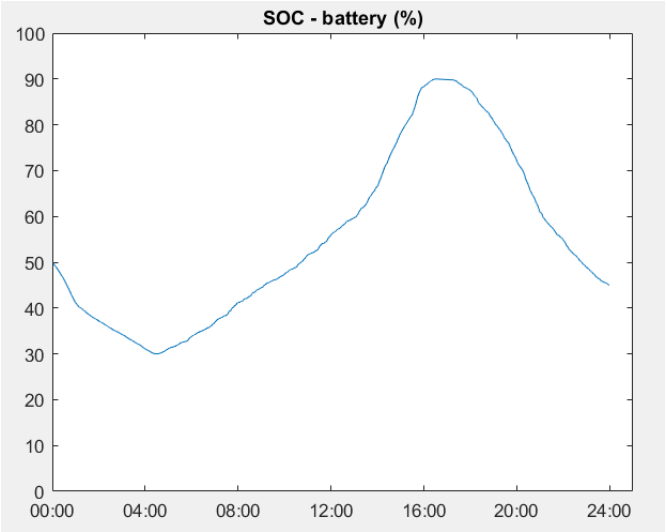

Fig. 6.22: SOC evolution when using the planification one-day ahead for reduction of energy costs

Note that the use of the storage helps to attenuate the variations of the power exchanged with the grid

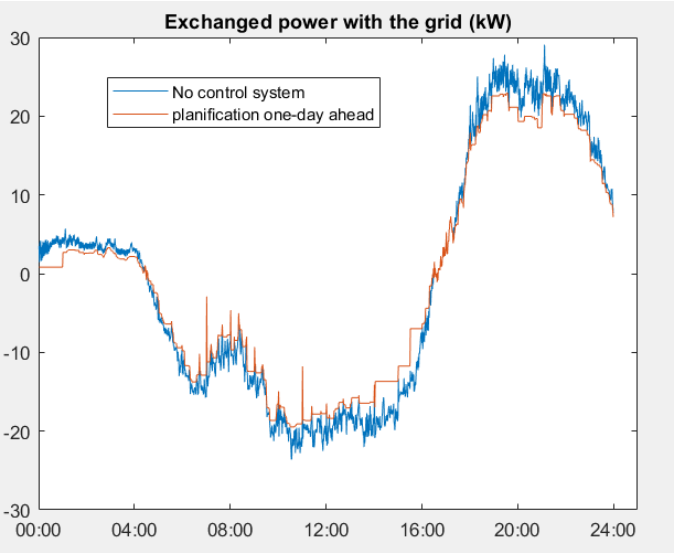

Fig. 6.23: Energy exchanged with grid profile produced by the planification one-day ahead for reduction of energy costs

6.3.2.2 MPC

Similarly to previous cases, the energy level in the battery and the power exchange with the grid follow their references

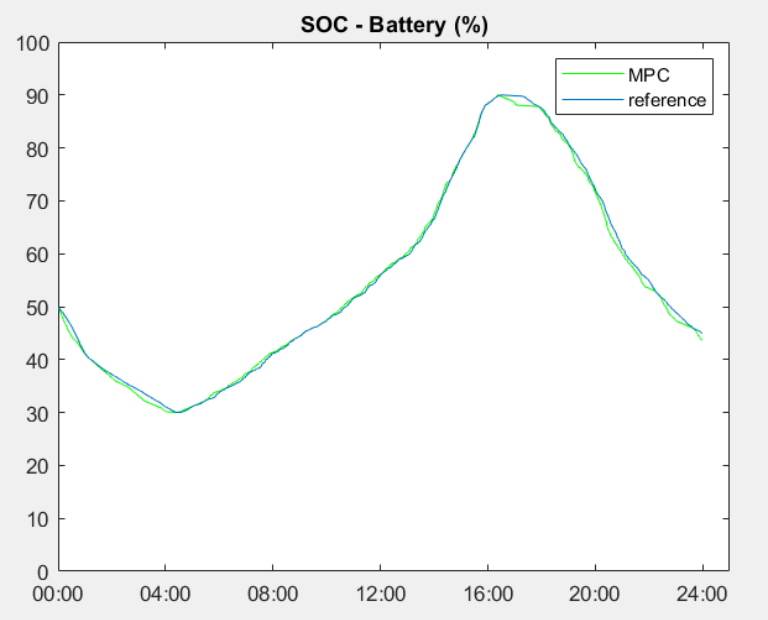

Fig. 6.24: Energy level in the battery when using MPC for reduction of energy costs

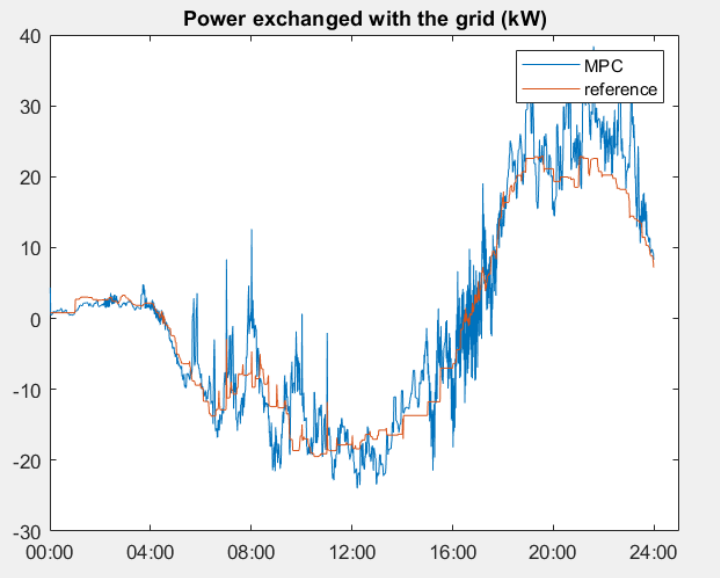

Fig. 6.25: Power exchanged with grid when using MPC for reduction of energy costs

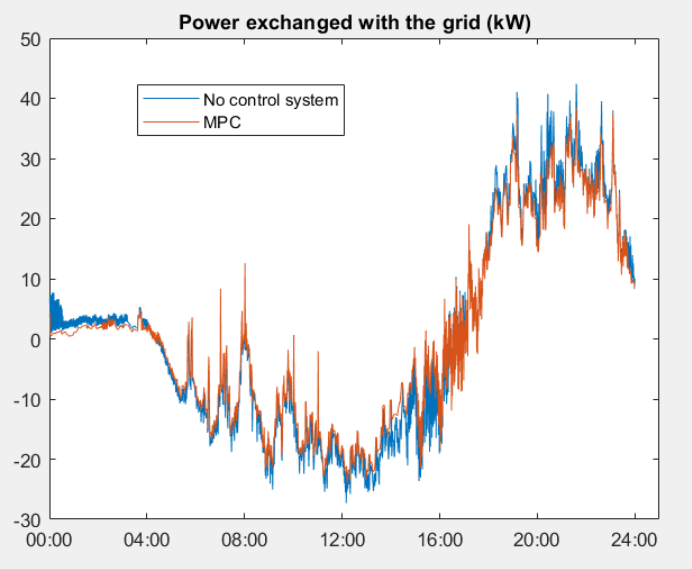

Fig. 6.26: Comparison between the energy exchanged with grid when using MPC for reduction of energy costs and not using any storage

In Fig. 6.27 is shown the power exchanged with the battery used to produce the previous profile of energy level

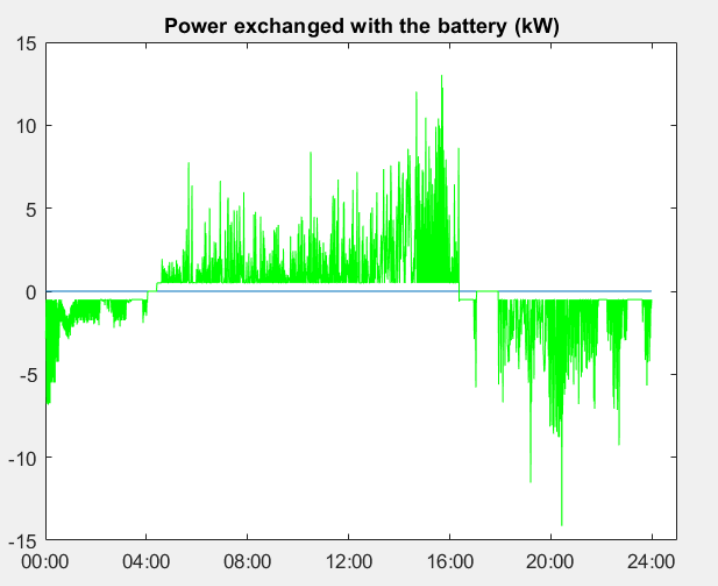

Fig. 6.27: Power references for the battery when using MPC for reduction of energy costs

6.3.2.3 Heuristic algorithm

Fig 6.28 shows the tracking of the reference using hysteresis

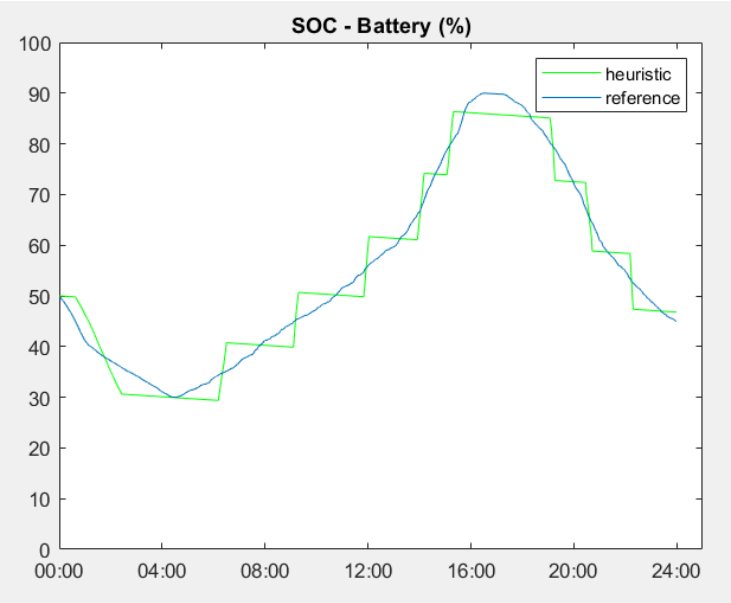

Fig. 6.28: Evolution of SOC when using the heuristic algorithm for reduction of energy costs

Similarly to the case of minimization of energy exchange, peaks of power are also produced

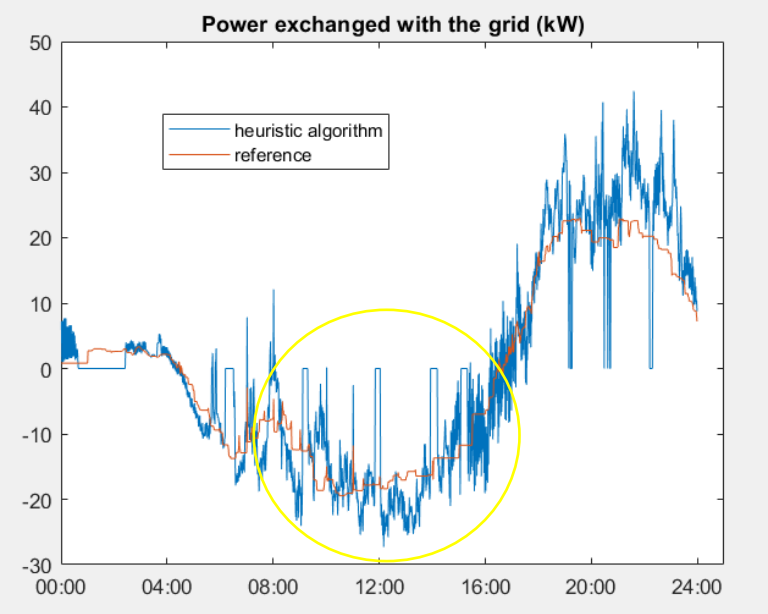

Fig. 6.29: Energy exchanged with the grid when using the heuristic algorithm reduction of energy costs in a microgrid with storage based on battery

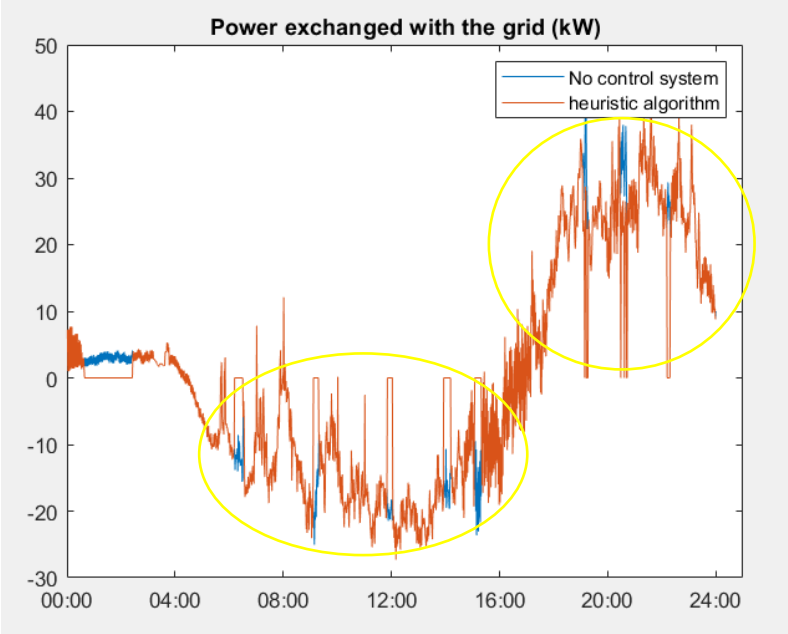

Fig. 6.30: Comparison between the power exchanged with the grid produced by the heuristic algorithm in a microgrid with battery for reduction of energy costs and not using any storage

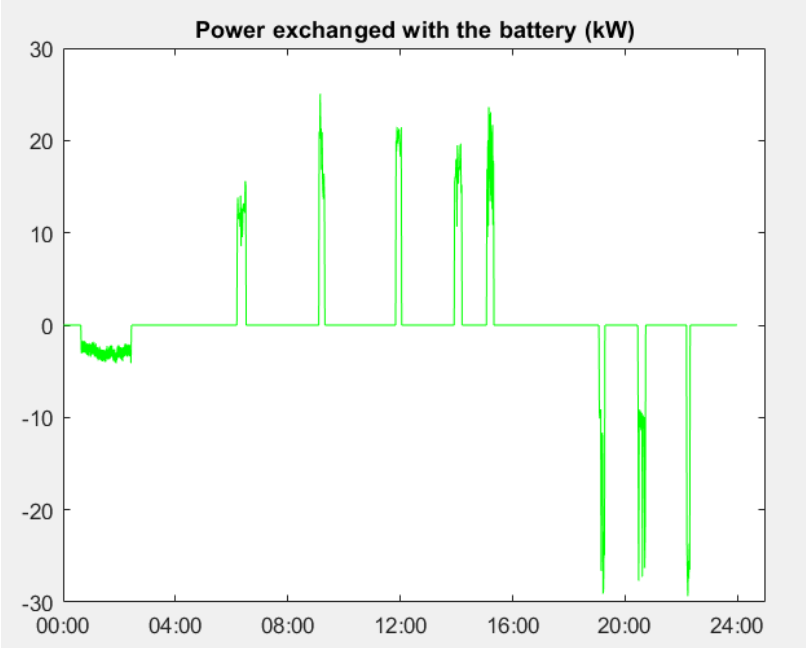

Fig. 6.31: Power references for the battery when using the heuristic algorithm for reduction of energy costs

6.3.3 Comparison

The criteria presented in equations 6.2 and 6.3 are used to compare the performance of the different control strategies applied to both types of microgrids. Additionally, these criteria are also used to compare the performance of the control strategies with the case of no using any storage in the microgrid. The results are presented in table 14:

	Battery storage		Hydrogen storage		No control system
	MPC	Heuristic	MPC	Heuristic	
Energy bill (€)	1464.11	1478.56	1511.84	1543.63	1543.63
Grid variation (kW)	2701.72	4805.43	4875.19	4923.90	4923.90

Table 14: Quantitative comparison for the case of reduction of energy costs

From these results the following can be stated:

- The use of hydrogen as a storage system does not give significant benefits. The main reason is that the round-trip efficiency of a storage based on hydrogen is too low when compared with a system with batteries.
- So, considering only the system based with batteries, MPC has better performance than the heuristic algorithm. It achieves not only lower energy costs but also lower variation of exchanged energy with the grid.

Chapter 7 Conclusions and future works

In this thesis, a control system structure is proposed to manage the operation of the storage system of a microgrid. It has been shown that this control structure can achieve different objectives subjected to operational constraints. The control system has a two-layer structure: a one-day ahead scheduling and a MPC controller. The prior planification uses forecasts of photovoltaic generation and demand for the next 24 hours and consists of an open-loop optimization problem to obtain similar levels of stored energy at the beginning and at the end of the day. The profiles of energy levels and power exchanged with the grid obtained by this optimization problem are sent as references to the MPC controller. At each time instant the MPC controller uses a forecast of generation and demand for the following 30 minutes, the references of the prior planification, the current energy level in the storage and the model of the system to state an optimization problem to find the optimal sequence of inputs to achieve a desired objective. From these inputs only the first input is applied to the real system and at the next time instant the energy level is measured. Then, new forecasts are generated again for the following 30 minutes and the optimization problem is stated again considering the new measured value of the storage. This strategy allows to compensate model and forecast errors.

For this study, two objectives were considered: minimization of energy exchange with the grid and reduction of energy cost and for each objective two types of storage systems of equivalent capacity for a microgrid were considered. The first type of storage is based on regeneration of hydrogen and the second is based on batteries. Results show that the storage based on hydrogen is better for minimization of energy exchange with the grid because its range of operation is greater than that of batteries. For the case of reduction of energy costs, the results show that it is better not to use of the storage based on hydrogen because of its low round-trip efficiency. Except for this case, it is also shown that the use of the storage system is better than not using it for both objectives. When compared to a simpler control strategy it was seen that the MPC control always performs better. It is important to mention that stability is achieved by imposing the constraint that during tracking the value of energy level in the storage must differ at most +/- 1% with respect to its reference. Additionally, the bounds of the exchanged power with the grid had high values, so to practical effects this variable is unbounded. This degree of freedom guarantees that there is always a feasible solution to the optimization problem.

The main objective of this thesis was to present a control strategy for a microgrid and evaluate its performance. However, the sizing of the components of the microgrids used for simulations was not optimally chosen. So, a future study should consider the following:

- Evaluate if it is convenient to relax the operation range of the batteries at the expense of reducing their lifetime.
- If the range of operation is not relaxed, it should be evaluated if it is convenient to increase the capacity of batteries considering the increase of space occupation and investments costs. It should also be considered that a similar increment of capacity for a storage based on hydrogen implies a lower increment of space occupation due to the high energy density of hydrogen.
- If a hydrogen system is used, then it should be considered to use a PEM electrolyser instead of an alkaline one because the PEM electrolyser does not have the restriction of minimum power and does not have inconvenient with frequent activation and deactivation.
- Determine the optimal value of the capacity of the storage that should be used for a determined photovoltaic generation and load.

Regarding the control system, future works should consider the following:

- Relaxation of the assumption that forecasts used by MPC are perfect and consider a more realistic case were at each time instant a prediction of the future generation and demand considering current values.
- In this thesis it was considered that the prices through the day are repeated every day. A future work should make predictions at each time instant of the energy prices based on the current conditions of the electrical.
- Include uncertainty in the models of the system
- Perform a formal analysis of feasibility and stability of the controller system

Bibliography

[1] J. K. James L. and J. L. Kirtley, Sources, Conversion, Distribution and Use, New York: John Wiley & Sons, Incorporated, 2010, p. 406.

[2] T. Sato, D. M. Kammen, B. Duan, M. Macuha, Z. Zhou, J. Wu, M. Tariq and S. A. Asfaw, "Specifications, Requirements, and Technologies," in *Smart Grid Standards*, Singapore, John Wiley & Sons, Incorporated, 2015, p. 484.

[3] H. Bevrani, B. François and T. Ise, Microgrid Dynamics and Control : A Solution for Integration of Renewable Power, Somerset: John Wiley & Sons, Incorporated, 2017, p. 715.

[4] A. Sumper and A. Baggini, Electrical Energy Efficiency: Technologies and Applications, Hoboken: John Wiley & Sons, Incorporated, 2012.

[5] N. D. Hatziargyriou, N. Jenkins, G. Strbac, J. A. P. Lopes, J. Ruela, A. Engler, J. Oyarzabal, G. Kariniotakis and A. Amorim, "Microgrids - Large scale integration of microgeneration," in *CIGRE 2006, Conseil International des Grands Réseaux Electriques*, Paris, 2006.

[6] N. (. Hatziargyriou, Microgrids : Architectures and Control, New York: John Wiley & Sons, Incorporated, 2014.

[7] K. R. Padiyar and A. M. Kulkarni, Dynamics and Control of Electric Transmission and Microgrids, Newark: John Wiley & Sons, Incorporated, 2019.

[8] A. Rogin, "Computational framework for evaluating the impact of power-to-gas technology on European transmission system with large penetration of renewable sources," Torino, 2018.

[9] M. A. Pellow, C. J. Emmott, C. J. Barnhart and S. M. Benson, "Hydrogen or batteries for grid storage? A net energy analysis," *Energy Environ. Sci,* vol. 2015, no. 8, pp. 1938-1952, 2015.

[10] A. Ursua, L. M. Gandia and P. Sanchis, "Hydrogen Production From Water Electrolysis: Current Status and Future Trends," *Proceedings of the IEEE,* vol. 100, pp. 410-426, 2012.

[11] L. Valverde-Isorna, D. Ali, D. Hogg and A. Abdel-Wahab, "Modelling the performance of wind–hydrogen energy systems: Case study the Hydrogen Office in Scotland/UK," *Renewable and Sustainable Energy Reviews,* vol. 53, pp. 1313-1332, 2016.

[12] Ø. Ulleberg, "Modeling of advanced alkaline electrolyzers: a system simulation approach," *International Journal of Hydrogen Energy,* vol. 28, no. 1, pp. 21-33, 2003.

[13] A. Dicks and D. A. J. Rand, Fuel cell systems explained, Hoboken: Willey, 2018.

[14] N. M. Sammes, Fuel Cell Technology, London: Springer, 2006.

[15] I. San Martin, A. Ursua and P. Sanchis, "Modelling of PEM Fuel Cell Performance: Steady-State and Dynamic Experimental Validation," *Energies,* vol. 2, no. 7, pp. 670-700, 2014.

[16] J. M. Correa, F. A. Farret, L. N. Canha and M. G. Simoes, "An electrochemical-based fuel-cell model suitable for electrical engineering automation approach," *IEEE Transactions on Industrial Electronics,* vol. 51, no. 5, pp. 1103-1112, 2004.

[17] I. D. Gimba, A. S. Abdulkareem and A. Jimoh, "Theoretical Energy and Exergy Analyses of Proton Exchange Membrane Fuel Cell by Computer Simulation," *Journal of Applied Chemistry,* vol. 2016, p. 15, 2016.

[18] J.-k. Park, Principles and Applications of Lithium Secondary Batteries, Weinheim, Germany: Wiley-VCH Verlag GmbH & Co. KGaA, 2012.

[19] B. Averill and P. Eldredge, Principles of general chemistry, Creative Commons, 2012.

[20] "A Guide to Understanding Battery Specifications," MIT Electric Vehicle Team, 2008.

[21] N. Mohammad, "Batteries and charging method," Milan, 2019.

[22] A. Chih-Chiang Hua and B. Zong-Wei Syue, "Charge and discharge characteristics of lead-acid battery and LiFePO4 battery," in *The 2010 International Power Electronics Conference - ECCE ASIA*, Saporo, 2010.

[23] H. Keshan, J. Thornburg and T. S. Ustun, "Comparison of lead-acid and lithium ion batteries for stationary storage in off-grid energy systems," in *4th IET Clean Energy and Technology Conference (CEAT 2016)*, Kuala Lumpur, 2016.

[24] C. Mittelsteadt, T. Norman, M. Rich and J. Willey, "Chapter 11 - PEM Electrolyzers and PEM Regenerative Fuel Cells Industrial View," in *Electrochemical Energy Storage for Renewable Sources and Grid Balancing*, P. T. Moseley and J. Garche, Eds., Elsevier, 2015, pp. 159-181.

[25] P. Kurzweil, "Chapter 16 - Lithium Battery Energy Storage: State of the Art Including Lithium–Air and Lithium–Sulfur Systems," in *Electrochemical Energy Storage for Renewable Sources and Grid Balancing*, P. T. Moseley and J. Garche, Eds., Elsevier, 2015, pp. 269-307.

[26] D. Rosewater, S. Ferreira, D. Schoenwald, J. Hawkins and S. Santoso, "Battery Energy Storage State-of-Charge Forecasting: Models, Optimization, and Accuracy," *EEE Transactions on Smart Grid,* vol. 10, no. 3, pp. 2453-2462, 2019.

[27] C. D. Maranas and A. R. Zomorrodi, "Modeling with Binary Variables and MILP Fundamental," in *Optimization Methods in Metabolic Networks*, 2016, pp. 81-106.

[28] A. Richards and J. How, "Mixed-integer programming for control," *Proceedings of the 2005, American Control Conference,* vol. 4, pp. 2676-2683, 2005.

[29] H. P. Williams, Model Building in Mathematical Programming, 5th Edition, John Wiley & Sons Ltd,, 2013.

[30] A. Bemporad and M. Morari, "Control of systems integrating logic, dynamics, and constraints," *Automatica,* vol. 35, no. 3, pp. 407-427, 1999.

[31] L. Ming-Hua, J. Gunnar Carlsson, D. Ge, J. Shi and T. Jung-Fa, "A Review of Piecewise Linearization Methods," *Mathematical Problems in Engineering,* vol. 2013, p. 8 pages, 2013.

[32] A. Bemporad, "Tutorial on model predictive control of hybrid systems," in *Proc. Adv. Process Control Appl. Ind. Workshop*, Vancouver, BC, Canada, 2007.

[33] A. Cataldo, "Model predictive control in manufacturing plants," 2016.

[34] D. Thomas, "RENEWABLE HYDROGEN: THE MISSING LINK BETWEEN THE POWER, GAS, INDUSTRY AND TRANSPORT SECTORS," 2018.

[35] J. E. Villa Londono, "GRID-CONNECTED OPERATION OF A HYBRID MICROGRID. Design, operation, and control of a Wind-Solar-Hydrogen Energy System.," 2019.

[36] A. M. Mansour, N. H. Saad and A. A. Sattar, "Maximum Power Point Tracking Of Ten Parameter Fuel Cell Model," *The Journal of American Science,* vol. 8(8), no. 139, pp. 941-946, 2012.

[37] "Gestore Mercati Energetici," [Online]. Available: https://www.mercatoelettrico.org/En/Default.aspx. [Accessed 2020].

[38] J. M. Bright, O. Babacan, J. Kleissl, P. G. Taylor and R. Crook, "A synthetic, spatially decorrelating solar irradiance generator and application to a LV grid model with high PV penetration," *Solar energy,* vol. 147, pp. 83-98, 2017.

[39] C. J. Smith, J. M. Bright and R. Crook, "Cloud cover effect of clear-sky index distributions and differences between human and automatic cloud observations," *Solar energy,* vol. 144, pp. 10-21, 2017.

[40] J. M. Bright, P. G. Taylor and R. Crook, "Methodology to stochastically generate synthetic 1-minute irradiance time-series derived from mean hourly weather observational data," in *ISES Solar World Congress 2015, 8th-12th November 2015*, Daegu, South Koreo, 2015.

[41] J. M. Bright, C. J. Smith, P. G. Taylor and R. Crook, "Stochastic generation of synthetic minutely irradiance time series derived from mean hourly weather observation data," *Solar energy,* vol. 115, pp. 229-242, 2015.

[42] J. M. Bright, P. G. Taylor and R. Crook, "Methodology to Stochastically Generate Spatially Relevant 1-Minute Resolution Irradiance Time Series from Mean Hourly Weather Data," in *5th Solar Integration workshop 2015, 19th-20th October 2015*, Brussels, Belgium, 2015.

[43] "Dateandtime.info," [Online]. Available: https://dateandtime.info/es/citycoordinates.php?id=3173435.

[44] T. Huld, R. Muller and A. Gambardella, "A new solar radiation database for estimating PV performance in Europe and Africa," *Solar Energy,* vol. 86, pp. 1803-1815, 2012.

[45] M. Z. Jacobson and V. Jadhav, "World estimates of PV optimal tilt angles and ratios of sunlight incident," *Solar Energy,* vol. 169, pp. 55-66, 2018.

[46] A. Colli and W. J. Zaaiman, "Maximum-Power-Based PV Performance Validation Method: Application to Single-Axis Tracking and Fixed-Tilt c-Si Systems in the Italian Alpine Region," *IEEE Journal of Photovoltaics,* vol. 2, no. 4, pp. 555-563, 2012.

[47] E. McKenna and M. Thomson, "High-resolution stochastic integrated thermal-electrical domestic demand model," *Applied Energy,* vol. Volume 165, pp. 445-461, 2016.